

8-2015

INVESTIGATING THE ROLE OF CHOLESTEROL METABOLISM AND SYNTHESIS IN METASTASIS AND RADIATION RESPONSE IN AGGRESSIVE SUBTYPES OF BREAST CANCER

Adam Wolfe

Follow this and additional works at: http://digitalcommons.library.tmc.edu/utgsbs_dissertations

 Part of the [Cancer Biology Commons](#), and the [Medicine and Health Sciences Commons](#)

Recommended Citation

Wolfe, Adam, "INVESTIGATING THE ROLE OF CHOLESTEROL METABOLISM AND SYNTHESIS IN METASTASIS AND RADIATION RESPONSE IN AGGRESSIVE SUBTYPES OF BREAST CANCER" (2015). *UT GSBS Dissertations and Theses (Open Access)*. Paper 601.

This Dissertation (PhD) is brought to you for free and open access by the Graduate School of Biomedical Sciences at DigitalCommons@The Texas Medical Center. It has been accepted for inclusion in UT GSBS Dissertations and Theses (Open Access) by an authorized administrator of DigitalCommons@The Texas Medical Center. For more information, please contact laurel.sanders@library.tmc.edu.

**INVESTIGATING THE ROLE OF CHOLESTEROL METABOLISM AND
SYNTHESIS IN METASTASIS AND RADIATION RESPONSE IN AGGRESSIVE
SUBTYPES OF BREAST CANCER**

by

Adam Ross Wolfe, B.S.

APPROVED:

Wendy Woodward, M.D.,Ph.D.

Advisory Professor

Russell Broaddus, M.D.,Ph.D.

Ann Klopp, M.D.,Ph.D.

Chandra Bartholomeusz, M.D.,Ph.D.

Kenneth Tsai, M.D.,Ph.D.

APPROVED:

Dean, The University of Texas

Graduate School of Biomedical Sciences at Houston

**INVESTIGATING THE ROLE OF CHOLESTEROL METABOLISM AND
SYNTHESIS IN METASTASIS AND RADIATION RESPONSE IN AGGRESSIVE
SUBTYPES OF BREAST CANCER**

A
DISSERTATION

Presented to the Faculty of
The University of Texas
Health Science Center at Houston
Graduate School of Biomedical Sciences
and
The University of Texas
M.D. Anderson Cancer Center
Graduate School of Biomedical Sciences

In Partial Fulfillment
of the Degree of

DOCTOR OF PHILOSOPHY

by

Adam Ross Wolfe, B.S.

Houston, Texas

August, 2015

Dedication

I dedicate my dissertation to my mother. Although our time in this world together was far too short, you are the inspiration to all of my dreams. You believed in me before anyone else and gave me the confidence to pursue this journey. Your love provided the light in my darkest days.

Acknowledgments

I would like to acknowledge the mentorship of Dr. Wendy Woodward during my PhD research years. She is a true mentor in every meaning of the word. She is an amazing clinician and brilliant researcher, and I was fortunate that my first google search for a summer research rotation brought her name up first. Through her guidance and support, I was able to develop a really interesting and clinically relevant research project. I owe a great deal of gratitude to her continued support and interest in my career goals.

Additionally, I would like to acknowledge the help of everyone in the Woodward laboratory, specifically Bisrat Debeb, Richard Larson, Li Li, Lara Lacerda, Rachel Atkinson, and Arvind Bambhroliya. I joined the lab with a subpar understanding of how to conduct basic research. Without their massive amounts of help I would have not been able to accomplish any of this dissertation.

I would also like to acknowledge my advisory committee: Dr. Ann Klopp, Dr. Russell Broaddus, Dr. Kenneth Tsai, and Dr. Chandra Bartholomeusz. Their evaluations and suggestions throughout the PhD process were instrumental. I would like to acknowledge Jo Cheatwood for helping me through the administrative process of the MD/PhD program.

Lastly, I want to acknowledge my family. My father has taught me the value of hard work and the importance of being a good father. My step mother Judy has been there for me without any question and has provided support for me when I always needed it. My beautiful wife, Tatiana, has forever changed my world for the better. Her unwavering love and support has kept me happy on this journey. *Você é o amor da minha vida.* To my son, Asher, may you always maintain a joy for life. You motivate me to be a better person. I love you both.

Investigating the role of cholesterol metabolism and synthesis in metastasis and radiation response in aggressive subtypes of breast cancer

Adam Ross Wolfe, B.S. Advisory Professor: Wendy A. Woodward, MD, PhD

Aggressive breast cancers, triple-negative breast cancer (TNBC) and inflammatory breast cancer (IBC), metastasize at a high rate and are notoriously resistant to standard treatments. Research has shown diets high in cholesterol increase the incidence of aggressive breast cancers and pre-clinical research has shown cholesterol can fuel the growth of breast cancer in vivo. Studies at MD Anderson have shown that IBC patients taking cholesterol lowering drugs, statins, have improved survival outcomes, and also statins can improve the response to radiation in vitro. Furthermore, statins have been shown to target the cells with stem like-properties called cancer stem cells (CSCs) which are known to be important in the pathogenesis of aggressive breast cancers. However, the effects of statins specifically on TNBC metastasis and the mechanism of action have not been explored. Furthermore, the transporters of cholesterol, high-density (HDL) and very low-density (VLDL) lipoproteins, have not been studied extensively in aggressive breast cancers. Due to the associations with cholesterol and incidence of breast cancer and the work done with statins and IBC, I hypothesized reductions in intracellular cholesterol content by statins or HDL inhibits downstream signaling regulating metastasis and radiation response, altering cellular functions in cancer cells and immune cells. Here I show for the first time that statins can inhibit TNBC cell metastasis in vivo, and is dependent on FOXO3a activation, demonstrate a potential role for dyslipidemia in radiation sensitivity and survival among IBC patients, reveal miR-33a regulates HDL-induced radiation sensitivity in breast cancer, and mesenchymal stem cells (MSCs) and macrophages can influence each other to increase the tumor promoting influence of each on IBC cells which can be inhibited with statins.

Table of Contents

Approval Signatures	i
Title Page	ii
Dedication	iii
Acknowledgements	iv
Abstract	v
Table of Contents	vi
List of Illustrations	ix
List of Tables	xi
Abbreviations	xii
Chapter 1 Introduction	1
1.1 Brief History of Breast Cancer	2
1.2 Aggressive Breast Cancers.....	4
1.3 Role of Cholesterol in Aggressive Breast Cancer.....	5
1.4 Statins and Breast Cancer.....	6
1.5 Lipoproteins and Breast Cancer.....	8
1.6 Breast Cancer Stem Cells.....	9
1.7 Inflammatory Breast Cancer Microenvironment.....	10
1.8 Conclusion.....	11
1.9 Conceptual Framework and Hypothesis.....	12
Chapter 2 Simvastatin prevents triple-negative breast cancer metastasis in pre-clinical models through regulation of FOXO3a.....	14
2.1 Abstract.....	15
2.2 Introduction.....	16
2.3 Methods and Materials.....	17
2.4 Results.....	25

2.5 Discussion.....	52
2.6 Conclusions.....	54
Chapter 3 High-density lipoprotein and very-low-density lipoprotein have opposing roles in regulating tumor-initiating cells and sensitivity to radiation in inflammatory breast cancer.....	55
3.1 Abstract.....	56
3.2 Introduction.....	58
3.3 Methods and Materials.....	60
3.4 Results.....	63
3.5 Discussion.....	76
3.6 Conclusions.....	77
Chapter 4 MiR-33a Regulates Radiation Sensitivity to High Density Lipoprotein in Breast Cancer.....	78
4.1 Abstract.....	79
4.2 Introduction.....	81
4.3 Methods and Materials.....	82
4.4 Results.....	85
4.5 Discussion.....	93
4.6 Conclusions.....	94
Chapter 5 Mesenchymal Stem Cells and Macrophage Cross-Talk through IL-6 to Promote Inflammatory Breast Cancer Cell Invasion and Self Renewal.....	95
5.1 Abstract.....	96
5.2 Introduction.....	98
5.3 Methods and Materials.....	99
5.4 Results.....	102
5.5 Discussion.....	115

5.6 Conclusions.....	116
Chapter 6 Discussion.....	117
6.1 Overall Conclusions.....	118
6.2 Research Significance.....	119
6.3 Future Investigations.....	120
Appendix.....	122
Bibliography.....	141
Vita.....	162

List of Illustrations

1.	Simvastatin reduces percentage of cycling cells, proliferation, and migration.....	27
2.	Simvastatin reduces the cancer stem cell-like population.....	28
3.	Simvastatin inhibits metastasis.....	34
4.	Simvastatin had no effects on tumor growth rate.....	35
5.	Imaging from mouse injected with SUM 149-GFP labeled cells.....	36
6.	Simvastatin regulates the expression of FOXO3a.....	39
7.	FOXO3a is a mediator of mammosphere and migration in TNBC cells.....	42
8.	High FOXO3a mRNA levels are associated with better clinical outcomes.....	48
9.	FOXO3a correlates with metastasis in vivo.....	51
10.	The impact of lipoproteins on mammosphere formation.....	64
11.	The effect of lipoprotein treatment on radiation response.....	66
12.	In vitro detection of cholesterol levels in SUM 149 cells by filipin staining.....	67
13.	HDL and VLDL have opposite effects on FOXO3a phosphorylation.....	69
14.	Kaplan Meir Curves for HDL outcomes.....	73
15.	Expression of miR-33 and the protein product of its target gene ABCA1.....	86
16.	Clonogenic survival curves indicate effect of miR-33.....	88
17.	Inhibition of miR-33a increases HDL-induced radiation sensitivity.....	89
18.	Ectopic expression of miR-33a inhibits HDL-induced radiosensitization.....	90
19.	High serum miR-33a level is associated with worse outcomes.....	92
20.	Model of Co-Culture System.....	103
21.	MSCs and M2 macrophages cross-talk through IL-6.....	104
22.	Crosstalk between educated MSCs and IBC cells increases IBC invasion.....	107

23.	Simvastatin blocks IL-6.....	109
24.	Blocking M2 macrophage recruitment in the in vivo IBC model	113

List of Tables

1.	List of breast cancer gene expression data sets included in the analysis.....	22
2.	Patients and tumor characteristics.....	23
3.	Tumor incidence and metastasis rate for tail vein and orthotopic in vivo.....	33
4.	RPPA analysis of simvastatin treated cells reveals FOXO3a as a target.....	38
5.	Correlations of FOXO3A expression with clinicopathological characteristics.....	49
6.	Univariate and multivariate analyses for MFS in breast cancer.....	50
7.	Patient Characteristics.....	71
8.	Univariate all patients.....	74
9.	Multivariate cox model for overall survival for HDL and VLDL.....	75

Abbreviations

ABCA1: ATP-Binding Cassette A1

ALDH: Aldehyde Dehydrogenase

ALL: Acute Lymphoblastic Leukemia

CSCs: Cancer Stem Cells

DEAB: Diethylaminobenzaldehyde

DFS: Disease-Free Survival

DMSO: Dimethyl Sulfoxide

ER: Estrogen Receptor

FPP: Farnesyl-Pyrophosphate

GFP: Green Fluorescent Protein

GPP: Geranylpyrophosphate

HDL: High-Density Lipoprotein

HER2: Human Epidermal Growth Factor Receptor 2

HMG-CoA: 3-Hydroxy-3-Methyl-Glutaryl-CoA

HSC: Hematopoietic Stem Cell

IBC: Inflammatory Breast Cancer

IMRT: Intensity-Modulated Radiation Therapy

LDL: Low-Density Lipoproteins

LRR: Local Regional Recurrence

MiRNAs: MicroRNAs

MSCs: Mesenchymal Stem Cells

OS: Overall Survival

PFS: Progression-Free Survival

PR: Progesterone Receptor

RPPA: Reverse-Phase Protein Assay

SREBP: Sterol Regulatory Element-Binding Protein 1

TAMs: Tumor Associated Macrophages

TNBC: Triple-Negative Breast Cancer

VLDL: Very Low-Density Lipoproteins

Chapter I
Introduction

1.1 Brief History of Breast Cancer

Breast cancer, in ancient Greece, was believed to be caused by dark and mysterious “black bile” circulating in the blood. The treatment of breast cancer in the Middle Ages was gruesome, including the usage of bloodletting, sulfur, and arsenic which did more harm than any good. It wasn’t until the turn of the 19th century that the idea of “transformed” normal cells being the cause of breast cancer took hold. The famous surgeon William Halsted in the late 1800s revolutionized the treatment of breast cancer, submitting the hypothesis that malignant breast cancer spread outward by invasion from the original tumor mass and therefore only “radical” mastectomy could hope to cure the patient. This surgery involved the surgical removal of the entire breast tissue, pectoralis major and minor muscles, and lymph nodes of the axilla. This surgery left women disfigured and the surgery only provided a 20-year survival rate of 50%.¹ It wasn’t until the 1970s that clinical trials showed that less radical surgeries had the same survivorship rates.

During the time of Halsted’s radical mastectomy, Wilhelm Conrad Röntgen discovered the X-ray for which he received the first Nobel Prize in physics.² Emil Grubbe was still in medical school remarkably when he first used X-rays to treat a woman with breast cancer in 1896. Marie Curie, the first woman to win the Nobel Prize, discovered two new elements, polonium and radium, which would become to be widely used in the early 1900s for neoplasms including breast cancer. Radium was replaced with cobalt therapy and caesium units in the mid-1900s.² Now the majority of breast cancers are treated with 3-D conformal therapy utilizing both photons and electrons. The use of intensity-modulated radiation therapy (IMRT) and protons are also being researched for their potential use in breast cancer.

At the end of World War II, sailors coming home exposed to mustard gas during the war were discovered to have toxic effects on their bone marrow. Thus, the era of chemotherapy began with the use of nitrogen mustard to treat lymphoma.³ In the 1950s in Boston, Sidney Farber showed folic acid compounds could cause remissions in children with acute leukemia. Clinicians Emil Frierech and Emil Frei introduced the idea, albeit to the horror of the medical community, of combination chemotherapies which sent children with leukemia to near-death but had the intended results of long-term remissions in children with acute lymphoblastic leukemia (ALL).³ From that point in history several classes of chemotherapies were discovered and tailored to breast cancer patients including drugs still used today including, doxorubicin, cyclophosphamide, and taxanes.

The last class of drugs used for breast cancer is hormonal therapy. At the turn of the 20th century Thomas Beatson in England discovered that performing an oophorectomy in women with advanced breast cancer prolonged their lives.⁴ His discovery revealed that the ovarian produced hormone, estrogen, had a pro-tumor effect on breast cancer. This same phenomenon was later shown 50 years later in prostate cancer by the testicular produced hormone, testosterone. Today, a drug that blocks the binding of estrogen to its receptor, Tamoxifen, is standard of care for all estrogen receptor (ER) positive breast cancer patients.⁴

All of these discoveries bring us to where we are today in the treatment of breast cancer. The three headed arsenal of surgery, radiation, and chemotherapy has given what was once thought impossible to breast cancer patients, a cure. Unlike some of the other stubborn cancers, such as pancreatic cancer, breast cancer death rates have plummeted over the past 20 years. The remaining battle in breast cancer is against what we in the field have labeled “aggressive breast cancers.”

1.2 Aggressive breast cancers

Aggressive breast cancers fall into two non-mutually exclusive classifications. The first is triple-negative breast cancer (TNBC), and the second being inflammatory breast cancer (IBC). TNBC is distinguished due to its lacking histologically of progesterone receptor (PR), ER, nor overexpression of human epidermal growth factor receptor 2 (HER2/neu). Between 12-15% of breast cancers in the United States annually will be of the TNBC subtype. TNBC patients have poor prognostic factors including disease-free survival (DFS) and overall survival (OS). More frequently compared to the other subtypes, TNBC occurs in younger women (<45) and African American women.⁵ Strikingly, 75% of TNBC are “basal-like”.⁶ Some often interchange the two. Basal-like tumors are higher grade and more aggressive.⁷ TNBC tumors have shortened disease free interval in the adjuvant and neoadjuvant setting and act more aggressively in the metastatic setting.⁸ They are highly resistant to chemotherapies and have a higher propensity to metastasize to the brain compared with luminal subtypes.⁹ A major viewpoint in the field is that the basal subtype of breast cancer represents a more undifferentiated stem cell like population compared to the luminal subtype. Cancer stem cells (CSCs) are known to be resistant to chemotherapy and radiation, initiate metastasis, and repopulate tumors after more differentiated cells are eliminated.¹⁰ The strong correlation between TNBC and the basal subtype leads to the speculation that TNBC contains a larger stem-cell like population compared to non TNBC thus leading to its aggressiveness.

IBC is the second class of aggressive breast cancer. The term inflammatory was added to the name because of the striking sudden appearance of an inflammatory like reaction of the breast that doctors even today misdiagnosis as mastitis. IBC comprises approximately 5% of all breast cancer cases but accounts for 10% of breast cancer mortalities.¹¹ IBC presents rapidly with the development of skin symptoms, including redness and skin edema identified by

prominent dermal hair follicles (peau d'orange), instead of as a mass detected by palpation or mammography. In IBC, the affected breast is often swollen, and nipple retraction is also common.¹² The percentage of IBC patients with TNBC is higher than non-IBC patients which suggest there is some overlap between these types of aggressive types of breast cancer. Like TNBC, IBC is found to be enriched in cancer stem cell signatures.¹³ The key to understanding the biology of these aggressive breast cancers and developing better treatment options might well in fact be found in the well-known observation that obese women are statistically more likely to develop not just breast cancer, but aggressive breast cancers such as TNBC and IBC.^{14,15}

1.3 Role of Cholesterol in Aggressive Breast Cancer

Western women are five times more likely than women in the developing world to develop breast cancer.¹⁶ This is most likely due to western diets considering women that migrate to the U.S. from the developing world increase their rate of breast cancer to the rate of U.S. women.¹⁷ Western diets contain high amounts of fats and cholesterol. Is there a connection between dietary cholesterol and breast cancer? Several clinical and pre-clinical studies lead us to believe that indeed there is.

In patient data, obesity increases the risk of post-menopausal ER positive breast cancer by 50%.¹⁴ Cholesterol was shown to be an independent risk factor of breast cancer.¹⁸ Post-menopausal women with the top quartile of cholesterol ingestion had a 50% increase risk of breast cancer.¹⁹ Llevarias et al in a set of in vivo experiments showed a cholesterol-rich diet exacerbates breast cancer progression and metastasis. PyMT female mice were fed a cholesterol-rich diet or regular chow diet for 12 weeks. The mice that received the cholesterol-rich diet had almost twice the amount of tumors as the regular diet mice.²⁰ More importantly the

tumors that developed in the cholesterol heavy diet were poorly differentiated and of higher histological grade with more angiogenesis. These mice developed more lung metastasis as well.²⁰ Nelson and colleagues set out to determine the mechanism by which elevated cholesterol is associated with increased breast cancer risk. Using the PyMT breast cancer model they showed that a byproduct of cholesterol, 27-hydroxycholesterol, acted much like estrogen to enhance breast cancer growth in vivo. The aggressiveness of the tumors was directly correlated with the expression of the enzyme that makes this metabolite of cholesterol.²¹ While these studies showed that cholesterol promoted ER⁺ tumor growth, we are more interested in how cholesterol affects the more aggressive breast cancers.

One of the only studies to focus on the differences of cholesterol metabolism in IBC vs non-IBC was performed by Martin et al. They found both non-IBC and IBC cells had increased cholesterol content compared with normal mammary epithelial cells. Importantly, IBC cells retained high cholesterol stores in the presence of a lipid-deficient environment, while the non-IBC cells decreased their lipid and cholesterol content in this same environment.²² They proposed breast cancer cells would migrate when they no longer could obtain extracellular cholesterol. What we found important from this study was that IBC cells had the ability to produce *de novo* cholesterol in the face of depleted cholesterol environments. The rate-limiting step in *de novo* cholesterol synthesis is the enzyme 3-hydroxy-3-methyl-glutaryl-CoA (HMG-CoA) reductase.²³ The inhibition of this enzyme has been utilized for cardiovascular disease for decades. This class of drugs, statins, is now being studied for their use in cancers including breast cancer.

1.4 Statins and Breast Cancer

Statins lower serum cholesterol and are effective therapies for patients with hypercholesterolemia. Because of the association of obesity and high cholesterol diets with breast cancer, statins have been studied for the correlation with incidence of breast cancer. There are conflicting evidence of statin use and breast cancer incidence, however; the majority of evidence support that statins can reduce breast cancer incidence and improve outcomes. A Danish study comparing local recurrence rates for stage I-III breast cancer between simvastatin users and nonusers showed a significant reduction in recurrence rates in the statin users after 10 years of follow-up.²⁴ Evidence from other cohort studies suggests that overall disease-free survival is improved in patients on statin therapy at the time of cancer diagnosis.²⁵ The pre-clinical data is massively extensive supporting statins as inhibitors of breast cancer. The anti-breast tumor effects have centered on the ability of statins to reduce the concentrations of the downstream molecule of HMG-CoA reductase, mevalonate. Mevalonate is a major precursor for several important cell processes including dolichol, geranylpyrophosphate (GPP), farnesylpyrophosphate (FPP).²⁶ GPP and FPP are critical for isoprenylation of G-proteins Ras and Rho, which are important in breast cancer proliferation, apoptosis, and motility.²⁷ Statins were shown to block cell-cycle progression in breast cancer by upregulating cell cycle inhibitors p27 and p21.²⁸ Statins can inhibit metalloproteinases,²⁹ decrease VEGF secretion from endothelial cells²⁵⁻²⁷,^{30,31} and induce proapoptotic protein expression, Bax and Bim.²⁸

In addition to their general anti-tumor effects in breast cancer, statins have been shown to target breast CSCs. Ginestier et al found CSCs were enriched in the mevalonate metabolic pathway. Using statins they showed a reduction in CSC formation through inactivation of RhoA and accumulation of p27 in the nucleus.³² The proposed importance of CSCs and the aggressiveness of breast cancer underscore the value of statin therapies in the clinic. Interestingly, in a retrospective analysis of 723 IBC patients from MD Anderson Cancer Center,

treatment with a hydrophilic statin was associated with significantly longer progression-free survival (PFS) than no statin.³³ Our lab showed that statins could be a good therapeutic option for IBC patients treated with radiation. The use of statins in a 519 IBC patient cohort reduced local regional recurrence (LRR) by 50% following radiotherapy. Multivariate analysis demonstrated an association of reduced local recurrence rates with statin use.³⁴ Simvastatin radiosensitized both TNBC non-IBC and IBC cells in vitro as well.

Statins are not the only way to lower serum cholesterol levels. To fully understand cholesterol metabolism, we need to understand the molecules that transport cholesterol from the point of ingestion to periphery tissues and back for storage in the liver. These proteins are named lipoproteins.

1.5 Lipoproteins and Breast Cancer

In the liver free cholesterol is packaged along with triglycerides and apolipoprotein B into very low-density lipoproteins (VLDL) and secreted into the blood. The resulting VLDL is further processed by hepatic lipase yielding low-density lipoproteins (LDL). LDL transports the cholesterol to the periphery tissue. LDL binds to the LDL receptor and is internalized by the periphery cells. Inside the periphery cells cholesterol concentrations are monitored by the sterol regulatory element-binding protein 1 (SREBP) which regulate genes that modulate intracellular cholesterol including ATP-binding cassette A1 (ABCA1) and ABCG1 transporters and miR-33. Cholesterol is effluxed out of the cell through the ABCA1 and ABCG1 transporters to apolipoprotein A which forms a mature high density lipoprotein (HDL). HDL then transports cholesterol back to the liver where it is stored or excreted.³⁵⁻³⁸ The concentrations of lipoproteins can have positive or negative effects depending on which lipoprotein is elevated. Increased LDL and VLDL are known to cause increased atherosclerosis and HDL the reverse.

One of the beneficial effects of statins is that they lower circulating LDL and increase circulating HDL.³⁹

While statins have been extensively looked at in breast cancer, lipoproteins have not been. One study have found low levels of HDL was associated with breast cancer risk.⁴⁰ The link between LDL and breast cancer has been both prognostic and non-significant.⁴¹ This suggests that lipoproteins might not have an effect on all subtypes of breast cancer. There have been limited studies to date looking at specifically in regards to either TNBC or IBC how lipoproteins effects breast cancer treatment resistance.

1.6 Breast Cancer Stem Cells

Normal stem cells are defined by three characteristics: self-renewal, differentiation into multiple lineages, and long lived proliferative potential. In the past 15 years, the identification of a small population of cells within solid tumors that closely parallels normal stem cell properties were identified and termed “cancer stem cells”.⁴² The first studies showed that there are biologically distinct “tumor-initiating” cells of the breast⁴³, brain⁴⁴, and hematological system^{45,46} that when orthotopically transplanted into immunocompromised mice regenerate solid tumors with neoplastic cells that demonstrate cellular heterogeneity. More recently, several studies of normal mammary gland stem cells have highlighted potential limitations of transplantation and called into question the use of this assay as the gold standard for demonstrating stem cell potential.⁴⁷⁻⁴⁹ However reviewing the sum of both approaches, Visvader and Stingl suggest transplantation may unleash a breadth of potential that in vivo is truly only seen at specific moments in development.⁵⁰ It is proposed that these cells in cancers mediate recurrence both through their ability to repopulate the tumor with cellular heterogeneity and through innate survival mechanisms to resist therapy. Since CSCs are important in resistance to

chemotherapy and radiation, drugs that can target CSCs will be of great importance in aggressive breast cancers.

1.7 The IBC Microenvironment

The study of IBC would be incomplete without understanding how the microenvironment influences and supports IBC. IBC presents uniquely with rapid onset of breast swelling and erythema, but is virtually indistinguishable from non-IBC at the pathologic and molecular level.⁵¹⁻⁵³ One difference was discussed earlier; IBC cells have a unique ability to regulate intracellular cholesterol which is vital for its growth and invasion.²² Understanding how the IBC microenvironment influences IBC incidence and progression will lead us to improving the outcomes in IBC patients. But first we need to review the important players in the microenvironment.

The hematopoietic stem cell (HSC) niche has been elucidated. The HSC niche is organized around a collection of normal and malignant cells in the bone marrow that coordinate between direct cell contact, hypoxia, and secreted factors.⁵⁴ A crucial player in the HSC niche is the nestin⁺ mesenchymal stem cell (MSC). In the niche, macrophages support the maintenance of MSCs.⁵⁴ There seems to be a symbiotic relationship between MSCs and macrophages that were highlighted by mouse studies showing macrophage depletion lead to the elimination of the HSC niche.⁵⁵ There is no current evidence of a similar IBC stem cell niche. However, we believe the current evidence supports the idea of a similar situation happening in IBC environment.

MSCs promoted IBC stem cells and in vivo tumor growth.⁵⁶ Our group further showed that MSCs could promote the IBC phenotype in vivo. Injecting MSCs with IBC cells into the mammary fat pad led to the hallmark pathological and skin erythema found in patients.⁵⁷ These

results suggest MSCs have a unique role in IBC promotion, but we do not yet know if macrophages also play a role similar like in the HSC stem cell niche. Macrophages infiltrating the breast tumor, or tumor associated macrophages (TAMs), demonstrated a negative correlation with breast cancer outcome.⁵⁸ TAMs have been shown in vivo to promote lymphatic emboli, the hallmark of IBC.⁵⁹ The state and plasticity of macrophages (tumor or normal adjacent) in IBC patients and models has not been examined nor has their interaction with other cell types in the IBC stroma been examined. Lack of such knowledge is important because these cells are potentially mediators of field effects that lead to the clinical characteristics of IBC, and targets for prevention and treatment of IBC.

1.8 Conclusions

This introductory chapter described the status of present day breast cancer treatment and the subtypes of breast cancer that still provide poor survival outcomes. Cholesterol was shown to be critical for the aggressiveness in breast cancers. The possible mechanisms through which cholesterol can impact breast cancer growth and metastasis was discussed. Also, the patient data was reviewed to show the relationship between high cholesterol diet and breast cancer incidence and outcomes. Next the statin data on breast cancer was discussed. Statins inhibit de novo cholesterol synthesis and several studies have shown their anti-tumor effect in breast cancer. Our group showed in IBC, statin users had better outcomes and statins radiosensitized IBC cells in vitro. The transporters of cholesterol, lipoproteins, were examined next. HDL, VLDL, and LDL mediate plasma and cellular cholesterol concentrations and studies suggest HDL might have a protective role in breast cancer. Breast CSCs are thought to be a driving force in aggressive breast cancers. A brief overview of the theory of CSCs was presented. Lastly, the IBC microenvironment was discussed. The lack of molecular differences between IBC and non IBC suggest something inherent in the normal breast is driving this aggressive phenotype. We

presented two stromal cells, macrophages and MSCs, that we believe play an important role in IBC.

1.9 Conceptual Framework and Hypothesis

The main goals of this thesis include challenging the current belief that the effects of statins in breast cancer are cholesterol independent inhibition of GPP and Ras prenylation. The concentrations of statins being used in existing studies might be too high to be relevant in patients. The inhibition of Ras, Rho, and Rap prenylation by statins requires a concentration as high as 50 μM . However, therapeutic levels of statins (50 nM to 3 μM) do not.⁶⁰ So the first aim of this thesis will be to study how a therapeutic concentration of a statin impacts TNBC metastases. Next, targeting cholesterol metabolism is an exciting proposition for aggressive breast cancer. Cancer cells require cholesterol for sustained proliferation and oncogenic signaling. Upsetting the tumor cell's ability to acquire and maintain cholesterol is a possible preventive and therapeutic strategy. Because radiation is a key component to aggressive breast cancer care, the second and third aims will focus on how disturbing cholesterol concentrations through lipoproteins changes radiation sensitivity. The final aim will look to understand how the tumor microenvironment plays a significant role in IBC and if statins can disrupt this IBC environment.

To summarize the entirety of my thesis, the central hypothesis is reductions in intracellular cholesterol content by statins or HDL inhibits downstream signaling regulating metastasis and radiation response, altering cellular functions in cancer cells and immune cells. To test this hypothesis I investigated specific aims:

1. To demonstrate that statins reduce the incidence of breast cancer metastasis in vivo and characterize relative mechanistic signaling:
 - a. Characterize in vitro and in vivo effects on metastasis of physiologic concentration of statins in aggressive breast cancer models
 - b. Investigate mechanistic signaling pathways involved in statins in aggressive breast cancer
2. To characterize changes in IBC cellular cholesterol through lipoprotein treatment alters self-renewal capacity and radiation sensitivity.
 - a. Characterize the effects of lipoproteins on in vitro stem cells and radiation response
 - b. Demonstrate lipoprotein effects on signaling pathways
3. To establish that differences in miR-33a expression in breast cancer cell line lines correlates to their radiation sensitivity to the exposure to HDL in vitro.
 - a. Manipulate the expression of miR-33 expression in high and low expressing breast cancer cell lines
 - b. Demonstrate radiation sensitivity in the presence or absence of HDL.
4. Demonstrate MSCs and Macrophages cross talk through cytokines to promote the Inflammatory Breast Cancer phenotype and can be inhibited by statins
 - a. To demonstrate tumor promoting macrophages change the MSC cytokine and migration potential (“educated MSCs”)
 - b. To elucidate if macrophage educated MSCs increase IBC invasion and sphere formation
 - c. To characterize that statins block the MSC promotion of the IBC phenotype

Chapter II

**Simvastatin prevents triple-negative breast cancer metastasis in pre-clinical models
through regulation of FOXO3a**

2.1 ABSTRACT

Purpose: Statins are being explored for their potential use in prevention of breast cancer. The purpose of our study was to examine the effect of statins on triple negative breast cancer (TNBC) cells metastatic potential.

Experimental Design: TNBC cells were treated with simvastatin and then studied for cell cycle progression and proliferation *in vitro*, and metastasis formation *in vivo*, following injection of statin-treated cells. Reverse-phase protein assay (RPPA) analysis was performed on statin-treated and control breast cancer cells. RNA interference targeting *FOXO3a* was used to measure the impact of simvastatin on FOXO3a-deficient SUM149 cells. The prognostic value of *FOXO3a* mRNA expression was examined in 8 public breast cancer gene expression data sets including 1,479 patients.

Results: Simvastatin increased G1/S phase arrest of the cell cycle and inhibited both proliferation and migration of TNBC cells *in vitro*. *In vivo*, pretreatment with simvastatin reduced metastases formation in both orthotopic-injection (p=0.017) and tail-vein-injection models (p=0.04). Phosphorylated FOXO3a was downregulated after simvastatin treatment in (RPPA) analysis. Ectopic expression of *FOXO3a* in low-expressing SUM159 cells enhanced mammosphere formation (p=0.005) and migratory capacity (p=0.14) *in vitro*. Consistently, knockdown of *FOXO3a* in high-expressing SUM149 cells attenuated the effect of simvastatin on mammosphere formation and migration. Furthermore, tumor *FOXO3A* mRNA downregulation was independently associated with shorter metastasis-free survival in all breast cancers, as well as in TNBC breast cancers.

Conclusions: Simvastatin can inhibit breast cancer cell metastasis *in vivo*, and is dependent on FOXO3a activation. Furthermore, high *FOXO3a* levels in patients predicted for longer distant free metastasis survival.

2.2 Introduction

Metastasis is the most common cause of death among women with breast cancer. Triple-negative breast cancer (TNBC) comprises 15% of breast cancers and has the poorest survival outcome of all breast cancer subtypes due to the high propensity for metastatic progression⁶¹ and absence of specific targeted treatments. Breast cancer metastases develop from dissemination of primary tumor cells into distant organs. The primary tumor cells most likely to metastasize are hypothesized to be cancer stem cells (CSCs). CSCs have unlimited self-renewal potential, can generate non-CSC progeny, are resistant to conventional therapies, and are capable of migration^{10,62}. In xenograft models of breast cancer, breast CSCs (i.e., cells expressing CD44) displayed increased metastasis compared to CD44⁻ breast cancer cells^{63,64}.

Recently, Ginestier et al. showed statins (3-hydroxy-3-methyl glutaryl coenzyme A reductase inhibitors) regulate breast CSCs through inhibition of RhoA³². Statins are widely used to reduce cholesterol and lipoprotein levels and thereby reduce mortality from cardiovascular disease; recently, statins have also been studied for their impact on cancer. A Danish study comparing local recurrence rates for stage I-III breast cancer between simvastatin users and nonusers showed a significant reduction in recurrence rates in the statin users after 10 years of follow-up²⁴. We showed previously that simvastatin radiosensitized triple negative cell lines in vitro⁶⁵. Statins have also been shown to have clinical benefits in lung, prostate, and colon cancer⁶⁶⁻⁶⁸. The mechanisms underlying the antitumor effects of statins have been studied extensively. Statins decrease EGFR dimerization⁶⁹, increase inducible reactive nitric oxide level⁷⁰, reduce metalloproteinase levels²⁹, decrease synthesis of inflammatory cytokines⁷¹, and reduced VEGF secretion in breast cancer models⁷². Statins effect on metastasis and its underlying mechanisms are unknown.

Herein we determined the effect of statins specifically on TNBC metastasis and observed inhibition of metastasis by statins. Further, we identified FOXO3a as a potential mediator of TNBC metastasis using in vitro and in vivo models, and show that statin therapy regulates FOXO3a activation, suggesting a potential mechanism for simvastatin's anti-metastatic effects.

2.3 Materials and Methods

Cell Culture and Drugs. SUM149 and SUM159 breast cancer cells were obtained from Asterand (Detroit, MI) and passaged in the laboratory for fewer than 6 months after receipt. Both types of cells were cultured in Ham's F12 medium supplemented with 10% fetal bovine serum, 1 $\mu\text{g}/\text{mL}$ hydrocortisone, 5 $\mu\text{g}/\text{mL}$ insulin, and 1% antibiotic-antimycotic. MDA-231 cells were obtained from ATCC and were cultured in α -media supplemented with 10% FBS, 1 $\mu\text{g}/\text{ml}$ hydrocortisone, 1 $\mu\text{g}/\text{ml}$ insulin, 12.5 ng/ml epidermal growth factor, sodium pyruvate, nonessential amino acids, 2 mM glutamine, and 1% antibiotic-antimycotic. Simvastatin (Sigma) was dissolved in DMSO at a stock concentration of 5 mM and stored at -80°C , and a final concentration of 2.5 μM was used in this study. DMSO alone was used as a control.

Mammosphere Formation Assay. Mammosphere formation has been used as a measure of the self-renewal capacity of breast CSCs and correlates closely with tumorigenicity⁷³. Treated and control cells were grown in standard mammosphere medium (serum-free, growth-factor-enriched medium) in low attachment plates at a concentration of 20,000 cells/mL. For secondary mammosphere assay, cells from primary mammospheres were dispersed with 0.05% trypsin, seeded in ultra-low attachment plates (20,000 cells/mL) in mammosphere medium, incubated for 7 days, and counted.

Aldefluor Assay. To further investigate the self-renewal capacity of cells, we used the Aldefluor assay following the manufacturer's guidelines (StemCell Technologies, Vancouver, Canada). Briefly, 5×10^5 cells were suspended in Aldefluor assay buffer containing ALDH substrate and incubated for 30 min at 37°C. As a negative control for each sample, cells were incubated with 50 mmol/L specific ALDH inhibitor diethylamino benzaldehyde (DEAB). Aldefluor fluorescence was excited at 488 nm, and fluorescence emission was detected using a Beckman Coulter machine. The data files were analyzed using FlowJo software (Treestar, Ashland, OR). For sorting, gates were established using ALDH-stained cells treated with DEAB as negative controls and taking the high negative and positive cells.

Cell Cycle Distribution and Cell Proliferation Assays. For assessment of cell cycle distribution, cells were fixed dropwise with 70% ice-cold ethanol overnight at 4°C. Then cells were suspended in 100 μ L of phosphate-citrate buffer (0.19 M Na_2HPO_4 , 4 mM citric acid), incubated for 30 min at room temperature, and resuspended in PBS containing 10 μ g/mL propidium iodide and 10 μ g/mL RNase A. The propidium iodide-stained cell samples were analyzed using FACSCalibur (Becton-Dickinson, San Jose, CA), and the percentage of cells in each phase of the cell cycle (G1, S, and G2/M) was analyzed with CELLQuest (Becton-Dickinson). For proliferation assay, pre-treated or DMSO treated cells were seeded at a density of 1.0×10^4 in 6 cm plates. After the specified number of days (24h-8 days), cells were trypsinized and viable cells counted with a Cellometer automated cell counter.

Migration assays. Cellular migration assays were performed using a Boyden chamber containing 24-well Transwell plates (Corning Inc.) with 8- μ m pores on the membrane. All experiments were performed in duplicate and repeated three times. Approximately 5×10^4 cells in 200 μ L culture medium supplemented with 10% FBS were seeded into the upper chamber. The lower chamber was filled with 500 μ L complete medium (with 10% FBS) as a

chemoattractant plus or minus simvastatin. After 24 hours of incubation at 37°C in a 5% CO₂ atmosphere, the membranes containing the cells were fixed and stained with crystal violet. The lower surfaces of the membranes were photographed at × 100 magnification. Five random fields were photographed for each chamber to determine the migration.

In Vivo Studies. Four-week-old female SCID/Beige mice (Harlan, USA) were housed and used in accordance with guidelines of The University of Texas MD Anderson Cancer Center under an Institutional Animal Care and Use Committee-approved protocol (ACUF 07-08-07213). Mice were anesthetized through intraperitoneal injection of a cocktail containing ketamine (100 mg/kg), xylazine (2.5 mg/kg), and acepromazine (2.5 mg/kg) in sterile saline solution, and fur at the surgical site was removed. The number-4 inguinal glands were cleared of mammary epithelium, and green fluorescent protein (GFP)-luciferin-labeled control SUM149 cells and simvastatin (1.25 μM)-treated GFP-luciferin-labeled SUM149 cells (8.0×10^5 in 15 μL of PBS) were injected into the cleared fat pads. Transplants were allowed to grow until tumors reached a volume of 500 mm³. Tumor growth was monitored weekly with caliper measurements. Tumors were resected under the above-mentioned institutional guidelines. A portion of each tumor was formalin-fixed, paraffin-embedded, sectioned, and stained with hematoxylin and eosin. After tumor resection, mice were injected weekly with D-luciferin (Biosynth) and imaged weekly for metastasis for 6 weeks after resection. Portions of xenografts were formalin-fixed, paraffin-embedded, sectioned, stained with hematoxylin and eosin, and used for immunofluorescence staining to detect FOXO3a.

To further investigate in vivo metastasis, we used a tail-vein-injection metastasis model. GFP-labeled SUM149 cells were treated with simvastatin (1.25 μM) in vitro. Twenty-four hours later, 1.0×10^6 GFP-labeled simvastatin-treated or DMSO-treated (control) SUM149 cells were injected via tail vein into 4-week-old female SCID/Beige mice. Mice were euthanized 8 weeks

after injection, and lung and brain metastatic colonization were assessed by fluorescent stereomicroscopy. All staining studies were performed with standard protocols, and staining was analyzed by a pathologist specializing in breast cancer.

RPPA Analysis. Cellular proteins were denatured by 1% SDS (with beta-mercaptoethanol) and diluted in five 2-fold serial dilutions in dilution buffer (lysis buffer containing 1% SDS). Serial diluted lysates were arrayed on nitrocellulose-coated slides (Grace Biolab) by Aushon 2470 Arrayer (Aushon BioSystems). Total 5808 array spots were arranged on each slide including the spots corresponding to positive and negative controls prepared from mixed cell lysates or dilution buffer, respectively. Each slide was probed with a validated primary antibody plus a biotin-conjugated secondary antibody. All sample analysis was performed at the MD Anderson RPPA Core Facility.

Immunoblotting and immunofluorescence. For immunoblotting, cells were lysed in 1x RIPA lysis buffer containing 1 μ M PMSF, and 40 μ g of protein was electrophoresed on SDS-polyacrylamide gels with a concentration gradient of 4% to 20% (Invitrogen). Membranes were incubated with primary antibodies, anti-FOXO3a, anti-phosphoFOXO3a (Ser253), anti-CDKN1B^{kip1} (Cell Signaling Technology). Actin antibody was used as a loading control. For immunofluorescence, xenograft tissue slides were incubated with heated Citrate buffer for antigen retrieval. Primary antibody FOXO3a (Cell Signaling) was added overnight at 4C. Slides were incubated with GFP labeled anti-rabbit secondary antibodies. The slides were viewed with a fluorescent microscopy following DAPI staining (Nikon).

FOXO3a Knockdown and overexpression. SignalSilence siRNA targeting FOXO3a and nontargeting siRNA were purchased from Cell Signaling. SUM149 cells (100,000/dish) were plated on 35 mm dishes. The following day, the cells were transfected with the siRNAs using XtremeGENE siRNA Transfection Reagent (Roche) according to the manufacturer's protocol. 48

hours after transfection, cells were washed collected for analysis of FOXO3a levels by western blotting and assayed for migration and mammosphere formation. Stable overexpression of FOXO3a in SUM159 cell line was conducted using overexpression plasmids purchased from Systems Biosciences according to the manufacturer's instruction. Briefly, overexpression FOXO3a plasmids were packaged along with plasmids pRSV-Rev, pMDLg-pRRE and pCMV-VSVG in 293T cells. Cell lines were then transduced as we described previously⁵⁶.

Gene expression data analysis. We analyzed *FOXO3A* mRNA expression in clinical samples in 8 public gene expression data sets selected as follows: pre-treatment sample of primary breast cancer, with at least one probe set representing *FOXO3A*, and with the following clinicopathological annotations (pathological axillary lymph node status pN, tumor size pT, and grade, and follow-up in term of metastatic relapse). Data sets were collected from the National Center for Biotechnology Information (NCBI)/Genbank GEO and ArrayExpress databases, and authors' website (1). The final pooled data set included 1,479 non-metastatic, invasive breast cancers. Their clinicopathological characteristics are summarized in (Table 2). Data analysis required pre-analytic processing. First, we normalized each data set separately using quantile normalization for the available processed data from the Agilent-based sets, and Robust Multichip Average (RMA)⁷⁴ with the non-parametric quantile algorithm for the raw data from the Affymetrix-based data sets. Normalization was done in R using Bioconductor and associated packages. Hybridization probes were then mapped across the different technological platforms. We used SOURCE (<http://smd.stanford.edu/cgi-bin/source/sourceSearch>) and EntrezGene (Homo sapiens gene information db, release from 09/12/2008, <ftp://ftp.ncbi.nlm.nih.gov/gene/>) to retrieve and update the Agilent annotations, and NetAffx Annotation files (www.affymetrix.com; release from 01/12/2008) to update the Affymetrix annotations. The probes were then mapped based on their

Reference	N° of samples	N° of analysed samples*	Technological platform	N° of probes	Source of data
van de Vijver et al., <i>N Engl J Med</i> 2002	254	254	Agilent Hu25k 60mer	25K	http://microarray-pubs.stanford.edu/wound_NKI/
van't Veer et al., <i>Nature</i> 2002	117	97	Agilent Hu25k 60mer	25K	http://www.rii.com/publications/2002/vantveer.html
Ivshina et al., <i>Cancer Res</i> 2006	448	243	Affymetrix U133 A+B	2x22K	GEO databaseGSE4922_1456
Sotiriou et al., <i>JNCI</i> 2006	80	73	Affymetrix U133 A	22K	GEO databaseGSE2990
Desmedt et al., <i>Clin Cancer Res</i> 2007	154	154	Affymetrix U133 A	22K	GEO databaseGSE7290
Merritt WM et al., <i>N Engl J Med</i> 2008	130	124	Affymetrix U133AAofAv2	23K	Array ExpressdatabaseE-MTAB-158
Schmidt M et al., <i>Cancer Res</i> 2008	200	200	Affymetrix U133A	22K	GEO databaseGSE11121
Sabatier et al., <i>PLoS ONE</i> 2011	352	334	AffymetrixU133 Plus 2.0	54K	GEO database GSE31448

* Only non-metastatic samples (M0)

Table 1: List of breast cancer gene expression data sets included in the analysis.

Characteristics	N (%)
Age, years	
<=50	657 (59%)
>50	463 (41%)
Pathological type *	
IDC	376 (78%)
ILC	35 (7%)
MIX	21 (4%)
other	48 (10%)
Pathological grade	
1	279 (19%)
2-3	1158 (81%)
Pathological axillary lymph node status, pN	
negative	866 (66%)
positive	443 (34%)
Pathological tumor size, pT	
pT1	607 (48%)
pT2-3	653 (52%)
ER status	
negative	403 (27%)
positive	1076 (73%)
PR status	
negative	632 (43%)
positive	847 (57%)
ERBB2 status	
negative	1313 (89%)
positive	166 (11%)
Metastatic relapse	
no	1069 (72%)
yes	410 (28%)
Median follow-up, months	93 (1-299)
5-year MFS [95CI]	77% [0.75-0.79]

* IDC, invasive ductal carcinoma; ILC, invasive lobular carcinoma; MIX, mixt

Table 2: Patients and tumor characteristics.

EntrezGeneID. When multiple probes mapped to the same GeneID, we retained the one with the highest variance in a particular dataset. To avoid biases related to immunohistochemistry (IHC) analyses across different institutions and thanks to the bimodal distribution of respective mRNA expression levels, estrogen receptor (ER), progesterone receptor (PR), and ERBB2 expressions (negative/positive) were defined at the mRNA level using gene expression data of *ESR1*, *PGR*, and *ERBB2* respectively, as previously described⁷⁵. Before analysis of *FOXO3A* expression, expression data were standardized within each data set as previously described⁷⁶. *FOXO3A* expression in tumors (T) was measured as discrete value after comparison with mean expression in normal breast samples (NB): downregulation, thereafter designated “down” was defined by a T/NB ratio ≤ 0.5 and no downregulation (“no down”) by a T/NB ratio > 0.5 .

Statistical Analysis. All data in graphs are presented as mean (standard deviation). For *in vitro* studies, all data are represented in graphs as means \pm SEM. A p-value inferior or equal to 0.05 in a paired two-sided test was considered statistically significant. For RPPA analysis, we used analysis-of-variance models to estimate 1) the overall effects of each treatment on each protein, and 2) the overall effects of all treatments combined on each protein. All treatment effects were computed using control as a reference. These results were averaged across all cell lines. Then the same analyses were repeated for each cell line, to determine which treatments worked the best for which cell line. Statistical analyses were conducted using SAS 9.4 for Windows (SAS Institute Inc., Cary, NC). Correlations between tumor groups and clinicopathological features were analyzed using the Fisher’s exact test. Metastasis-free survival (MFS) was calculated from the date of diagnosis until the date of distant relapse, and the follow-up was measured from the date of diagnosis to the date of last news for event-free patients. Survivals were calculated using the Kaplan-Meier method and curves were compared with the log-rank test. Univariate and multivariate survival analyses were done using Cox regression analysis (Wald test). Variables

tested in univariate analyses included patients' age at time of diagnosis (≤ 50 years vs > 50), pathological type, axillary lymph node status (pN: negative vs positive), tumor size (pT: pT1 vs pT2-3), and grade (1 vs 2-3), ER, PR and ERBB2 statuses, and *FOXO3A* expression-based group ("down" vs "no down"). Variables with a p-value < 0.05 in univariate analysis were tested in multivariate analysis. Statistical analysis was done using the survival package (version 2.37) in the R software (version 2.15.2; <http://www.cran.r-project.org/>). We followed the reporting REcommendations for tumor MARKer prognostic studies (REMARK criteria)⁷⁷. Results with P-values less than 0.05 were regarded as significant.

2.4 Results

Simvastatin Inhibits Breast Cancer Metastatic Related Endpoints *In Vitro*

We analyzed the effects of simvastatin on cell proliferation, cell cycle distribution, and cell migration in TNBC cell lines. After 24 hours of pre-treating of SUM149, SUM159, and MDA-231 cells with simvastatin, we observed a significant decrease in cell proliferation as early as 48 hours and as long as 8 days (**Figure 1A, B, C**). Simvastatin decreased the S-phase fraction and increased G1/S arrest in both SUM149 and SUM159 TNBC cell lines (**Figure 1D**). Next we used the Boyden chamber assay to measure migration of DMSO- or simvastatin-treated TNBC cell lines *in vitro*. Simvastatin treatment significantly reduced the number of SUM149 cells, SUM 159, and MDA-231 cells that migrated through the pores in the membrane (**Figure 1E**). The migratory ability of simvastatin pre-treated SUM149/SUM159 cells was rescued by co-treatment with mevalonate. These results demonstrate simvastatin inhibited surrogates of metastasis *in vitro* in multiple TNBC cell lines. As CSCs have been hypothesized as the metastatic initiating cells⁶², we used two *in vitro* stem cell surrogate assays to test for the effect of simvastatin on CSC properties. The mammosphere assay developed by Dontu et al for normal

mammary gland has been adapted for cancer cell lines as an assay that correlates to cancer cell self-renewal capacity. This has been validated in particular in triple negative breast cancer cell lines^{32,73}. Confirming the findings of Ginestier et al³², we found that primary sphere formation in TNBC cell lines SUM149 and SUM159 cells pretreated with simvastatin were reduced 78% and 75%, respectively, compared to DMSO-treated control cells ($p < 0.01$) (**Figure 2A, B**). The addition mevalonate (10 mM), the organic compound downstream of simvastatin inhibition, rescued mammosphere formation back to control levels. Similarly, secondary sphere formation was inhibited ($P < 0.01$) in simvastatin-treated cells compared to DMSO-treated cells for both cell lines. Moreover, the spheres were smaller in simvastatin-treated cells compared to DMSO-treated control cells (**Figure 2A, 2B**). The Aldefluor assay is an alternative surrogate assay to test for CSCs⁶³. We found that the proportions of ALDH-positive cells among simvastatin-treated SUM149 and SUM159 cells were 23% and 70%, respectively, relative to the proportions of ALDH-positive cells among DMSO-treated control cells ($P < 0.05$) (**Figure 2C, D**). The proportions of ALDH-positive cells were also rescued to the levels seen in DMSO-treated control cells after administration of mevalonate (**Figure 2C, D**). Thus, simvastatin reduced two independent in vitro surrogates for self-renewal capacity in TNBC cell lines through inhibition of the mevalonate pathway.

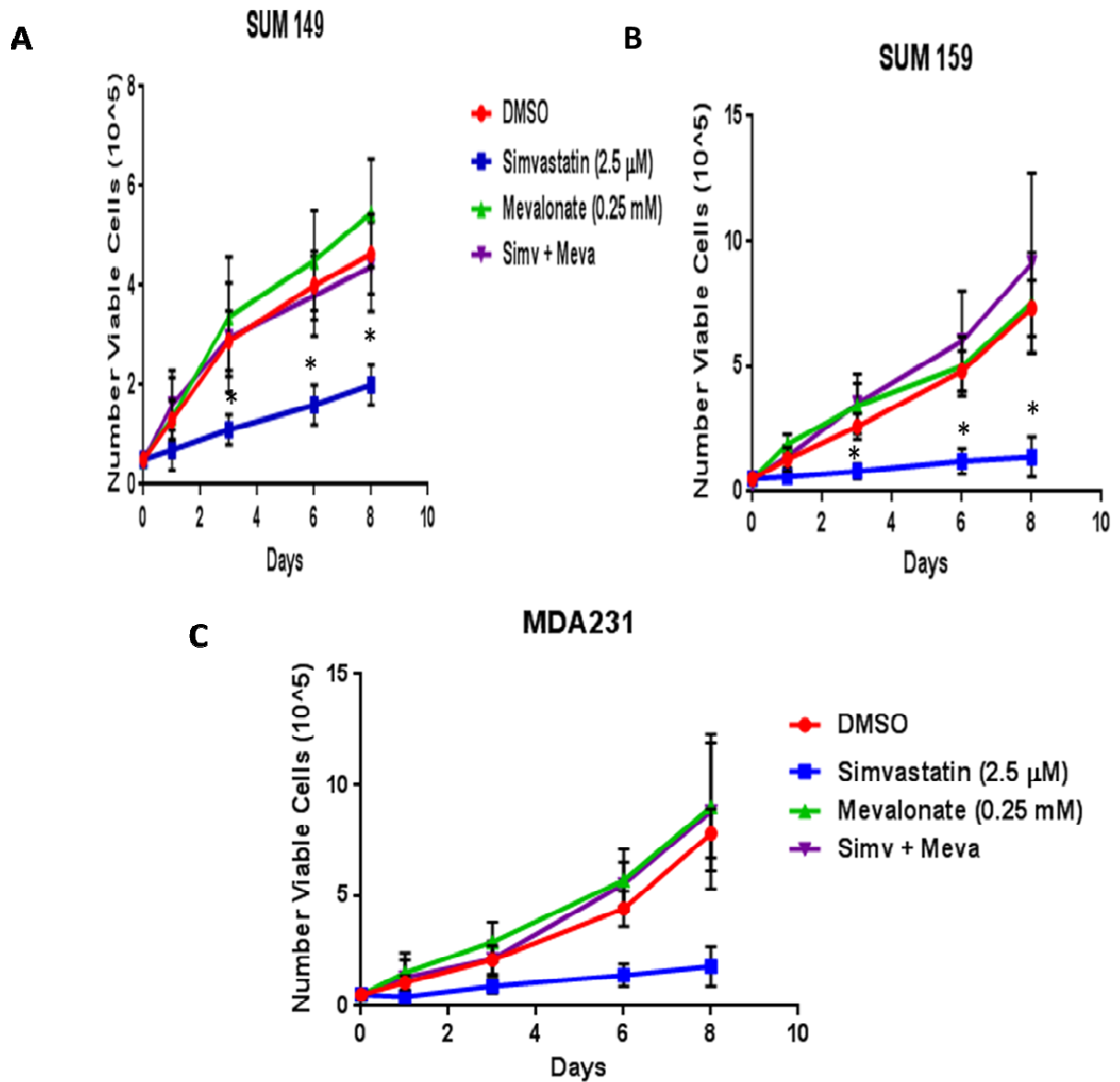


Figure 1. Simvastatin reduces percentage of cycling cells, proliferation, and migration.

Cell proliferation assay conducted to assess proliferation rates in (A) SUM149, (B) SUM159, or (C) MDA-231 cell populations pretreated for 24h with 2.5 μM simvastatin, 10 mM mevalonate, both, or vehicle (DMSO). *, P < 0.05 for unpaired 2-tailed Student's t-test (n = 3).

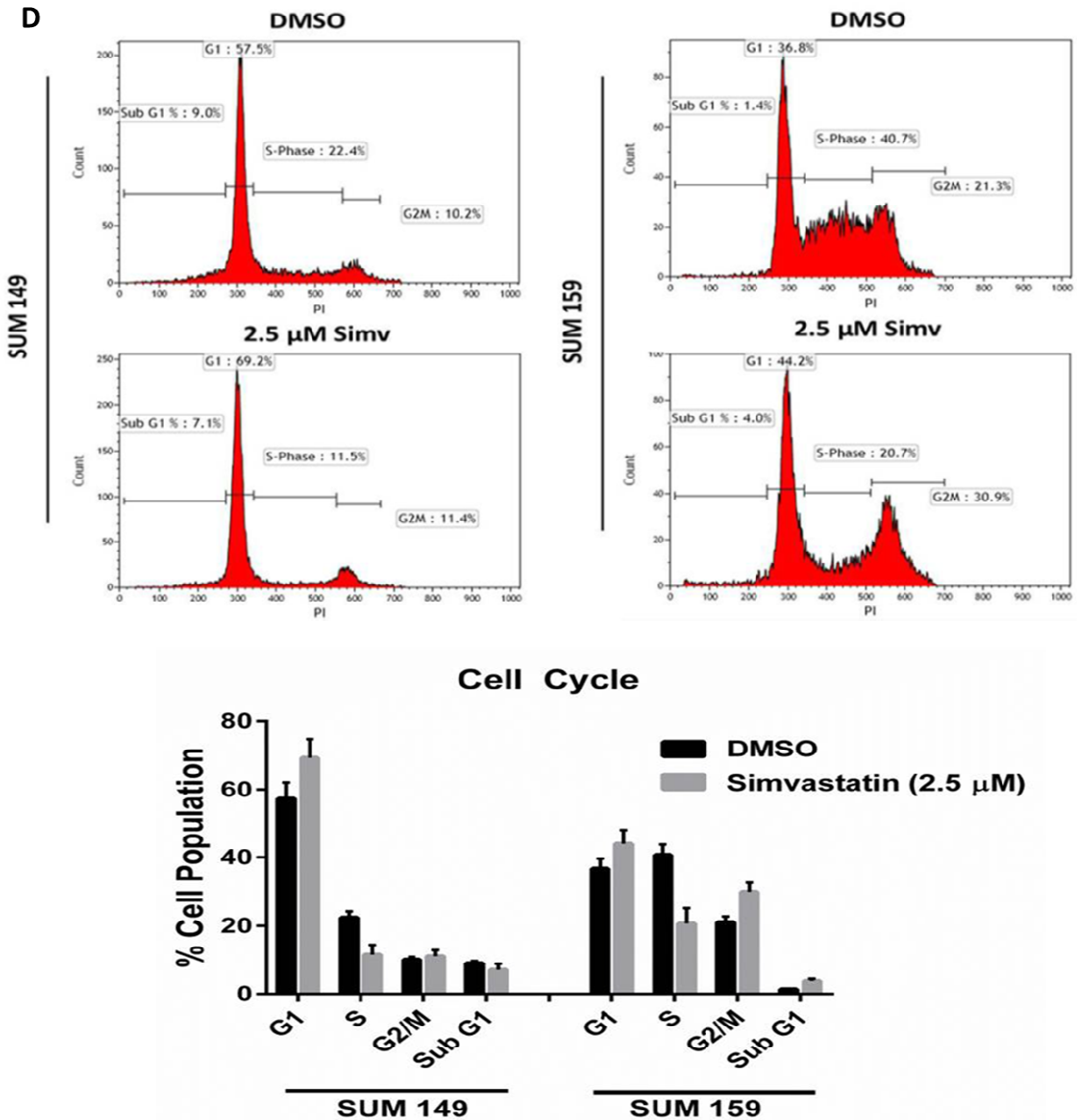


Figure 1. Simvastatin reduces percentage of cycling cells, proliferation, and migration. (D) SUM149 and SUM159 cells were profiled for their cell cycle pattern after they were pretreated 2.5 μ M simvastatin of vehicle for 24 hours and stained with PI. : *, $P < 0.05$ for unpaired 2-tailed Student's t-test ($n = 3$). Abbreviations: PI, propidium iodide.

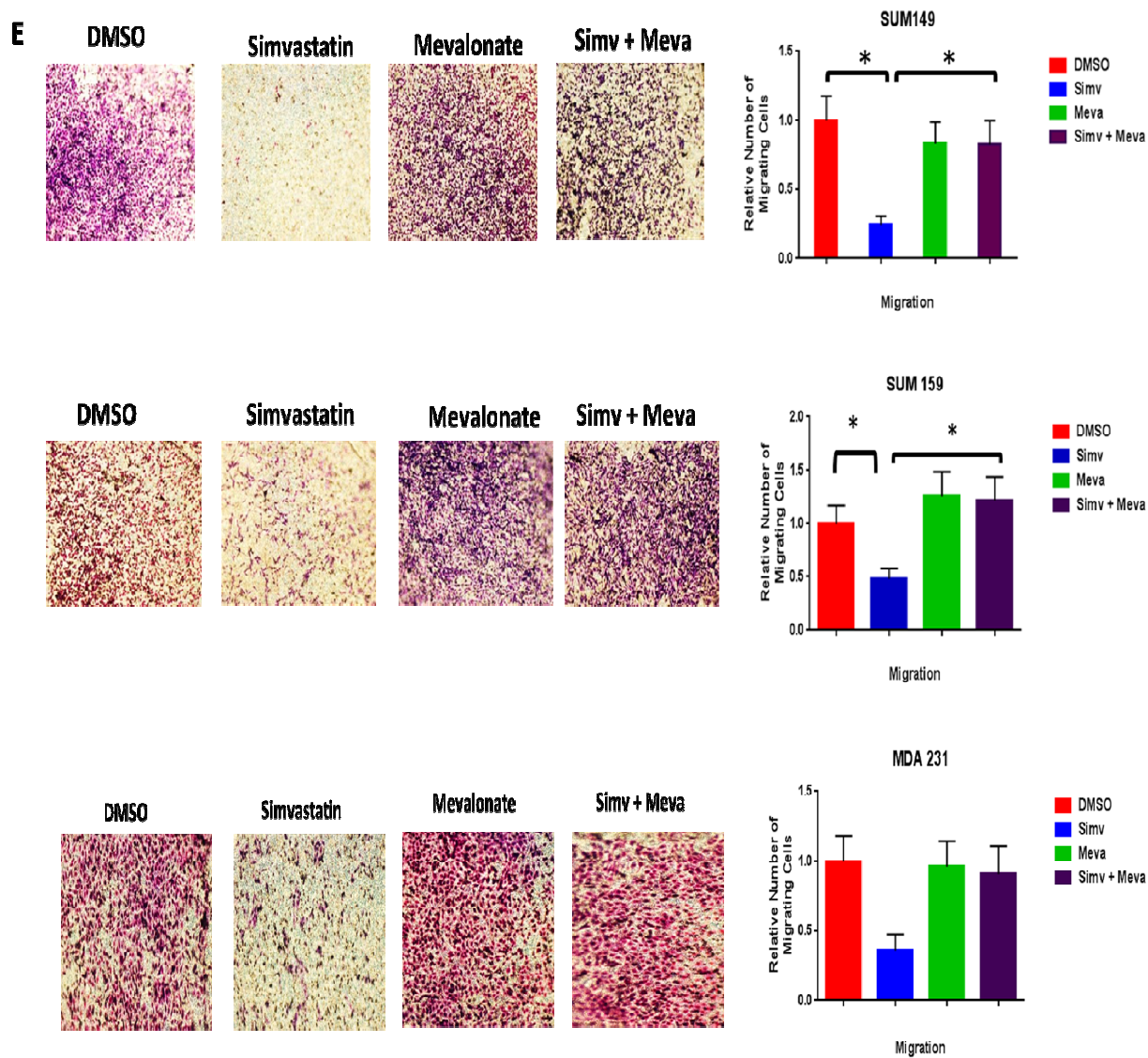


Figure 1. Simvastatin reduces percentage of cycling cells, proliferation, and migration. (E) SUM149, SUM159, and MDA-231 cells migrated through an 8 μm pore in the presence of 2.5 μM simvastatin, 10 mM mevalonate, both, or vehicle (DMSO). The number of cells that passed through the transwell membrane was counted. Significant differences are shown as follows: *, $P < 0.05$ for unpaired 2-tailed Student's t-test ($n = 3$). Abbreviations: PI, propidium iodide.

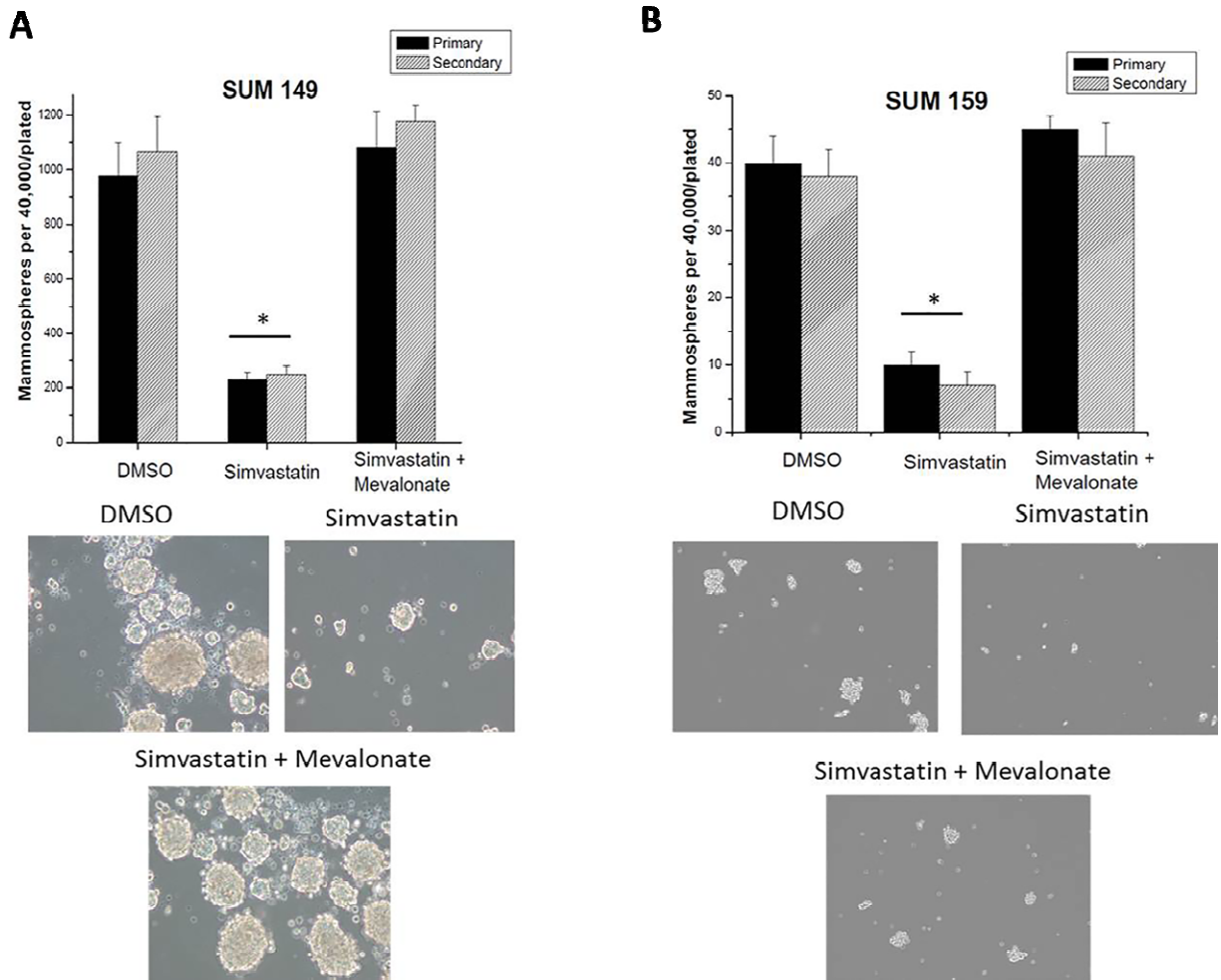


Figure 2. Simvastatin reduces the cancer stem cell-like population. (A) SUM149 and (B) SUM159 cells exposed to simvastatin (2.5 μ M) treatment (24 h) or simvastatin plus mevalonate (10 mM) and seeded in self-renewal promoting suspension culture conditions. There is an increase in both primary and secondary mammosphere formation in the simvastatin-treated cells and spheres were smaller on light microscope (40X). Significant differences are shown as follows: *, $P < 0.05$ for unpaired 2-tailed Student's t-test ($n = 3$).

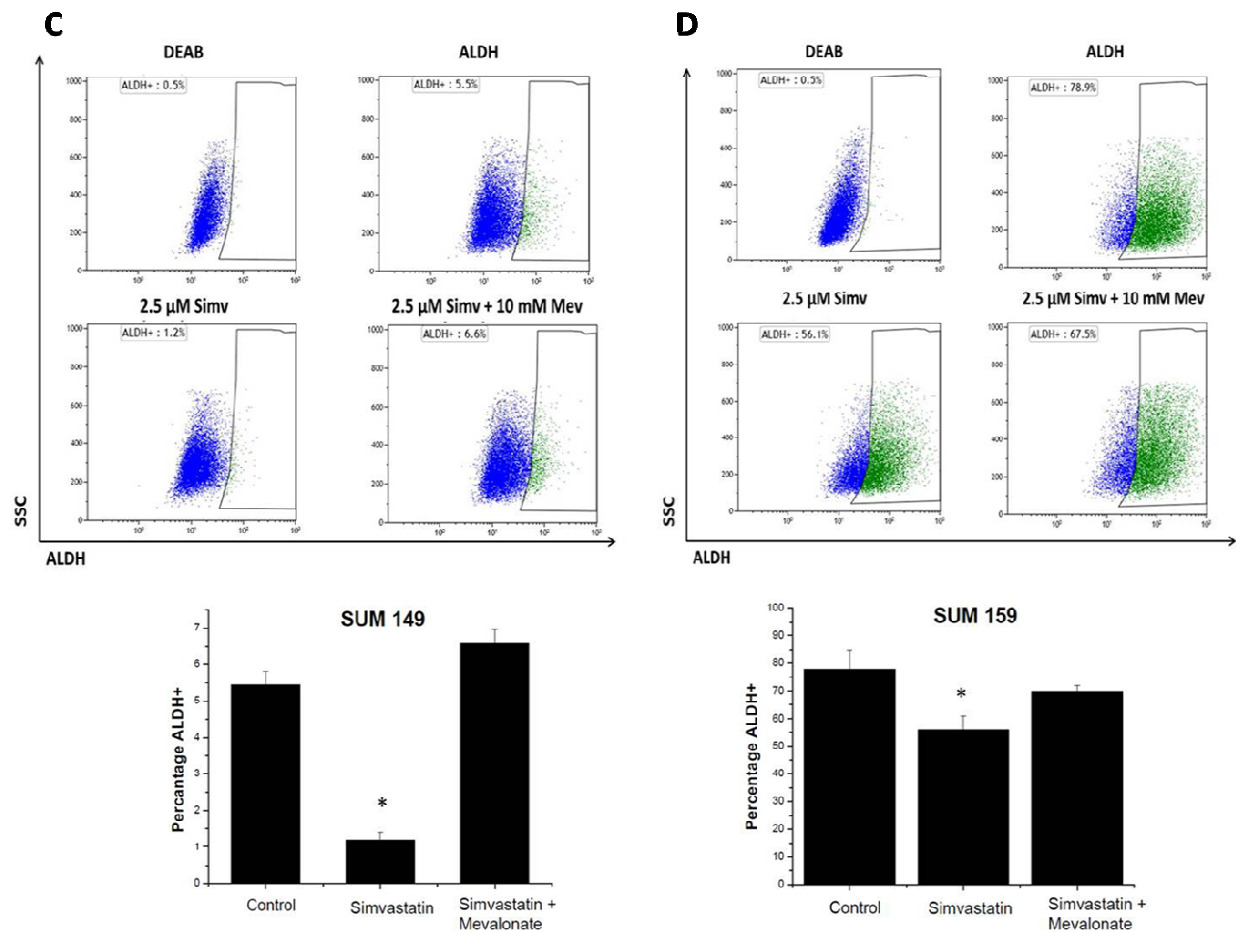


Figure 2. Simvastatin reduces the cancer stem cell-like population. Flow cytometry plot illustrating the gating strategy used to isolate ALDH+ (C) SUM149 and (D) SUM159 cells based on ALDH. Gating is set to DEAB-inhibitor control cells. Percentage of ALDH+ cells generated from SUM149 and SUM159-sorted ALDH+ cells pretreated for 24h with 2.5 μ M simvastatin or simvastatin plus 10 mM mevalonate or vehicle (DMSO). Results are mean \pm average number of spheres per 40,000 cells plated \pm SEM; representative data are shown. Results are mean \pm SEM from at least two biological replicates. SEM from at least two biological replicates. Abbreviations: ALDH, aldehyde dehydrogenase; DEAB, diethylaminobenzaldehyde; DMSO, dimethyl sulfoxide.

Simvastatin Inhibits Tumor Formation and Metastasis In Vivo

To examine the metastatic potential of TNBC cells exposed to simvastatin versus control cells, we used two separate *in vivo* models, an orthotopic xenograft model and an experimental metastasis model via tail vein injection. 20 weeks after orthotopic injection, tumors developed in 67% of the mice injected with simvastatin-treated SUM149 cells compared to 95% of the mice injected orthotopically with DMSO-treated SUM149 cells (**Table 3**, $p=0.04$). Primary tumors were resected at 20 weeks and mice were followed for an additional 8 weeks to evaluate the formation of distant metastasis. Of the mice in which tumors developed, 27% of the mice injected with simvastatin-treated SUM149 cells had developed metastasis in distant organs compared to 79% of the mice injected with DMSO-treated SUM149 cells (**Figure 3A**, $P=0.017$). Metastasis free survival was thus significantly longer in the simvastatin group (**Figure 3B**, $p<0.01$) despite no change in the primary tumor growth rate (**Figure 4**). In the tail-vein-injection experimental metastasis model, the control group developed distant metastases (either lung or brain) at a higher rate than the simvastatin pre-treated group (86% control, 22% simvastatin) ($P=0.04$, **Figure 5**), confirming that the establishment of colonies within the lung or brain was significantly inhibited by simvastatin pre-treatment of the cell lines.

Group	Number of mice	Tumor Incidence (%)	Metastasis rate (%)
<u>Orthotopic Injection</u>			
DMSO	19	18/19 (95)	11/14 (79)
Simvastatin	18	12/18 (67)	3/11 (27)
P		0.04	0.017
<u>Tail Vein Injection</u>			
DMSO	7	N/A	6/7 (86)
Simvastatin	9	N/A	2/9 (22)
P			0.04
<p>Note: For orthotopic injection tumors grew to a volume of 500 mm³ and resected after which metastasis was monitored through luciferase imaging weekly for 6 weeks. For tail vein injection mice were sacrificed after 8 weeks and lungs and brains imaged for GFP positive metastasis. The fisher exact test was used to compare tumor incidence and metastases rate.</p>			

Table 3. Tumor incidence and metastasis rate for tail vein and orthotopic in the DMSO control and simvastatin-treated SUM 149 group.

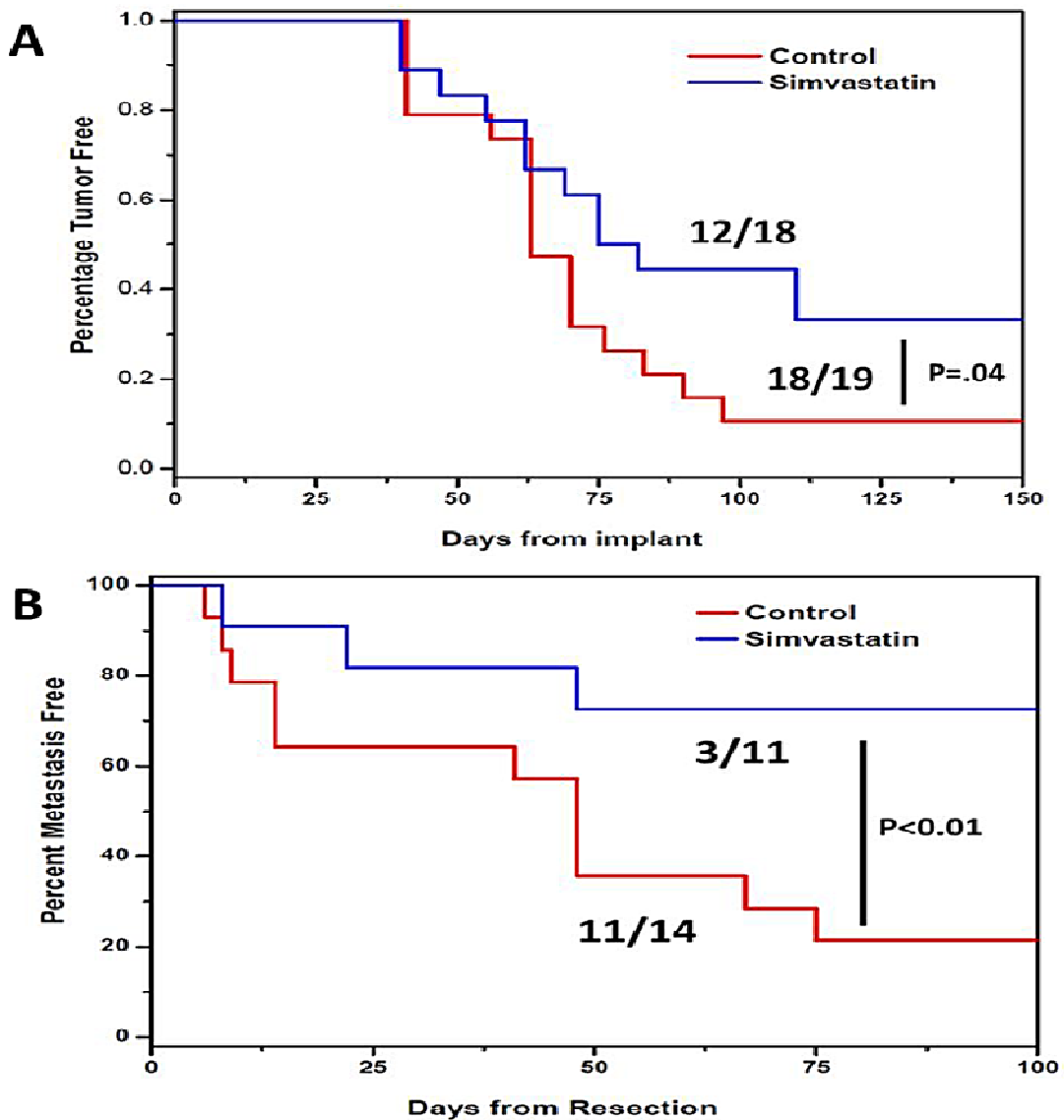


Figure 3. Simvastatin inhibits metastasis in both orthotopic and tail-vein in vivo

experiments. GFP labeled SUM149 cells were treated in vitro with simvastatin (1.25 μM) and injected either orthotopically or into the tail vein of mice and tumor metastasis was assessed. (A) Cells were injected into the mammary fat pad and tumor volume monitored every week until the tumors reached a volume of 500 mm^3 . A tumor was registered following 3 consecutive measurements (B) Following tumor resection mice were imaged with Luciferin for metastasis every two weeks.

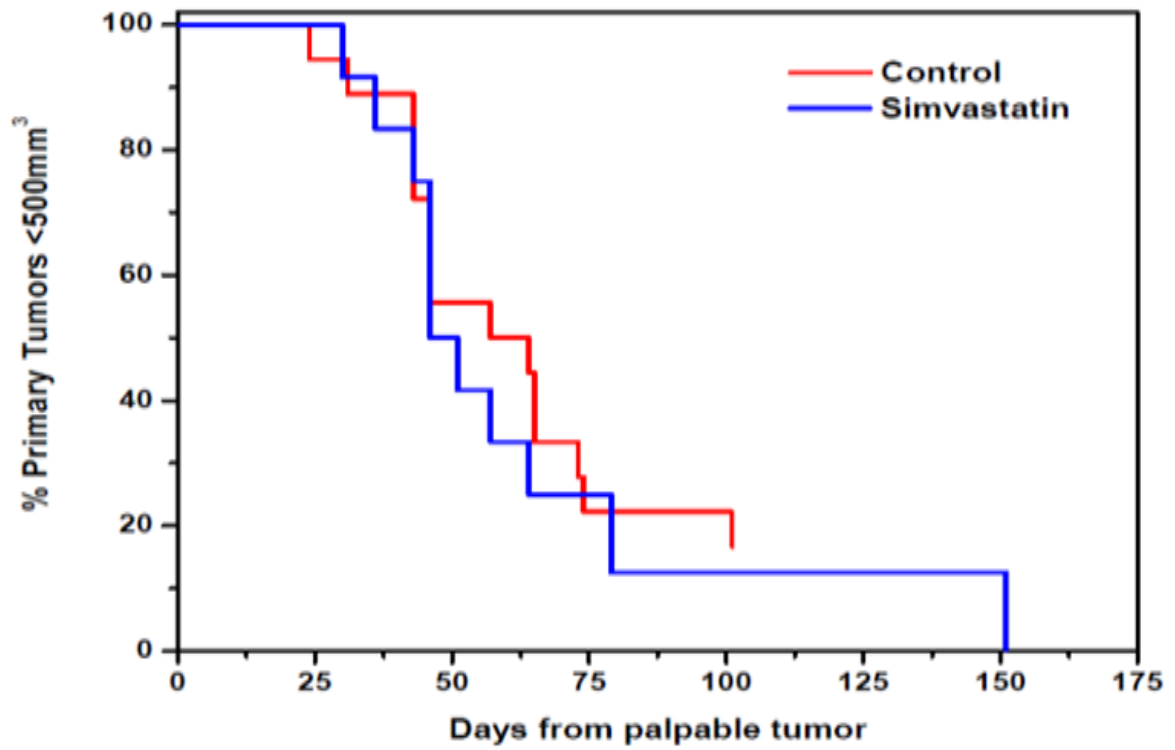
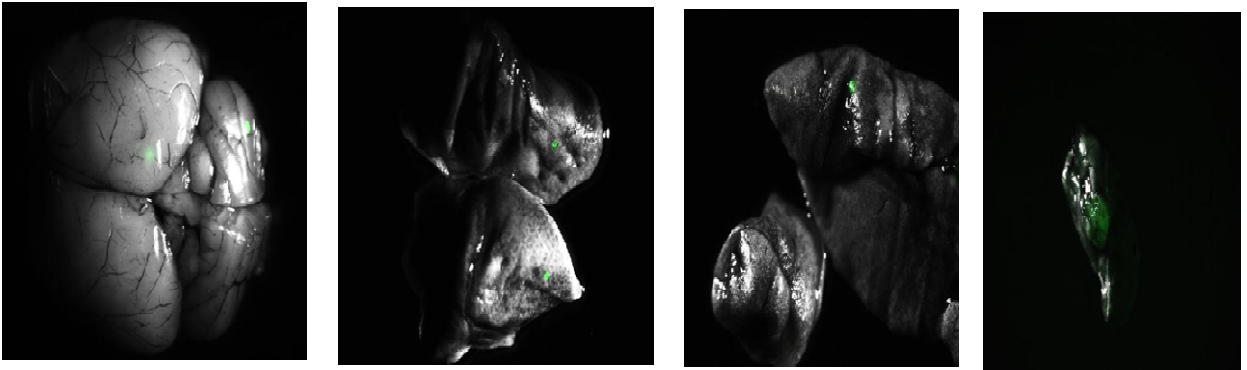


Figure 4. Simvastatin had no effects on tumor growth rate. Graph of Kaplan-Meier survival curve for the duration of time from first palpable tumor to time of resection (500 mm³).

DMSO-Control



Simvastatin

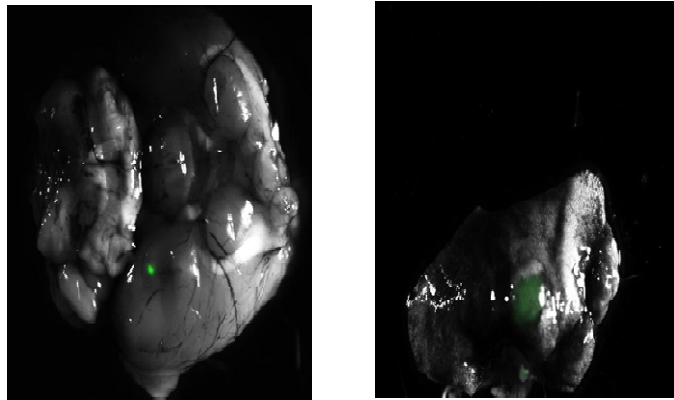


Figure 5. Imaging from mouse injected with SUM 149-GFP labeled cells in the tail vein. 8 weeks after of lung and brain metastatic colonization assessed by fluorescent stereomicroscopy.

Simvastatin regulates FOXO3a in TNBC cells

To identify pathways targeted by simvastatin we utilized RPPA to compare protein activation state in simvastatin treated versus untreated SUM149 and SUM159 cells. We found that phosphorylated FOXO3a and Akt were two of several proteins that were significantly downregulated (**Table 4**). FOXO3a is a known tumor suppressor that is targeted for degradation by phosphorylation (27). Akt is activated by phosphorylation following growth factor binding to cell membrane receptors such as epidermal growth factor (EGF). Following activation Akt regulates FOXO3a through phosphorylation leading to subsequent nuclear exclusion and degradation.⁷⁸ The possibility of increasing expression of a tumor suppressor is intriguing so we examined the relative expression of both phosphorylated and total FOXO3a and Akt proteins in SUM149 cells treated with simvastatin or vehicle control. We found that simvastatin inhibited phosphorylation of FOXO3a and Akt, and simvastatin decreased degradation of the total FOXO3a protein in the presence of EGF (**Figure 6A**). In order to further examine the function role of FOXO3a protein in TNBC metastasis, we evaluated its expression in three triple negative breast cancer cell lines. We found that SUM149 had a high level of FOXO3a expression and SUM159 and MDA-MB-231 had no protein expression of FOXO3a (**Figure 6B**). We used the FOXO3a high-expressing SUM149 and low/non-expressing SUM159 cell lines for further loss and gain of function experiments to examine whether simvastatin suppresses metastases by upregulating FOXO3a. A model of our working hypothesis is shown in **Figure 6C**.

Gene	Estimate	StdErr	tValue	Probt
IGFBP2	0.236541974	0.068937	3.431301	0.001948
JUN	0.147423042	0.069742	2.113839	0.042953
STMN1	0.102551778	0.048798	2.101559	0.045061
IRS1	0.062318964	0.030328	2.054806	0.049692
SCD1	0.056442084	0.021708	2.60002	0.014933
NOTCH1	0.043475254	0.017653	2.46277	0.020453
PAK4	0.04069914	0.019735	2.062269	0.048925
SMAD4	0.031210876	0.014996	2.081273	0.047021
CD29	0.013757838	0.005735	2.398885	0.023618
PTK2	-0.021843653	0.009895	-2.207436	0.035967
FOXO3a_pS318_S321	-0.023552701	0.009433	-2.496808	0.018687
MAP2K1	-0.027897861	0.013049	-2.13789	0.041395
CDKN1B1	-0.031618252	0.01503	-2.103695	0.044514
RAB25	-0.054924702	0.019028	-2.88652	0.007574
TTF1	-0.055480414	0.021997	-2.522187	0.017865
YAP1	-0.063656188	0.028464	-2.236384	0.033474
CHEK2	-0.128682305	0.044851	-2.869118	0.007899
EEF2	-0.129430725	0.04224	-3.064175	0.004906
CHEK1	-0.133710375	0.060976	-2.192843	0.03621
RAF11	-0.15511963	0.072606	-2.136453	0.041522
STAT3_pY705	-0.157584782	0.053725	-2.933161	0.006764
CHEK1	-0.166654442	0.075576	-2.205117	0.035827
Akt_pS473	-0.219314209	0.085809	-2.55584	0.016537
RPTOR	-0.233392901	0.102815	-2.270037	0.030553
FOXM1	-0.242775981	0.117432	-2.067379	0.048054
RPTOR	-0.282740455	0.129336	-2.186087	0.03733
RB11	-0.60117363	0.235042	-2.557732	0.016237
CAV1	-0.981896649	0.44709	-2.196197	0.036847
CCNB1	-1.405263027	0.428065	-3.282824	0.002759

Table 4. RPPA analysis of simvastatin treated cells reveals FOXO3a as a target. SUM149 and SUM159 cells were treated with 2.5 μ M simvastatin for 24 hours and submitted for RPPA analysis. Analysis-of-variance models were used to estimate 1) the overall effects of each treatment on each protein and 2) the overall effects of all treatments combined on each protein. All treatment effects were computed using control as a reference. The proteins with a $P < 0.05$ difference between the control are listed in the table.

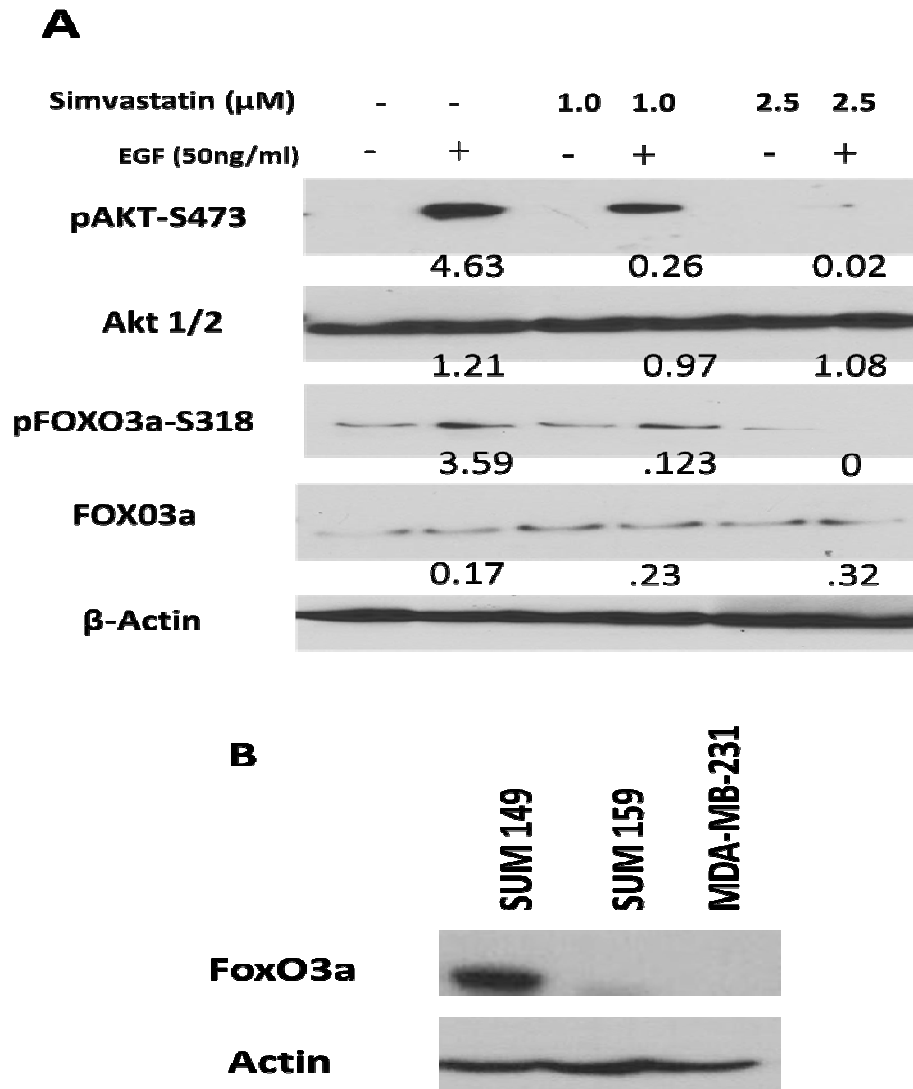


Figure 6. Simvastatin regulates the expression of FOXO3a (A) Immunoblot with anti-pFOXO3a, anti-FOXO3a antibodies, anti-Akt, and anti-pAkt in SUM149 cells treated with 1.25 or 2.5 μM simvastatin or vehicle control. Cells were treated with EGF 10 ng/mL for 15 minutes following 24 hours of simvastatin treatment or DMSO treatment. Beta-actin was used as a loading control. **(B)** Three breast cancer cell lines were probed with anti-FOXO3a antibody.

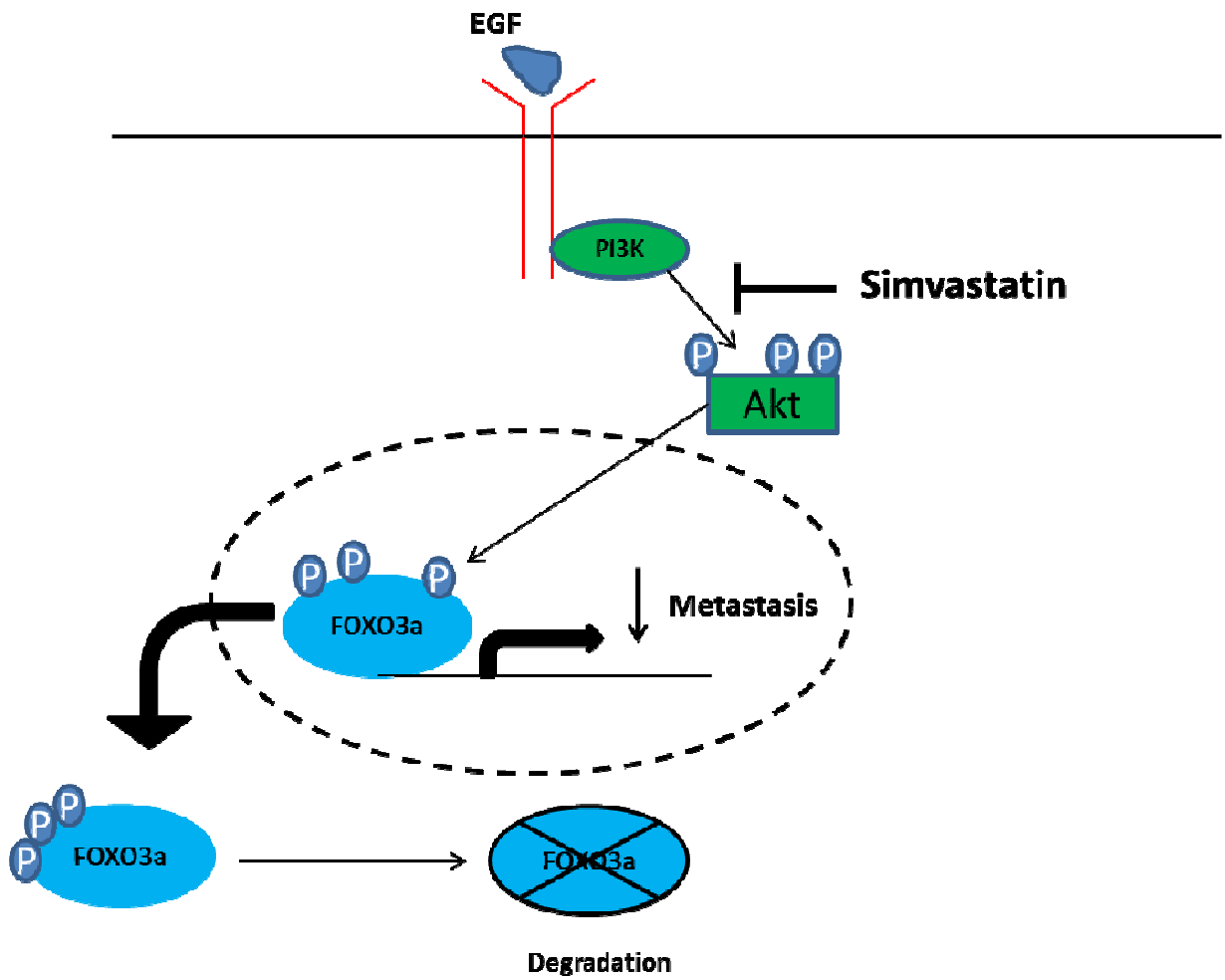


Figure 6. Simvastatin regulates the expression of FOXO3a (C) A model of how simvastatin regulates FOXO3a.

Next, we stably expressed FOXO3a in the low-expressing SUM159 using a lentiviral overexpression vector. Protein expression of FOXO3a and the downstream target CDKN1B in the SUM159 cells was increased compared with SUM159 cells stably transfected with empty vector (**Figure 7A**). Ectopic expression of FOXO3a significantly inhibited mammosphere formation (**Figure 7B**, $p=0.005$) and migration of SUM159 cells (**Figure 7C** $p=0.014$) in line with the effects observed with simvastatin treatment.

To mimic the effect of high FOXO3a phosphorylation leading to increased degradation, we knocked down FOXO3a in the high expressing SUM149 cell and examined the effect of simvastatin on these cells lacking FOXO3a. We tested for increased self-renewal and migration in vitro following RNA interference targeting FOXO3a in a metastatic TNBC breast cancer cell line, SUM149. RNA interference of FOXO3a in SUM149 inhibited the expression of FOXO3a (**Figure 7D**). Knockdown of FOXO3a significantly increased the mammosphere-forming efficiency of SUM149 cells compared to control cells (**Figure 7E**). While pretreatment with simvastatin significantly inhibited mammosphere formation in SUM149 cells transfected with control siRNA- consistent with our earlier findings - simvastatin had no effect on the FOXO3a-knockdown cells (**Figure 7E**). Similarly, knockdown of FOXO3a resulted in increased migration of SUM149 cells, and the treatment of these cells with simvastatin was unable to inhibit migration (**Figure 7F**). These results suggest that not only does FOXO3a regulate migration and self-renewal, but that simvastatin inhibition is mediated through regulation of FOXO3a.

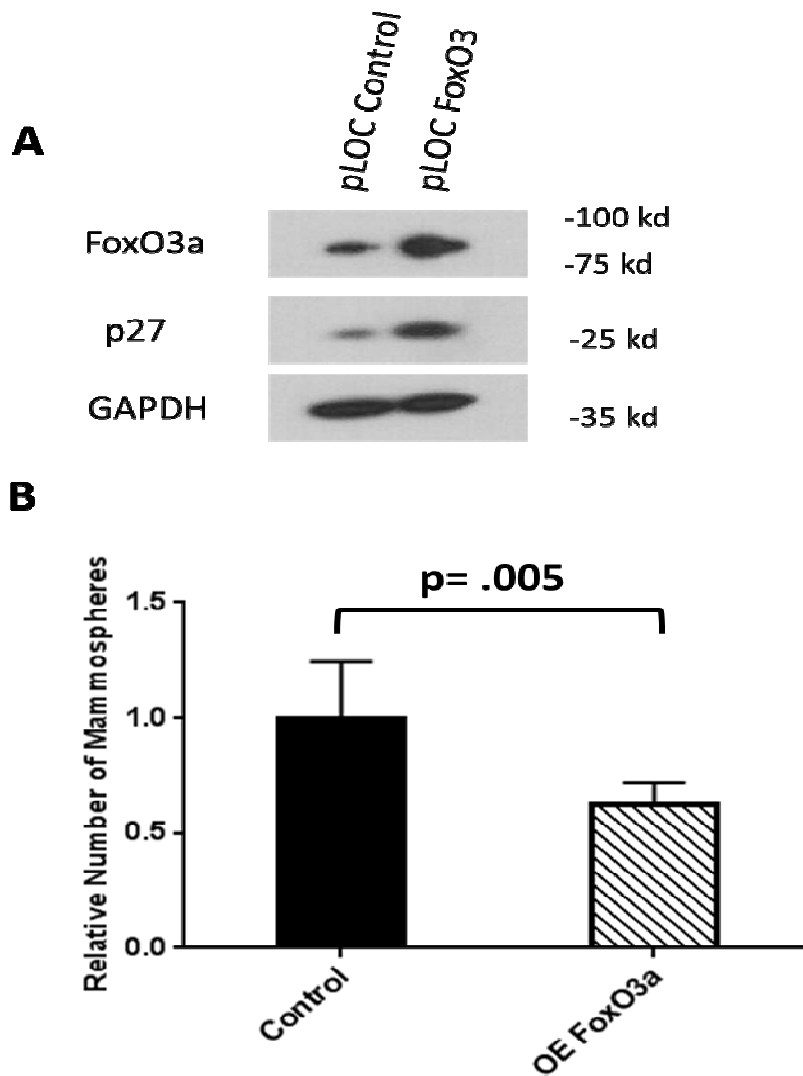


Figure 7. FOXO3a is a mediator of mammosphere and migration in TNBC cells. (A) Western blot assay to identify the overexpression efficiency of the plasmids for FOXO3a in SUM159 cells. (B) Mammosphere formation presented as the average number of spheres per 40,000 cells plated relative to the control plasmid \pm SD; representative data are shown.

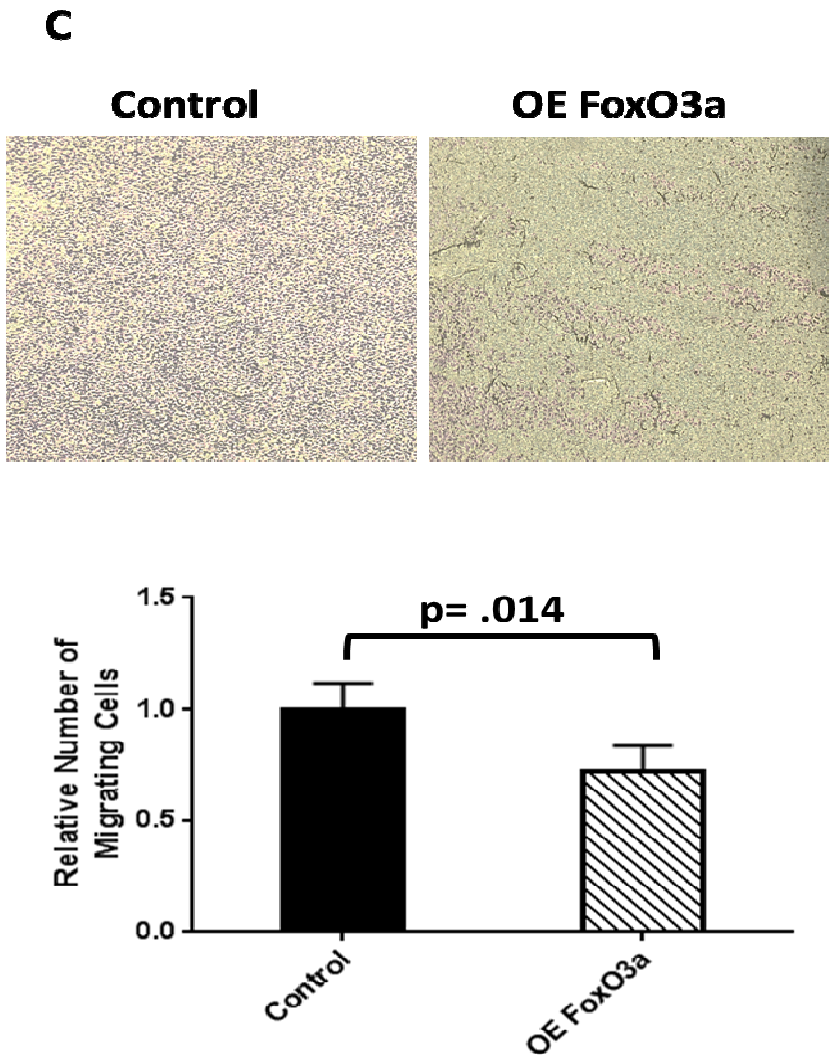


Figure 7. FOXO3a is a mediator of mammosphere and migration in TNBC cells. (C)

Representative images of the Transwell assays (magnification, $\times 40$). Quantification of the

numbers of migrating cells relative to the control plasmid is presented as mean \pm SD.

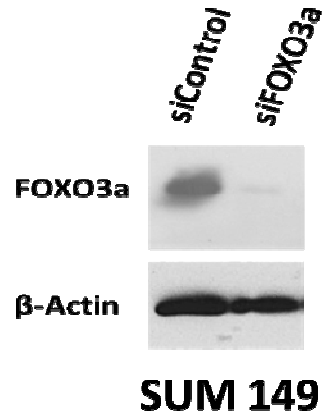
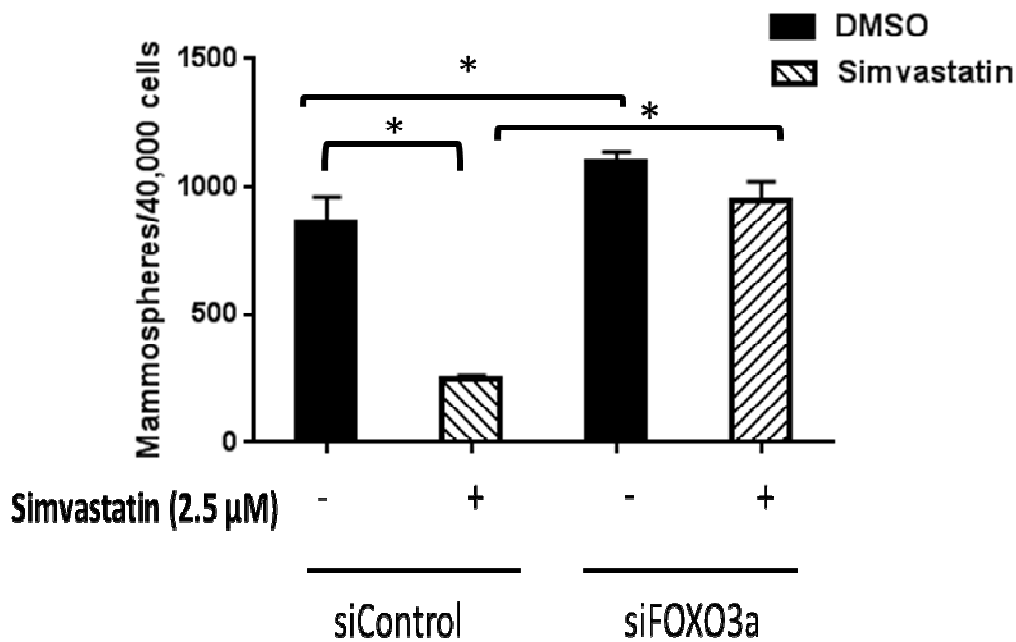
D**E**

Figure 7. FOXO3a is a mediator of mammosphere and migration in TNBC cells. (D)

Immunoblot with anti-FOXO3a antibodies in SUM149 cells transfected with either siRNA

targeting FOXO3a or scrambled control siRNA for 48 hours. Beta-actin was used as a loading

control. (E) SUM149 cells transfected with either siFOXO3a or scrambled siControl exposed to

simvastatin (2.5 μ M) treatment (24 h) and seeded in self-renewal promoting suspension culture

conditions. Mammosphere formation presented as the average number of spheres per 40,000

cells plated \pm SEM; representative data are shown.

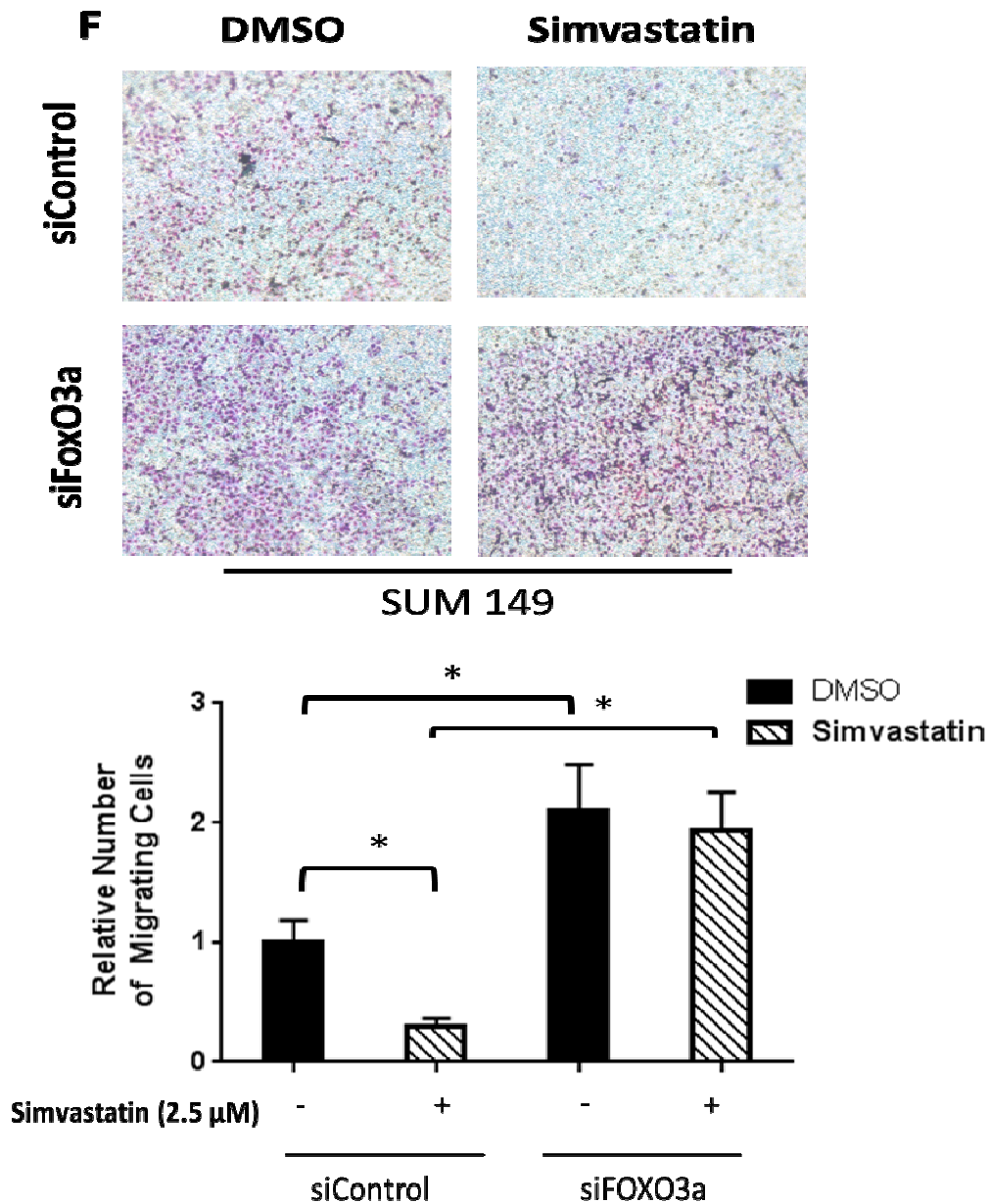


Figure 7. FOXO3a is a mediator of mammosphere and migration in TNBC cells. (F)

SUM149 cells transfected with either siFOXO3a or scrambled siControl migrated through an 8 μ m pore in the presence of 2.5 μ M simvastatin or vehicle (DMSO). The number of cells that passed through the transwell membrane was counted. Significant differences are shown as follows: *, $P < 0.05$ for unpaired 2-tailed Student's t-test ($n = 3$).

FOXO3a Levels Are Increased in Mouse Xenograft Primary Tumors Treated with Simvastatin

To confirm whether FOXO3a expression is correlated to simvastatin exposure, we tested FOXO3a protein expression with immunofluorescence in primary mouse tumors obtained from the orthotopic transplantation experiment described earlier. We found the expression of FOXO3a was lower in the vehicle pre-treated cells consistent with their increased rate of metastases. In the simvastatin treated tumors, the expression of FOXO3a was higher and as described these mice developed fewer distant metastases following tumor resection (**Figure 8**). This result suggests FOXO3a has a role in breast cancer metastasis and that simvastatin treatment could be a potential therapeutic therapy for preventing breast cancer metastasis.

FOXO3a Predicts For Distant Metastasis Free Survival in Breast Cancer Patients

To determine whether FOXO3a expression correlates with prognosis in patients with breast cancer, we analyzed *FOXO3A* mRNA expression in 8 public gene expression data sets, including 1,479 breast cancers clinically annotated. *FOXO3A* expression was heterogeneous with a range of intensities over 11 units in log₂ scale: 759 tumors (51%) showed downregulation when compared to normal breast (“*FOXO3A*-down” group), and 720 (49%) did not (“*FOXO3A*-no down” group). We searched for correlations between *FOXO3A* expression status (down-versus no down- groups) and clinicopathological variables (**Table 5**). No correlation was found with patients’ age, grade, pN, pT, and PR status, whereas *FOXO3A* downregulation was associated with ductal type, ER-positive status and ERBB2-negative status (Fisher’s exact test). Regarding survival, 1,069 patients remained metastasis-free during a median follow-up of 93 months (range, 1 to 299) and 410 displayed metastatic relapse. The 5-year MFS rate was 77% [95CI, 0.75-0.79]. In univariate analysis (**Table 6**), axillary lymph node involvement, large

tumor size, high grade, ER-negative status, PR-negative status, and ERBB2-positive status were associated with poor MFS, as was the *FOXO3A*-down group (p=0.028, Wald test; HR=1.24 [1.02-1.51], and p=0.028, log-rank test, **Figure 9**). In multivariate analysis (**Table 6**), all these features, except ER status, remained associated with poor MFS, including the *FOXO3A*-down group (p=0.024, Wald test; HR=1.29 [1.03-1.60]). The MFS analysis was done in each molecular subtype separately. As shown in **Figure 9**, *FOXO3A* expression influenced MFS in the TN subtype and the HR+/ERBB2- subtype, but not in the ERBB2+ subtype. These results suggest that FOXO3a may have a prognostic value for breast cancer metastasis, which is consistent with our mechanistic findings.

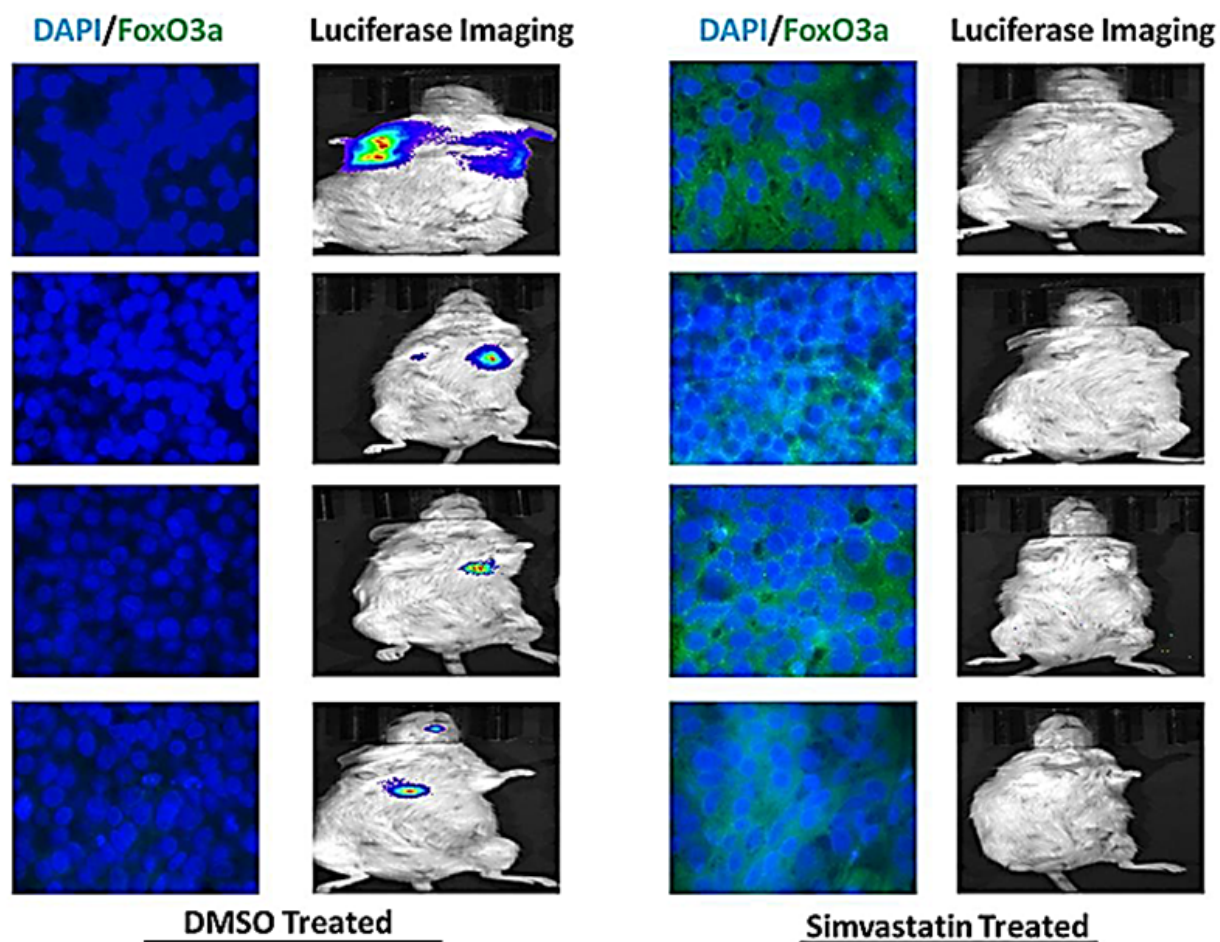


Figure 8. FOXO3a correlates with metastasis *in vivo*. Immunofluorescence images of primary xenografts and bioluminescence imaging of mice injected orthotopically with vehicle-DMSO or simvastatin treated SUM149 cells. Xenografts were stained with an anti-FOXO3a antibody (Green) and DAPI (Blue). Images are at 100X magnification. Bioluminescence imaging was obtained after 8 weeks following primary xenograft resection. Mice were injected with D-Luciferin and imaged in an IVIS NOVIS Lumina imager.

Characteristics*	N	FOXO3A expression-based groups		p-value
		no down (N=720)	down (N=759)	
Age, years				0.467
<=50	657	322 (57%)	335 (60%)	
>50	463	238 (42%)	225 (40%)	
Pathological type				1.43E-02
IDC	376	196 (74%)	180 (84%)	
ILC	35	25 (9%)	10 (5%)	
MIX	21	10 (4%)	11 (5%)	
other	48	34 (13%)	14 (7%)	
Pathological grade				0.424
1	279	142 (20%)	137 (19%)	
2-3	1158	557 (80%)	601 (81%)	
Pathological axillary lymph node status, pN				0.381
negative	866	432 (67%)	434 (65%)	
positive	443	209 (33%)	234 (35%)	
Pathological tumor size, pT				0.955
pT1	607	301 (48%)	306 (48%)	
pT2-3	653	322 (52%)	331 (52%)	
ER status				4.18E-03
negative	403	221 (31%)	182 (24%)	
positive	1076	499 (69%)	577 (76%)	
PR status				0.599
negative	632	313 (43%)	319 (42%)	
positive	847	407 (57%)	440 (58%)	
ERBB2 status				1.34E-02
negative	1313	624 (87%)	689 (91%)	
positive	166	96 (13%)	70 (9%)	
5-year MFS [95CI]	1479	80 [0.77-0.83]	74 [0.71-0.77]	2.79E-02

Table 5: Correlations of *FOXO3A* expression with clinicopathological characteristics in breast cancer.

Characteristics		Univariate			Multivariate		
		N	HR [95CI]	p-value	N	HR [95CI]	p-value
<i>FOXO3A</i> expression-based group	down vs. no down	1479	1.24 [1.02-1.51]	2.82E-02	1228	1.29 [1.03-1.6]	2.40E-02
Age, years	>50 vs. <= 50	1120	0.97 [0.77-1.21]	0.76			
Pathological type	ILC vs. IDC	480	1.30 [0.74-2.27]	0.213			
	MIX vs. IDC		0.66 [0.27-1.63]				
	other vs. IDC		0.53 [0.25-1.15]				
Pathological grade	2-3 vs. 1	1437	2.89 [2.06-4.06]	7.56E-10	1228	2.08 [1.45-2.99]	6.42E-05
Pathological axillary lymph node status, pN	positive vs. negative	1309	1.63 [1.32-2.01]	5.29E-06	1228	1.35 [1.08-1.70]	9.87E-03
Pathological tumor size, pT	pT2-3 vs. pT1	1260	1.64 [1.32-2.04]	8.81E-06	1228	1.41 [1.12-1.77]	3.12E-03
ER status	positive vs. negative	1479	0.58 [0.47-0.71]	1.11E-07	1228	0.88 [0.67-1.17]	0.40
PR status	positive vs. negative	1479	0.57 [0.47-0.69]	8.40E-09	1228	0.70 [0.54-0.91]	7.26E-03
ERBB2 status	positive vs. negative	1479	1.58 [1.20-2.08]	1.04E-03	1228	1.37 [1.01-1.86]	4.51E-02

Table 6: Univariate and multivariate analyses for MFS in breast cancer

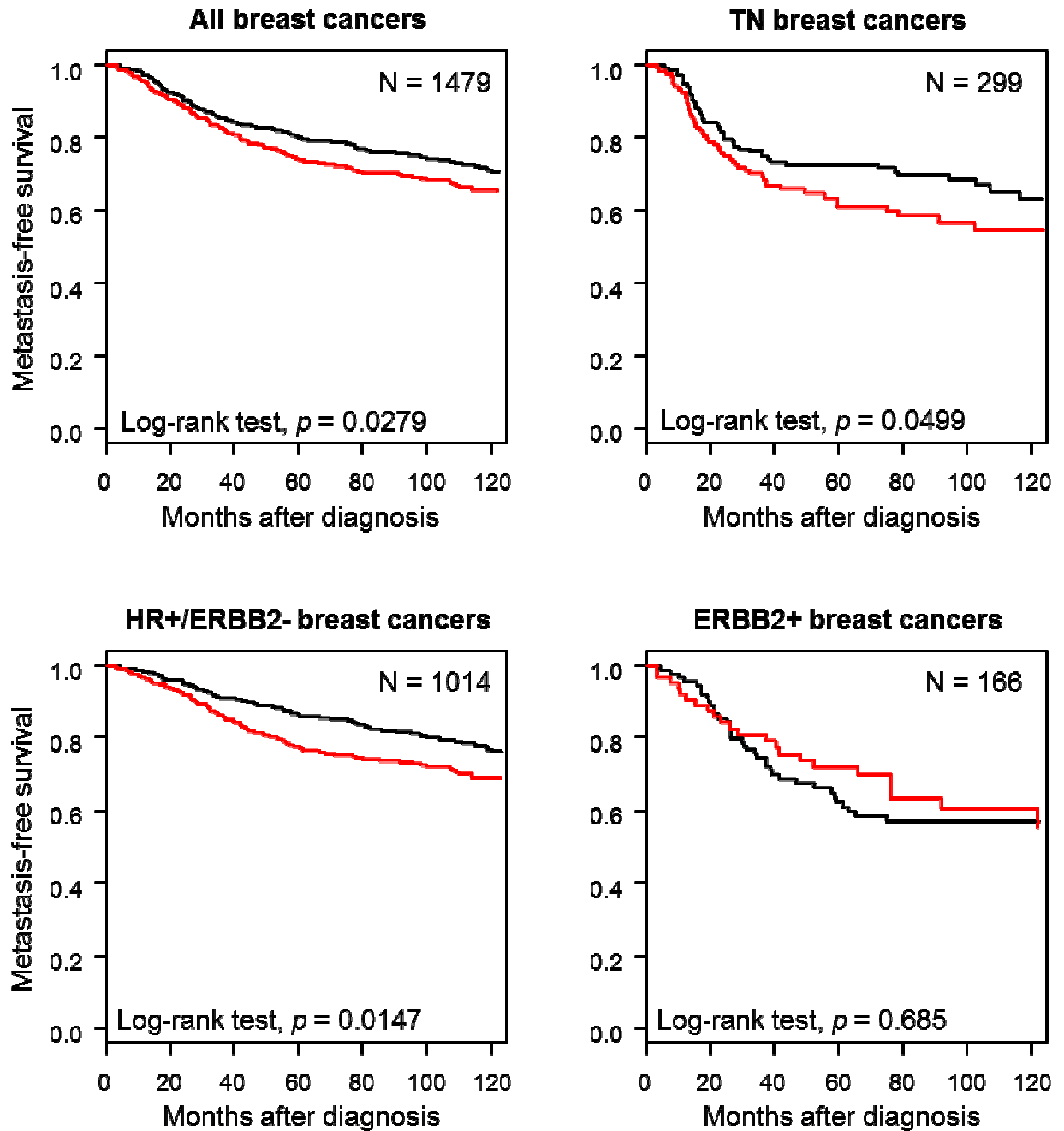


Figure 9. High FOXO3a mRNA levels are associated with better clinical outcomes in metastatic patients. Kaplan-Meier curves showing high *FOXO3a* mRNA levels were associated with longer metastasis free survival (5 year survival, 81% vs 72%; $p=0.0004$).

2.5 Discussion

Our results show that TNBC cells pre-exposed to simvastatin had less metastasis-associated in vitro characteristics and formed less metastasis in vivo, and that reduction of metastasis in vivo after simvastatin pre-treatment was correlated with intact FOXO3a signaling. We further showed that FOXO3a mRNA expression levels are positively correlated with patients' distant-metastasis-free survival.

In the current proposed clinical model, the use of statins is for primary tumor prevention and treatment⁷⁹, but our study suggests simvastatin should be further considered for metastasis prevention. The anti-tumor effects of statins were observed over 20 years ago^{80,81}. Subsequent research confirmed statins inhibit breast cancer proliferation in vitro and tumor growth in vivo⁸²⁻⁸⁶. The association between statin use in patients and breast cancer incidence has not been as clear. Undela et al. investigated the relationship of statin use and breast cancer risk in 24 observational studies, reporting data from more than 2.4 million participants, including 76,759 breast cancer cases. Their findings showed no association of statin use with reduced risk of breast cancer⁸⁷. To move forward with any clinical trials of the efficacy of statins in treating metastasis, biomarkers are necessary to separate patients into groups that would be predicted to be responsive to the effects of the drug.

FOXO3a has been previously described as a tumor suppressor in various tumors, including breast cancer, and is regulated by Akt, a pathway commonly deregulated in breast cancer⁷⁸. FoxO3 acts as a transcription factor and triggers apoptosis through induction of death genes such as *FasL* and *Bim1*⁸⁸. Ni et al showed that FOXO3a silencing promoted invasiveness of renal cancer cells and metastasis of renal cancer cells in vivo⁸⁹. Furthermore, Gopinath et al demonstrated a functional requirement for FOXO3a as a regulator of the Notch signaling pathway, a pathway critical for the self-renewal and maintenance of CSCs⁹⁰. Our data further

showed that *FOXO3a* mRNA levels were a significant predictor of distant-metastasis-free survival in breast cancer patients implying FOXO3a could be useful as a marker for metastatic outcomes in breast cancer patients. A recent study by Jiang and colleagues showed high expression level of *FOXO3a* was significantly correlated with long-term survival⁹¹. Whether it may be predictive of response to statin therapy remains to be examined. Our data showed that FOXO3a-knockdown cells were resistant to simvastatin treatment. The results of our study suggest a model wherein simvastatin treatment leads to increased activity of FOXO3a and finally inhibition of metastasis (**Figure 6**). Our observation that simvastatin decreased the rate of G1-to-S-phase progression is consistent with previous studies showing statins increase the expression of cell cycle inhibitors, which have been shown to decrease the self-renewal capacity of CSCs⁹²⁻⁹⁴. FOXO3a also mediates decreased transcription of CDKN1B⁹⁵, and therefore the increased activity of FOXO3a through simvastatin treatment could be the mechanism underlying the cell cycle arrest that we observed. This inhibition of the G1-to-S-phase transition could be the mechanism underlying the decreased CSC self-renewal capacity observed in our study.

Our data are consistent with data from previous statin studies showing that statins can inhibit self-renewal capacity. Ginestier et al showed that simvastatin targeted CSCs through RhoA/CDKN1B signaling³². Similarly, Ni et al. observed downregulation of FOXO3a increased metastasis and predicted worse metastasis-free survival in patients with renal cell carcinoma⁸⁹. This paper distinguishes itself from Ginestier et al because they looked at tumor initiation and this study focused on metastasis initiation. This study's focus was not on a treatment of metastasis and as such these results suggest statins could be used for preventing metastasis. Consistent with the clinical data in IBC showing it only helps in stage III, i.e. too late in those who develop metastasis in spite of statins⁶⁵.

The major strengths of this study are the use of two in vivo assays to study metastasis formation and the use of a large-scale screening tool in RPPA. Our study also has limitations. We pretreated cells before injection; therefore, we do not know how long the effects of simvastatin lasted once the cells were injected in vivo. Future studies involving treatment of mice with daily simvastatin and measurement of metastasis are warranted. The mammosphere and Aldefluor assays both measure tumor initiation capacity but are only surrogates for CSC likeness. To more effectively study simvastatin's effect on CSCs, additional studies using in vivo serial dilutions are warranted.

2.6 Conclusions

We showed that simvastatin inhibits breast cancer cells' ability to form metastases in spontaneous and experimental metastasis models. Furthermore, for the first time, we showed that FOXO3a in breast cancer is regulated by simvastatin and that *FOXO3a* mRNA expression levels in breast cancer patients correlated with distant-metastasis-free survival. Our findings underscore the potential of statins for breast cancer therapy.

Chapter III

High-density lipoprotein and very-low-density lipoprotein have opposing roles in regulating tumor-initiating cells and sensitivity to radiation in inflammatory breast cancer

This chapter is based upon the journal article “High-Density and Very-Low-Density Lipoprotein Have Opposing Roles in Regulating Tumor-Initiating Cells and Sensitivity to Radiation in Inflammatory Breast Cancer. Wolfe, A.R., R.L. Atkinson, J.P. Reddy, B.G. Debeb, R. Larson, L. Li, H. Masuda, T. Brewer, B.J. Atkinson, A. Brewster, N.T. Ueno, and W.A. Woodward, International Journal of Radiation Oncology*Biography*Physics, 2015. 91(5): p. 1072-1080.” It was approved by the publisher for reuse in this thesis.

3.1 Abstract

Purpose: We previously demonstrated that cholesterol-lowering agents regulate radiosensitivity of inflammatory breast cancer (IBC) cell lines *in vitro* and are associated with less radioresistance among IBC patients who undergo postmastectomy radiation. We hypothesized decreasing IBC cellular cholesterol induced by treatment with lipoproteins increases radiation sensitivity. Here, we examined the impact of specific transporters of cholesterol (i.e., lipoproteins) on the responses of IBC cells to self-renewal and to radiation *in vitro* and on clinical outcomes in IBC patients.

Methods and Materials: Two patient-derived IBC cell lines, SUM 149 and KPL4, were incubated with low-density, very-low-density, or high-density lipoproteins (LDL, VLDL, or HDL) for 24 hours prior to irradiation (0-6 Gy) and mammosphere formation assay. Cholesterol panels were examined in a cohort of patients with primary IBC diagnosed between 1995 and 2011 at XXX. Lipoprotein levels were then correlated to patient outcome using the log rank statistical model and examined in multivariate analysis using Cox regression.

Results: VLDL increased and HDL decreased mammosphere formation compared to untreated SUM 149 and KPL4 cells. Survival curves showed enhancement of survival in both IBC cell lines when pretreated with VLDL, and conversely radiosensitization in all cell lines when

pretreated with HDL. In IBC patients, higher VLDL values (>30 mg/dL) predicted a lower 5-year overall survival rate than normal levels (HR [95% CI] = 1.9 [1.05-3.45], P= 0.035). Lower than normal patient HDL values (<60 mg/dL) predicted a lower 5-year overall survival rate than values higher than 60 mg/dL (HR [95% CI] = 3.21 [1.25-8.27], P=0.015).

Conclusions: This study discovered a relationship between the plasma levels of lipoproteins, overall patient response, and radioresistance in IBC patients and IBC patient-derived cell lines. A more expansive study is needed to verify these observations."

3.2 Introduction

Inflammatory breast cancer (IBC) comprises approximately 5% of all breast cancer cases and is a rare, phenotypically distinct, highly aggressive form of locally advanced breast cancer.¹¹ IBC is highly invasive and has a high propensity to invade into the dermal lymphatics and metastasize to distant organs.⁹⁶ These features confer to IBC an extremely high metastatic potential, which accounts for its poor prognosis: the 5-year overall survival (OS) rate is only 40.5%.⁹⁷ Even with dose escalation and modified treatment regimens, local recurrence rates after radiation remain high, and morbidity due to local failure is significant. In the search for methods to sensitize IBC tumors to conventional therapies, the plasticity of IBC tumor cells has been extensively studied.⁹⁸

IBC is enriched in gene signatures identified in tumor initiating cells (TICs), TICs have been defined several ways but most conservatively are prospectively identified cells that self-renew to initiate tumors in transplantation assays. Enrichment for gene expression found in TICs may contribute to IBC resistance to standard therapies.⁹⁸ TICs have been shown to be important in resistance to therapies such as radiation and chemotherapy,⁹⁹⁻¹⁰¹ and new strategies for advanced cancer therapies increasingly include TIC-targeting drugs. Studies have shown cells that share markers with TICs have an enhancement in DNA repair including increases in CHK1, CHK2, and RAD51.^{102,103}

Inhibitors of 3-hydroxy-3-methylglutaryl coenzyme A (HMG CoA) reductase, or statins, have been shown to increase self-renewal of tumor cells via inactivation of Ras homolog family member A and increased accumulation of P27^{kip1} in the nucleus.³² Interestingly, in a retrospective analysis of 723 IBC patients from MD Anderson Cancer Center, treatment with a hydrophilic statin was associated with significantly longer progression-free survival (PFS) than

no statin.³³ Statins are known to regulate concentrations of lipoproteins in the blood, and the lipoproteins—low-density lipoprotein (LDL), high-density lipoprotein (HDL), and very-low-density lipoprotein (VLDL)—mediate cholesterol homeostasis in the blood.¹⁰⁴ Martin and van Golen recently demonstrated that IBC cells display differences in uptake and storage of cholesterol compared to non-IBC cells. IBC cells were able to maintain intracellular stores of cholesterol in cholesterol-depleted environments, while non-IBC cells could not.²² Even though statins are known to decrease the “bad” cholesterol, LDL and VLDL, and increase “good” cholesterol, HDL,^{79,105} the effects of regulating these lipoproteins was never established at the cellular level. Furthermore, the role of specific cholesterol transport lipoproteins on TIC survival and radiosensitivity in IBC cell lines has not been reported.

We hypothesized altering IBC cellular cholesterol induced by treatment with lipoproteins increased radiation sensitivity. *Here, we examined the impact of specific transporters of cholesterol (i.e., lipoproteins) using in vitro assays of self-renewal and radioresistance of IBC cells and on clinical outcomes in IBC patients.* Together, our analyses of patient outcomes and preclinical data specifically demonstrates that radiosensitization of IBC by statins was due to changes in HDL and VLDL levels, and that dyslipidemia (i.e., clinically low HDL and high VLDL) was associated with worse outcomes among IBC patients.

3.3 Methods and Materials

Cell culture and reagents

The SUM 149 IBC cell line is commercially available (Asterand, Detroit, MI). Cells were incubated in normal cell culture conditions with Hams–F12 cell culture medium supplemented with 1 µg/mL hydrocortisone, 5 µg/mL insulin, and 1% antibiotic-antimycotic. The KPL4 IBC cell line was maintained in DMEM/F-12 medium supplemented with 10% fetal bovine serum. Lipoproteins VLDL, LDL, and HDL were purchased from Sigma-Aldrich (St. Louis, MO). For all experiments including lipoproteins, serum was not added to the media to remove the cholesterol and lipoprotein contained in fetal bovine serum.

Mammosphere formation assay

To generate primary mammospheres, cells in monolayer culture, pretreated with lipoproteins for 24 hours or untreated, were grown in standard mammosphere medium (serum free, growth factor enriched). Low-attachment plates were used, as described previously [16]. For secondary mammosphere assay, cells from primary mammospheres were dispersed with 0.05% trypsin, seeded in ultra-low-attachment plates (20,000 cells/mL) in mammosphere medium, incubated for 7 days, and counted. All 3 lipoproteins were used at a concentration of 10 µg/mL in all *in vitro* experiments to simulate normal cholesterol lipoprotein levels found in human blood samples.

Clonogenic survival assays

Clonogenic viability of the SUM 149 and KPL4 cells was tested in triplicate in both standard monolayer conditions (referred to here as 2D culture) and 3D culture conditions. Cells in 2D culture were incubated for 14 days after treatment with VLDL, LDL, or HDL and irradiation.

Crystal violet staining (10%) was used to mark colonies with 50 cells or more ($\geq 300 \mu\text{m}$ diameter). Survival curves were obtained for all groups and curves were fitted on the basis of the linear-quadratic model.

Delivery of radiation

Cell lines were grown to 75% confluence and lipoproteins were added to the cell culture medium 24 hours prior to irradiation. Cells were irradiated using a ^{137}Cs source (Shepherd Irradiator, J.L. Sheperd and Associates, San Fernando, CA). Cells were washed twice with phosphate-buffered saline solution (PBS) and plated for 2D culture; 14 days later, colonies were stained with crystal violet. For 3D culture, cells were plated for 7 days immediately following irradiation. Spheres with a minimal size of $50 \mu\text{m}$ were counted using a Gelcount colony counter (Oxford Optronix, Oxford, UK).

Cholesterol staining

SUM 149 cells were incubated with HDL or VLDL for 24 hours and fixed and stained with cholesterol-specific stain filipin III (Abcam Cholesterol Kit Catalog # ab133116), a bacterial by-product that fluoresces after interacting with an isomer of cholesterol. Image J software was used to quantify the mean fluorescence for a sample of 6 images.

Immunoblotting

Western blot analysis was performed with precast gradient gels (Novex Life Technologies) using standard methods. Briefly, cells were lysed in the RIPA buffer containing protease inhibitors and phosphatase inhibitors (Sigma). Membranes were probed with the specific primary antibodies, followed by peroxidase-conjugated secondary antibodies. The following

antibodies were used: antibodies against pEGFR, EGFR, Akt, pAkt, FOXO3a, and pFOXO3a (Cell Signaling).

Immunofluorescence

Following irradiation at time points of 30 min, 4 hours, and 24 hours, cells were cultured in chamber slides overnight and fixed with 4% formaldehyde in PBS for 30 min, followed by permeabilization with 0.1% Triton X-100 in PBS for 1h. Cells were then blocked for nonspecific binding with 1% BSA in for 1h, and incubated with the γ H2AX antibody (1:400, Cell Signaling) overnight at 4°C. Alexa Fluor 488 goat anti-rabbit IgG (1:400, Cell Signaling) for 1 h at RT. Coverslips were mounted on slides using anti-fade mounting medium with DAPI (Cell Signaling).

Patient data

Patient and tumor characteristics for women with stage III or stage IV primary IBC diagnosed between January 12, 1995, and January 27, 2011, at MD Anderson Cancer Center were reported previously under a protocol approved by the MD Anderson Cancer Center Institutional Review Board [11]. Data on lipid and cholesterol levels were available for 193 of the women in this cohort and were extracted from the laboratory results database. These data were merged into the patient/tumor data, which included statin use, and these 193 patients comprised the cohort examined in this analysis.

Statistical analysis

For *in vitro* studies, statistical significance was determined by using the Student *t*-test, calculated by Origin software. For patient data, associations between categorical variables were assessed via cross-tabulation and the X^2 -test or Fisher exact test, where appropriate. Five-year

OS was estimated by using the Kaplan-Meier method. Both univariate and multivariate Cox proportional hazard models were applied to assess the effect of covariates of interest on OS.

3.4 Results

In vitro lipoprotein treatment of IBC cells results in changes in self-renewal and radiosensitivity.

We determined the effects of treatment with lipoproteins on the capacity of IBC cells to form secondary mammospheres in 3D culture conditions. Secondary mammosphere forming efficiency is an in vitro assay of self-renewal, a critical attribute of stem-like cells. VLDL significantly increased primary and secondary mammosphere forming efficiency (MSFE) in both SUM 149 and KPL4 cells compared to untreated cells (**Figure 10**). In SUM 149 cells, the effect of VLDL on secondary mammosphere formation was slightly greater than that on primary mammosphere formation (50% vs. 33% enhancement; $P < 0.05$). For KPL4 cells, primary and secondary mammosphere formation was enhanced 42% by VLDL treatment. Conversely, HDL treatment significantly reduced the number of mammospheres formed compared to untreated cells in both cell lines: mammosphere formation by SUM 149 cells was reduced by 21% and mammosphere formation by KPL4 cells was reduced by 70% (Fig. 10; $P < 0.05$). LDL treatment, on the other hand, was associated with no significant difference in mammosphere formation compared to untreated IBC cells (**Figure 10**). These findings suggest that VLDL increases and HDL decreases self-renewing cells that survive in low attachment, serum free conditions.

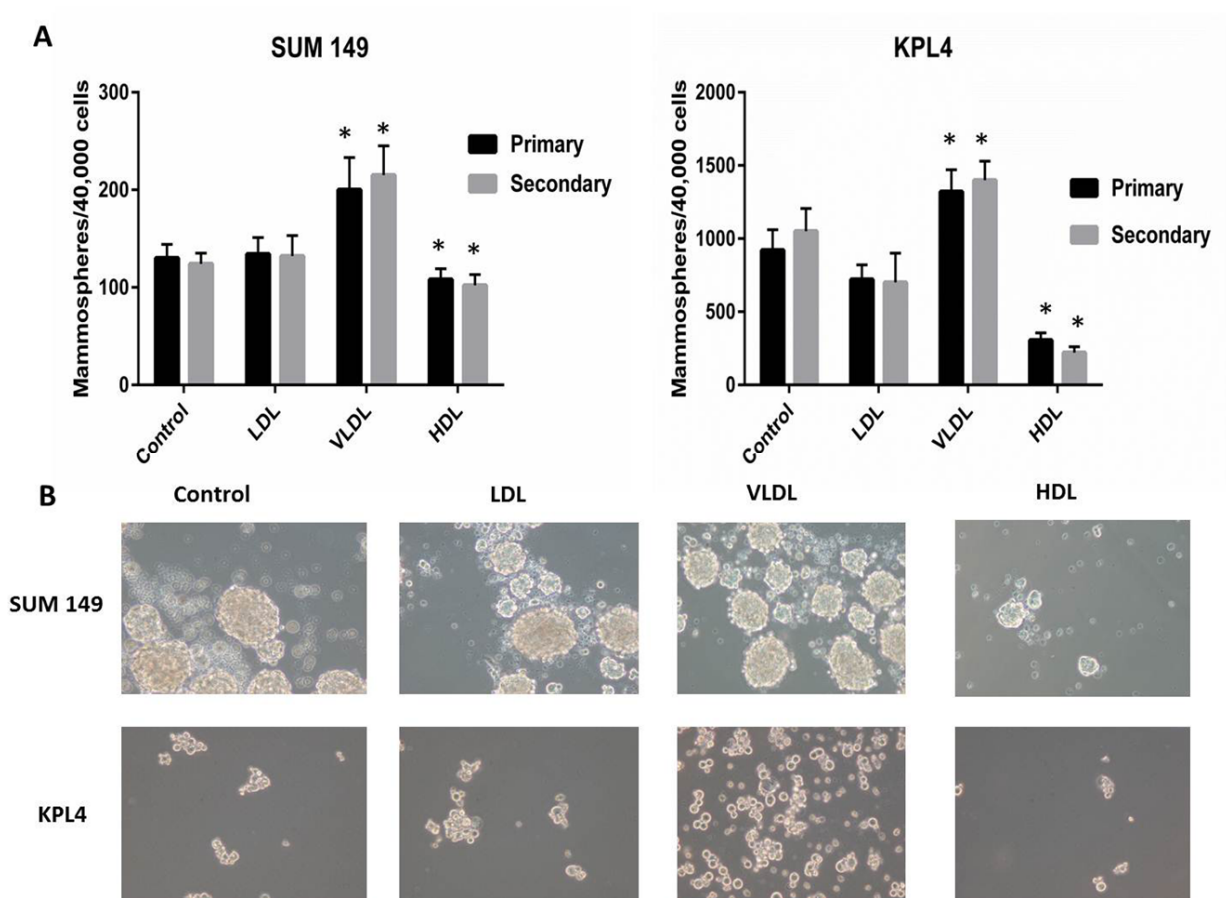


Figure 10. The impact of lipoproteins on mammosphere formation was demonstrated in 3D culture. (A). SUM 149 (left) and KPL4 cells (right) were treated with LDL, HDL, or VLDL (10 μ g/mL) and incubated for 24 hours to evaluate mammosphere formation (* $P < 0.05$ in triplicate independent experiments). **(B)** Light-microscope images (40 \times) of the primary mammospheres in culture. VLDL was observed to increase growth of primary and secondary mammospheres, and HDL to inhibit this growth.

In light of the radiation resistance of cells capable of growing as mammospheres and our previous work demonstrating statin treatment radiosensitizes mammospheres,⁶⁵ we investigated the effect of lipoprotein treatments on radiosensitivity of IBC cells. Clonogenic assays were performed with SUM 149 and KPL4 cells treated in the same conditions as for the mammosphere formation assay (10 µg/mL of VLDL, HDL, or LDL). After 24 hours of lipoprotein treatment, cells were irradiated with increasing doses of radiation between 0-6 Gy and then seeded in 2D or 3D culture conditions (**Figure 11**). Consistent with the findings on mammosphere-forming efficiency, VLDL increased radioresistance and HDL enhanced radiosensitivity of both IBC cell lines. These findings led us to hypothesize that radiosensitization of IBC could be due to the increased and decreased cellular levels of cholesterol induced by VLDL and HDL, respectively.

Decreased IBC cellular cholesterol concentrations correlate with decreased growth factor signaling and increased DNA repair following radiation

To elucidate the role of cholesterol transport in the response to radiation, we sampled cells from the clonogenic assays treated with VLDL or HDL to image intracellular levels of cholesterol before irradiation. VLDL-treated cells showed a 1.3-fold increase in cholesterol content in the intracellular environment ($P=.03$), while cells treated with HDL showed a 3-fold decrease in intracellular cholesterol content ($P<.01$) (**Figure 12**). To explore the mechanistic connection between lipoprotein treatment and response to radiation we examined reverse phase protein array (RPPA) data from statin treated breast cancer cells (Chapter 2) and observed Akt and FOXO3a to be regulated by statins. In addition Van Laere et al have previously shown higher (Akt) and lower (FOXO3a) expression in IBC patients compared to non-IBC.⁹⁸

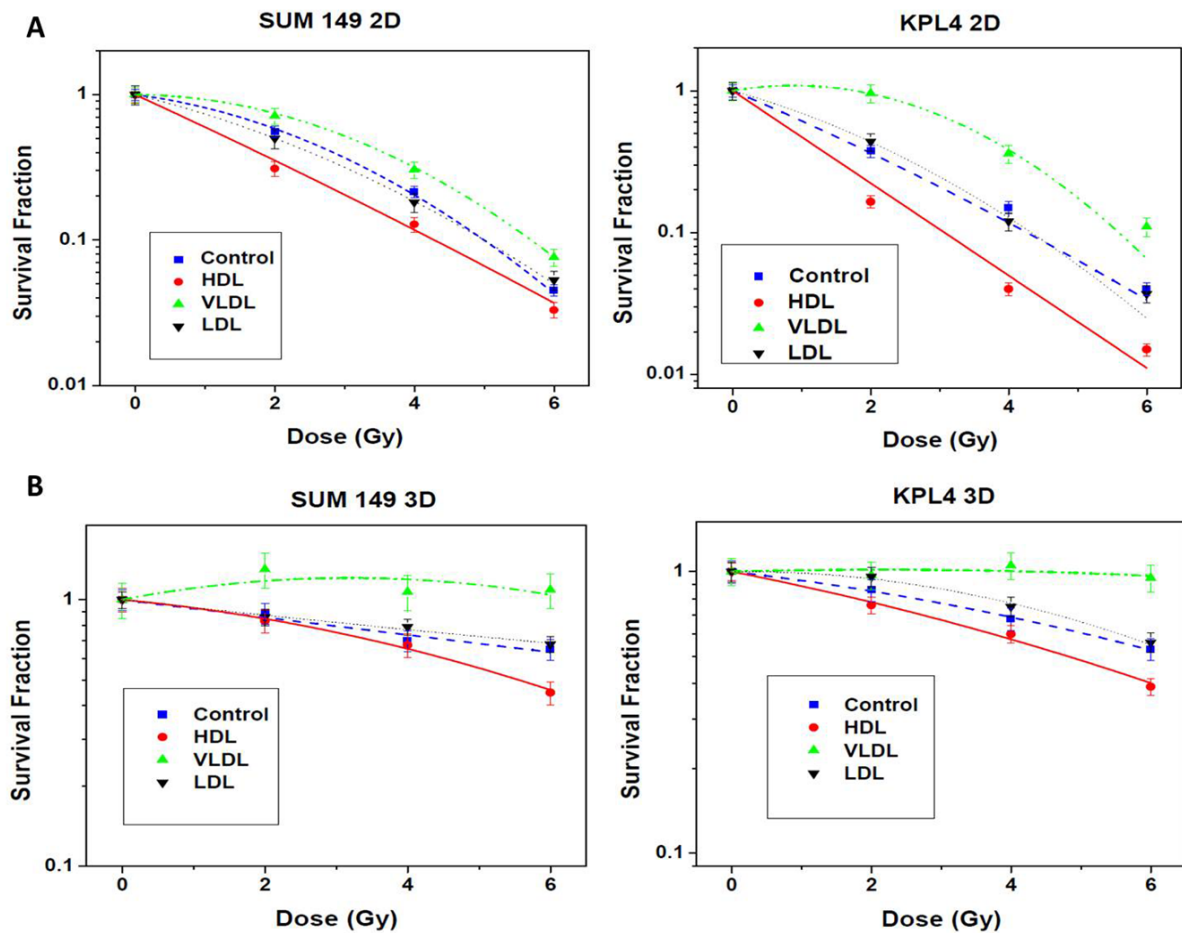


Figure 11. The effect of lipoprotein treatment on radiation response of SUM 149 and

KPL4 cells. (A). We observed in 2D cultures that VLDL caused radioprotection, HDL

radiosensitized, and LDL showed no effect on radiation response in both IBC cell lines. **(B).**

The same effects were observed in mammosphere 3D culture. Left panels represent SUM 149

and right panels KPL4.

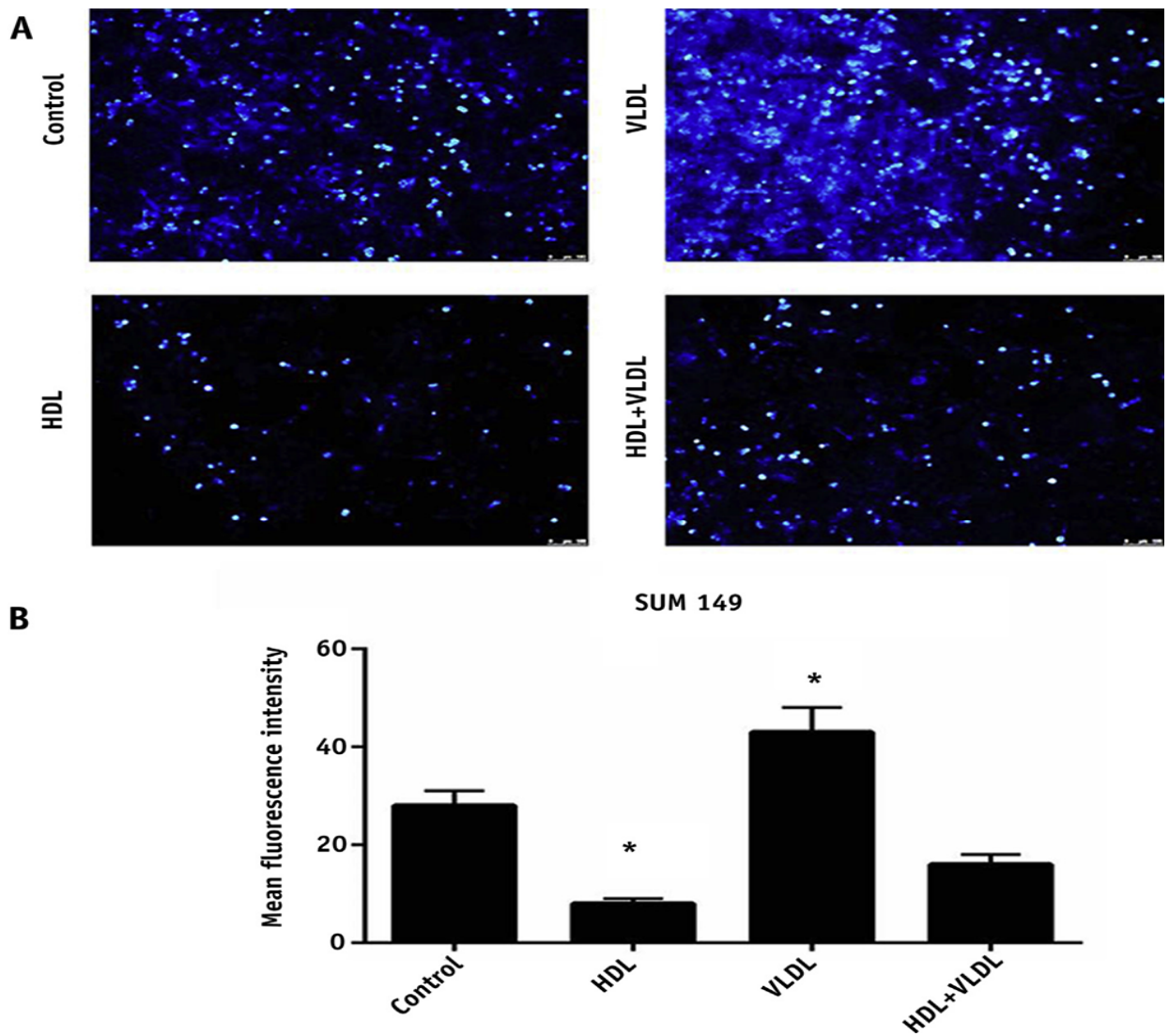


Figure 12. In vitro detection of cholesterol levels in SUM 149 cells by filipin staining. (A).

Leica microscopy images (40×) demonstrating intracellular cholesterol-rich domains after treatment with VLDL, HDL, or a combination. **(B).** Quantification of mean fluorescence activity is shown.

AKT and FOXO3A signaling is a key cytoprotective response in many cell types downstream of the EGFR family receptor.^{106,107} SUM 149 (**Figure 13A**) and KPL4 cells (**Figure 13B**) treated with HDL or VLDL 24 hours prior to EGF (15 ng/mL) stimulation displayed lower (HDL) and higher (VLDL) protein ratios of pEGFR:EGFR, pAKT:Akt, and pFOXO3a:FOXO3a compared with control SUM 149 and KPL4 cells.

Gamma-H2AX (γ H2AX) is a marker for DNA double strand repair after ionizing radiation treatment and γ H2AX foci persist longer in radiosensitive cell lines than in radioresistant lines.¹⁰⁸ We observed persistence (HDL treated) and decreased (VLDL treated) γ H2AX foci at 4 hours after 4 Gy ionizing radiation treatment (HDL, 4.27 fold increase P=.001, VLDL, 0.15 fold decrease P=.009) and continued differences at 24 hours (HDL, 5.5 fold increase P=.001, VLDL, 0.1 fold decrease P=.005) (**Figure 13C**), indicating HDL treated IBC cells were less able to repair DNA lesions and VLDL treated IBC cells were better able to repair DNA lesions. It is important to highlight, HDL treated SUM 149 cells had higher baseline γ H2AX foci starting at 0.5 hours following irradiation (1.8 fold increase, P=.002), while VLDL treated SUM 149 showed similar γ H2AX foci (0.8 fold decrease P=0.27) after 0.5 hours.

Dyslipidemia in IBC patients predicts overall survival

To expand the relevance of this work to patients, we correlated lipoprotein levels to OS in the cohort of 193 patients with stage III or stage IV IBC. Their lipid and cholesterol panels were analyzed; patients with stage III or IV disease were analyzed together as there was no significant difference by stage (P = 0.1). A summary of patient characteristics is presented in **Table 7**. Lipid panels were drawn per physician preference and practice and presumably represent a bias toward women with known dyslipidemia or risk factors for dyslipidemia.

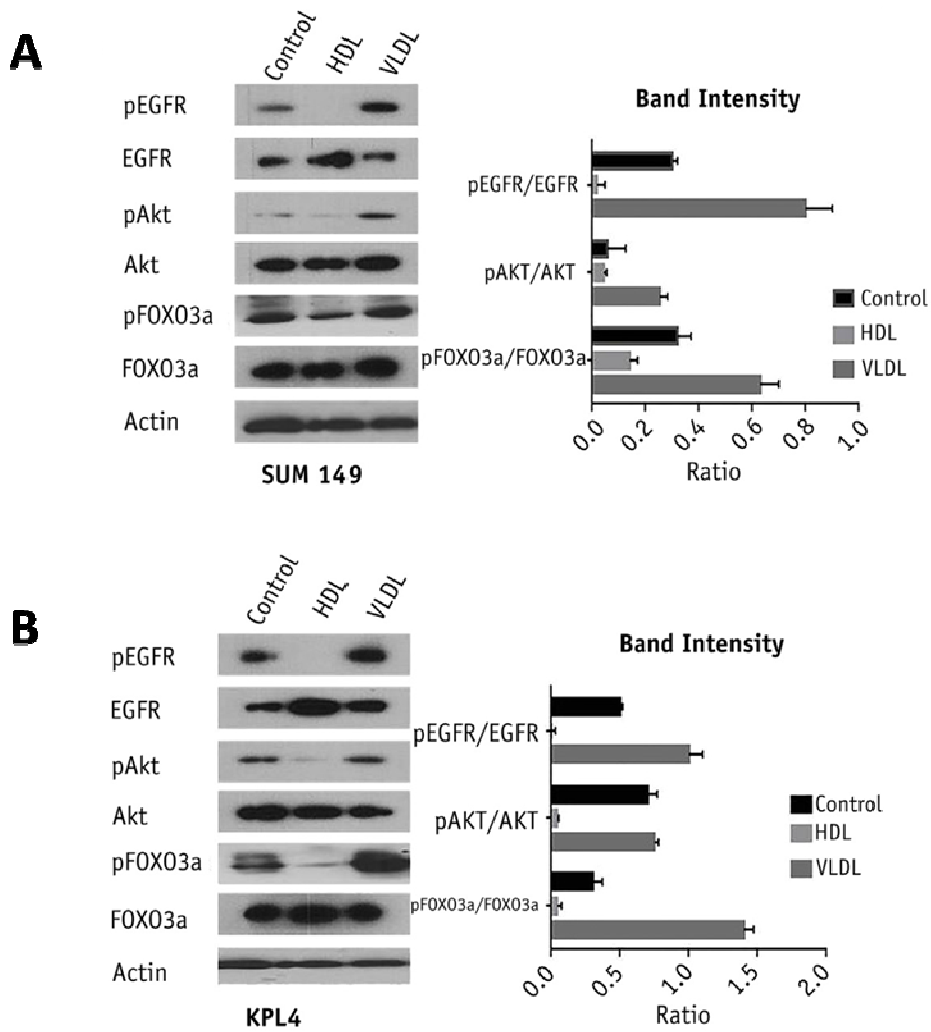
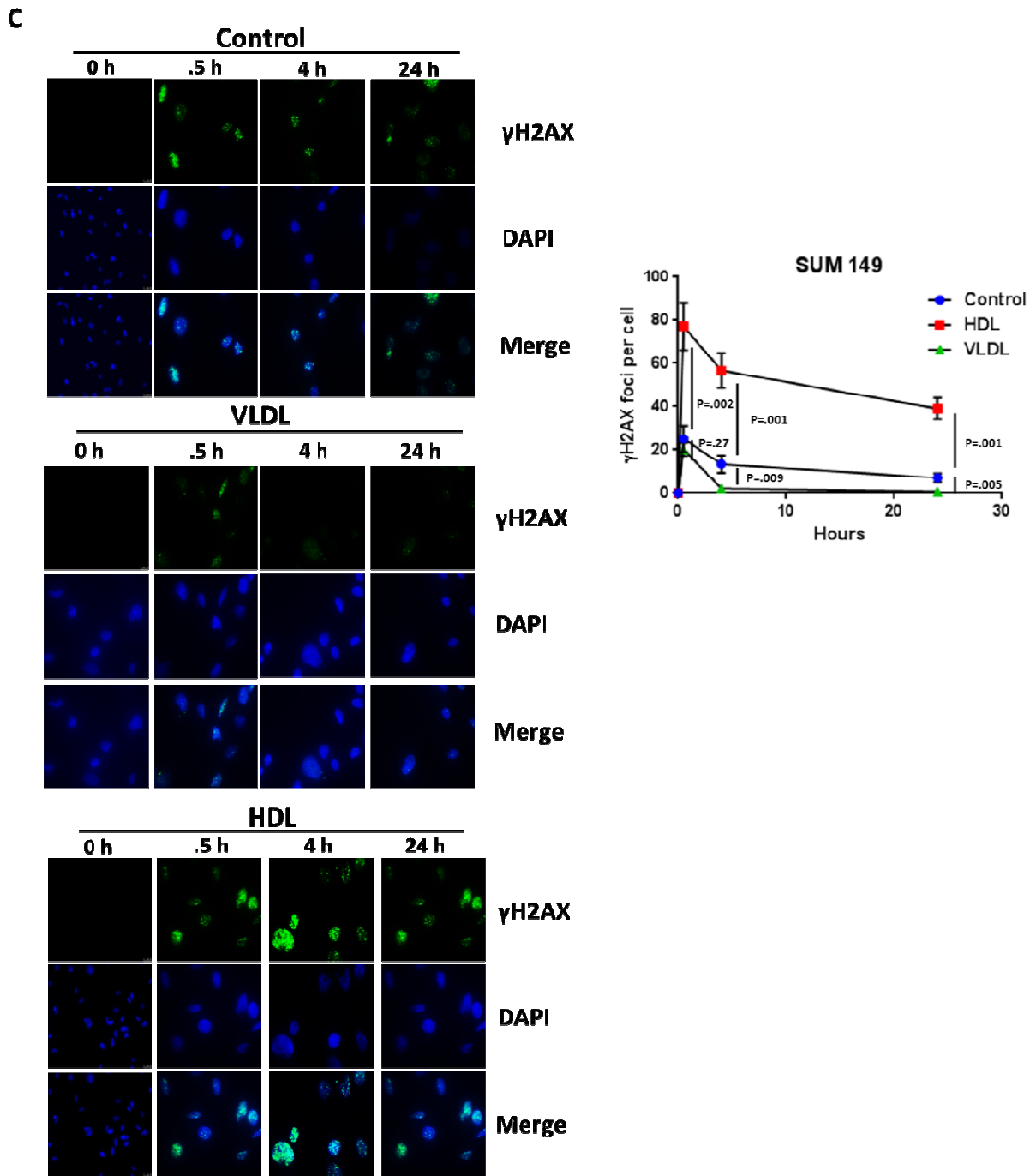


Figure 13. HDL and VLDL have opposite effects on FOXO3a phosphorylation and DNA Damage Response. (A) Immunoblotting of pEGFR, pAKT, pFOXO3a, and Actin in SUM 149 and **(B)**. KPL4 cells treated with either HDL or VLDL for 24 h.



Patient Characteristics (n=193)				
	Percentage	Number	Mean	Range
Age of Diagnosis				
≥ 45	78.24	42	52.17	(26-81)
< 45	21.76	151		
Body Mass Index				
<25	21.76	42	31.2	(17-71)
25>30	29.53	57		
>30	48.70	94		
Race				
Non-Hispanic White	77.20	149		
All others	22.80	44		
Menopausal status				
Postmenopausal	60.62	117		
Premenopausal	39.38	76		
ER status				
Positive	54.95	100		
Negative	45.05	82		
PR status				
Positive	36.11	65		
Negative	63.89	115		
Her2 status				
Positive	42.86	75		
Negative	57.14	100		
Triple Negative				
Positive	19.55	35		
Negative	80.45	144		
Radiation Therapy				
Yes	75.65	146		
No	24.87	47		
Statin Use				
Current	23.83	46		
Never	76.17	147		
Cholesterol levels				
Normal (≤200)	50.54	94	204	(110-411)
High (>200)	49.46	92		
HDL levels				
Normal (≥60)	26.45	41	51	(7-107)
Low (<60)	73.55	114		
LDL levels				
Normal (≤100)	36.36	56	119	(30-246)
High (>100)	63.64	98		
VLDL levels				
Normal (≤30)	61.69	95	29	(9-77)
High (>30)	38.31	59		
TRIG levels				
Normal (≤150)	52.84	93	177	(50-948)
High (>150)	47.16	83		

Table 7. Patient Characteristics

The demographic and clinical characteristics of this subset of 193 women were similar to those of the larger cohort.³³ The women were older (78% older than 45 years), demonstrated high body mass index (48% BMI >30), and were predominantly postmenopausal (60.6%). Approximately 20% of the patients had triple-negative disease, and the majority of patients received radiation therapy (75%). The patients had higher than normal LDL (>100 mg/dL, 63%) and VLDL (>30 mg/dL, 38%) levels and lower than normal HDL levels (<60 mg/dL, 73%). Statin users comprised 24% of the total number. Statin users had significantly better locoregional control of disease (82% vs. 54%, $P = 0.003$). No local failures occurred among statin users during the 36 months after treatment. Patients with an HDL level higher than 30 mg/dL had a significantly higher 5-year local/regional recurrence-free survival rate than patients with an HDL level less than 30 mg/dL (98% vs. 74% respectively, $P=0.003$) Kaplan Meier curves for 5 year OS and local/regional recurrence-free survival by baseline HDL levels are shown in **Figure 14**.

The risk factors that were included in the multivariate model ($P<0.25$ in univariate analysis) were ER status ($P=0.02$), PR status ($P=0.04$), HER2 status ($P=0.11$), triple-negative status ($P<0.0006$), total cholesterol level ($P=0.11$), HDL level ($P=0.03$), VLDL level ($P=0.06$), statin use ($P=0.23$), and menopausal status ($P=0.13$) (**Table 8**). In the final multi-covariant Cox model, triple-negative breast cancer, HDL, and VLDL were significant predictors of 5-year OS (**Table 9**). Patients with a higher than normal VLDL level had a significantly lower 5-year OS rate than patients with a normal VLDL level (HR [95% CI] = 1.9 [1.05-3.45], $P= 0.035$). Similarly, patients with a lower than normal HDL level had a significantly lower 5-year OS rate than patients with a normal HDL level (HR [95% CI] = 3.21 [1.25-8.27], $P=0.015$). Of the 72 patients who had died by January 27, 2011, 68 died of disease. Of the other 4 patients, 3 were in the no statin group; one died of a fall, one of metastatic endometrial cancer, and one of

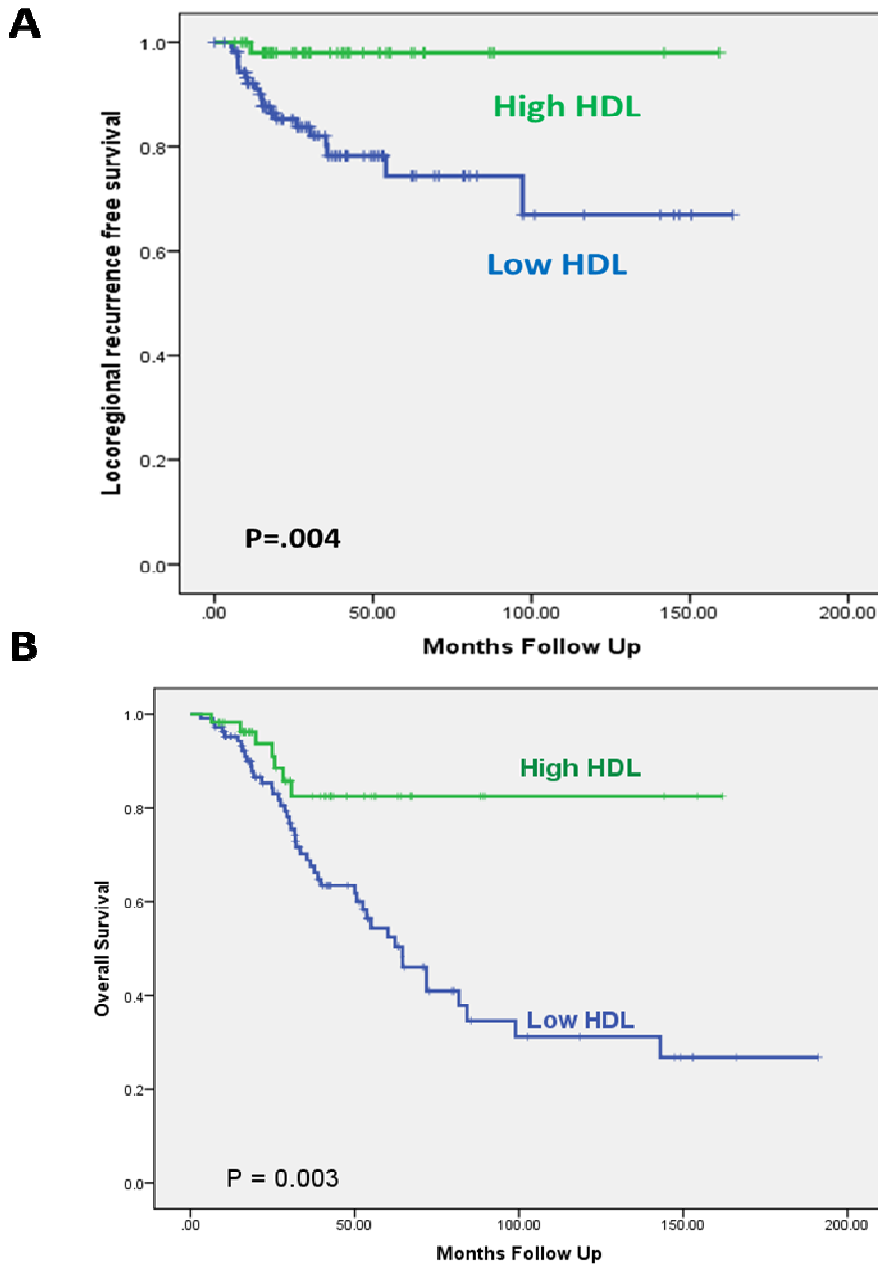


Figure 14. Kaplan Meir Curves for HDL outcomes. (A). Locoregional recurrence-free survival curve comparing patients with high HDL level (>30 mg/dL) and those with low HDL level (<30 mg/dL; P=0.004). **(B).** Overall survival curves comparing patients with normal vs. abnormal serum HDL levels determined from blood samples collected at the time of IBC diagnosis.

Prognostic Factors	Number of Patients/ Number of Deaths	5-Year OS (95% CI)	P value
Age of Diagnosis			
≥ 45	151/56	65.90 (55.6 – 74.3)	0.83
< 45	42/17	62.4 (42.2 – 77.3)	
Race			
Non-Hispanic White	149/54	64.8 (54.3 – 73.5)	0.43
All others	44/19	65.2 (45.9 – 79.1)	
ER Expression			
Negative	82/36	58.2 (44.1 – 69.49)	0.02 *
Positive	100/30	74.1 (61.2 – 83.3)	
PR Expression			
Negative	115/47	60.8 (48.2 – 70.8)	0.04 *
Positive	65/18	76.8 (60.9 – 86.9)	
HER2 Expression			
Negative	100/48	64.7 (52.6 – 74.5)	0.11 *
Positive	75/17	70.2 (54.2 – 81.5)	
Triple-negative status			
No	144/43	72.4 (61.8 – 80.5)	<0.0006 *
Yes	35/23	46.0 (27.0 – 63.1)	
Total Cholesterol			
Normal	94/39	56.6 (42.8 – 68.3)	0.11 *
High	92/29	73.8 (60.6 – 83.3)	
HDL			
Normal	41/5	94.5 (79.6 – 98.6)	0.03 *
Low	114/44	63.9 (52.1 – 73.5)	
Statin Use			
No	147/63	61.3 (51.1 – 70.0)	0.23 *
Yes	46/10	81.4 (62.4 – 91.5)	
Triglyceride			
Normal	93/36	66.2 (52.7 – 76.2)	0.41
High	83/25	69.1 (54.7 – 79.7)	
VLDL			
Normal	59/24	76.9 (62.8 – 86.2)	0.06 *
High	95/25	57.7 (40.6 – 71.5)	
BMI			
Normal	42/14	59.9 (35.5 – 77.6)	0.84
Overweight	57/25	61.5 (45.4 – 74.1)	
Obese	94/34	66.4 (53.0 – 76.8)	
Menopausal Status			
Post	117/49	61.7 (49.9 – 71.5)	0.13 *
Pre	76/24	69.1 (53.5 – 80.3)	

Table 8. Univariate analysis of all patients.

Table 9.
Multivariate Cox model for OS

	HR (95% CI)	P-value
Triple Negative Status	2.52 (1.35-4.68)	0.003
HDL (<60 mg/dL)	3.21 (1.25-8.27)	0.015
VLDL (>30 mg/dL)	1.90 (1.05-3.45)	0.035

unknown cause. Removing stage IV, the LRR and OS remain significant for high HDL vs not, 97 vs 68% LRR, $P = .004$, 84% vs 59%, $P = .015$. The trend remains for OS in stage IV patients but is not significant suggesting using the entire cohort makes the results more conservative rather than biasing them.

3.5 Discussion

In this study we demonstrated that lipoproteins VLDL and HDL had opposite effects on IBC cells grown as mammospheres and on these cells' radioresistance *in vitro*, and the level of both lipoproteins predicted 5-year OS in IBC patients.

Previous studies have shown that cholesterol and lipoproteins LDL and VLDL are significantly elevated in breast cancer patients compared to controls.³⁵ In addition, hypercholesterolemia was discovered to be an independent risk factor for breast cancer in postmenopausal women.¹⁰⁹⁻¹¹¹ The cholesterol metabolite 27-hydroxycholesterol increased ER-positive breast tumor growth *in vivo* through a liver X receptor agonist mechanism.²¹ Furthermore, mice fed a high cholesterol diet developed more aggressive tumors and had significantly more metastasis in a breast cancer model.²⁰ We have previously shown statins, which inhibit de novo cholesterol synthesis, were shown to radiosensitize inflammatory breast cancer cells *in vitro*.⁶⁵ Herein we observed *in vitro*, intracellular levels of cholesterol in IBC cells are altered by HDL and VLDL treatment, ultimately modifying response to radiation by reducing (HDL) or increasing (VLDL) self-renewal of these cells, as shown by our mammosphere-forming assay. Importantly, a clinical correlation between HDL and local control after post-mastectomy radiation is identified. Of course independent validation is critical and it

remains to be seen if this effect is limited to IBC as might be predicted by the in vitro work by Martin and van Golen showing unique cholesterol properties in IBC cells.²²

Cholesterol plays an important role in cell membrane integrity and fluidity.¹¹² Several growth factor signaling receptors are located in cholesterol rich domains in the membrane and RPPA analysis of statin treated and untreated cells suggested signaling downstream of EGFR were regulated by statins. Interestingly, EGFR is well described to be activated by association with cholesterol mediated lipid rafts in the membrane.^{113,114} We examined these as potentially regulated signals in direct lipoprotein treatments HDL inhibited phosphorylation of EGFR, Akt, and FOXO3a and VLDL was observed to increase these phosphorylated levels. Phosphorylated Akt is downstream of EGFR and has been shown to be important in radiation resistance.¹¹⁵⁻¹¹⁷ FOXO3a is a tumor suppressor, inactivated by phosphorylation, which increases cell death following DNA damage from radiation.¹¹⁸ We showed DNA damage repair was decreased with HDL treatment and increased in VLDL treatment following radiation (**Figure 13**). We speculate that cholesterol enriched IBC membranes promote EGFR signaling through lipid raft formation and that HDL can directly reduce lipid raft mediated signaling by removing cholesterol from the membrane.

3.6 Conclusions

Our results demonstrate a potential role for dyslipidemia in radiation sensitivity and survival among IBC patients. We also highlight the urgent need for further studies on the potential benefit of aggressively correcting dyslipidemia in IBC patients at the time of diagnosis and the role of altering lipid profiles in IBC patients without clinical dyslipidemia.

Chapter IV

MiR-33a Regulates Radiation Sensitivity to High Density Lipoprotein in Breast Cancer

4.1 Abstract

Purpose: We previously showed that high-density lipoprotein (HDL) radiosensitizes inflammatory breast cancer (IBC) cells *in vitro* (*chapter 3*). Since the microRNA miR-33 family controls expression of ABCA1, a cellular transporter of cholesterol efflux to HDL, we hypothesized that differences in miR-33a expression in breast cancer cell lines correlates with their radiation sensitivity following exposure to HDL *in vitro*.

Materials and Methods: miR-33a expression was analyzed by reverse transcriptase–polymerase chain reaction in five cell lines representing common clinical breast cancer subtypes. Cell lysates were subjected to western blot analysis for ABCA1 expression. Clonogenic survival *in vitro* was determined following overexpression or knockdown of miR-33 via transfection of miR-33a mimic or anti-miR-33a constructs, respectively. The radiosensitivity of the breast cancer cell lines was quantified at baseline and following HDL treatment. Kaplan-Meier analysis determined the clinical impact of miR-33a expression on distant relapse-free survival (DRFS) of 210 cases downloaded from the Oxford breast cancer dataset.

Results: Expression levels of miR-33a varied among the five breast cancer cell lines. Clonogenic survival following 24 hours of HDL treatment was decreased in response to irradiation in the low miR-33a–expressing cell lines, SUM 149 and KPL4, but survival following HDL treatment did not change in the high miR-33a–expressing cell lines, MDA-MB-231 and SUM 159. In the high miR-33a–expressing cell lines, anti-miR-33a transfection decreased cell survival. Conversely, in the low miR-33a–expressing cell lines, miR-33a mimic reversed the HDL-induced radiosensitization observed previously. Breast cancer patients in the top quartile of miR-33a expression had markedly lower rates of DRFS than the bottom quartile ($p= 0.0228$, log-rank test).

Conclusions: Our results reveal miR-33a regulates HDL-induced radiation sensitivity in breast cancer.

4.2 Introduction

The majority of breast cancer patients receive radiation therapy because of its efficacy in reducing local recurrence.¹¹⁹ We do not yet have biological markers that accurately identify patients with the highest likelihood of recurrence following radiation therapy. Therefore, our ability to personalize the decision to administer radiation therapy is limited. Our group has found a relationship between outcomes of an aggressive type of breast cancer, inflammatory breast cancer (IBC), and cholesterol regulation, including local recurrence after radiation therapy and overall survival. A previous study showed that IBC patients taking a statin (a drug that lowers serum cholesterol level) had lower local recurrence rates following radiation therapy than patients not taking a statin, and preclinical studies showed that statins radiosensitized both IBC and non-IBC cells.⁶⁵ A follow-up study looked at the same patient cohort to determine if lipoproteins (which transport serum cholesterol) also predicted patient outcome. IBC patients with a higher than normal level of high-density lipoprotein (HDL, which transports cholesterol from peripheral tissues to the liver), had longer overall survival than patients with a lower than normal HDL level. *In vitro* studies showed that treatment of IBC cell lines with HDL led to increased radiation sensitivity.¹²⁰

Preclinical studies have supported the role of cholesterol regulation in breast cancer progression, mostly in estrogen receptor–positive (ER+) subtypes.^{20,21,121} The exact mechanism by which cholesterol promotes breast cancer progression and radiation resistance is not clearly understood. The main mediators of cholesterol efflux from intracellular to extracellular HDL are the adenosine triphosphate–binding cassette (ABC) transporters ABCA1 and ABCG1.³⁶ ABCA1 deficiency in cancer cells was shown to increase cellular cholesterol, leading to increased cell survival.¹²² In prostate cancer, hypermethylation of the *ABCA1* promoter, which

led to elevated cholesterol levels, was detected in high-grade prostate cancers but not in normal prostate tissues.¹²³

MicroRNAs (miRNAs) are noncoding small RNAs that repress translation and cleave mRNA by binding to the 3'-untranslated region of their target gene.¹²⁴ MiR-33 is known to inhibit the expression of cholesterol transport genes, including *ABCA1* and *ABCG1*.¹²⁵ MiR-33 silencing *in vivo* increased hepatic expression of *ABCA1* and plasma HDL levels.³⁷ Additional studies showed that miR-33 can promote glioma-initiating cells¹²⁶ and was upregulated in patients with chemoresistant osteosarcoma.^{127,128}

The connection between cholesterol transport and radiation sensitivity has not been described. We hypothesized that expression of miR-33 regulates HDL-induced breast cancer radiosensitivity by inhibiting *ABCA1* and *ABCG1*. We tested our hypothesis by manipulating the expression of miR-33 in high and low miR-33-expressing breast cancer cell lines and testing their radiation sensitivity in the presence or absence of HDL. Our results indicate that miR-33a expression correlates with HDL-induced radiosensitivity *in vitro*.

4.3 Materials and Methods

Cell culture and drugs

Five breast cancer cell lines were chosen to represent a variety of breast cancer subtypes. SUM149 (ER-/human epidermal growth factor receptor 2 [HER2]-) and SUM159 (ER-/HER2-) cells were obtained from Asterand (Detroit, MI). Both types of cells were cultured in Ham F12 medium supplemented with 10% fetal bovine serum (FBS), 1 µg/mL hydrocortisone, 5 µg/mL insulin, and 1% antibiotic-antimycotic. MDA-231 cells (ER-/HER2-) were obtained from

American Type Culture Collection (Manassas, VA) and were cultured in α -media supplemented with 10% FBS, 1 $\mu\text{g}/\text{mL}$ hydrocortisone, 1 $\mu\text{g}/\text{mL}$ insulin, 12.5 ng/mL epidermal growth factor, sodium pyruvate, nonessential amino acids, 2 mM glutamine, and 1% antibiotic-antimycotic. KPL4 IBC cells (ER-/HER2+) were maintained in DMEM/F-12 medium supplemented with 10% FBS. MCF-7 (ER+/HER2-) cells were cultured as monolayer in modified Eagle's medium (MEM) supplemented with 10% FBS, 0.1 mM nonessential amino acids, 1 mM sodium pyruvate, 5 $\mu\text{g}/\text{ml}$ insulin, 1 $\mu\text{g}/\text{ml}$ hydrocortisone, and 1% antibiotic-antimycotic. Human HDL was purchased from Sigma-Aldrich (St. Louis, MO). For all experiments including lipoproteins, serum was not added to the medium to prevent contamination/confounding of the results by the cholesterol and lipoprotein contained in FBS.

RNA isolation and miRNA PCR

Total RNA was isolated from the cell lines by using Trizol reagent (Invitrogen, Grand Island, NY) according to manufacturer's protocol. To isolate the miRNAs, RNA isolated from cell lines was reverse-transcribed to cDNA using the TaqMan MicroRNA Reverse Transcription kit (Applied Biosystems, Foster City, CA) following the manufacturer's instructions and subjected to polymerase chain reaction (PCR) in a Thermal Cycler (BioRad, Hercules, CA) at 16°C for 30 minutes, 42°C for 30 minutes, and 85°C for 5 minutes. The expression levels of mature miR-200 family members were measured by quantitative reverse-transcription PCR (qRT-PCR) using TaqMan MicroRNA assays (Applied Biosystems) according to the manufacturer's instructions. The reaction was performed in a 7300 real-time PCR system (Applied Biosystems) at 95°C for 10 minutes and 40 cycles at 95°C for 15 seconds and 60°C for 60 seconds. U6 was used as a reference.

Immunoblotting

For immunoblotting, cells were subjected to lysis in 1× RIPA lysis buffer containing 1 μM phenylmethylsulfonyl fluoride, and 40 μg of protein was subjected to electrophoresis on sodium dodecyl sulfate–polyacrylamide gels with a concentration gradient of 4% to 20% (Invitrogen). Membranes were incubated with primary antibodies anti-ABCA1 and anti-ABCG1 (Novus Biologicals, Littleton, CO). Actin antibody was used as a loading control.

miR-33a and anti-miR-33a transfection

SUM149 and KPL4 were transfected with 40 nM miRIDIAN miR-33a mimic (miR-33a) and SUM159 and MDA-MB-231 cells with 60 nM miRIDIAN miRNA inhibitor (anti-miR-33a) (Dharmacon, Lafayette, CO), utilizing Oligofectamine (Invitrogen), for 48 hours. All control samples were treated with an equal concentration of a non-targeting control mimic sequence or negative control inhibitor sequence to detect non–sequence-specific effects. miR-33a overexpression and knockdown were verified by using qRT-PCR as described above.

Clonogenic survival assays

Clonogenic viability of the breast cancer cells was tested in triplicate in standard monolayer conditions. Following 48 hours of miR-33a or anti-miR-33a transfection, cells were washed with phosphate-buffered saline solution (PBS) and supplemented with serum-free medium with or without 100 μg/mL of HDL for a total of 24 hours. After treatment with HDL, cells were irradiated and then incubated for 14 days. Cells were then subjected to crystal violet staining (10%) to mark colonies with 50 cells or more (≥ 300 -μm diameter). Survival curves were obtained for all groups, and curves were fitted on the basis of the linear-quadratic model. Cells were irradiated by using a ^{137}Cs source (Shepherd Irradiator, J.L. Shepherd and Associates, San Fernando, CA).

Patient outcomes

The Oxford breast cancer dataset was downloaded from the U.S. National Center for Biotechnology Information (NCBI) GEO website (GSE22216).¹²⁹ Expression values for miR-33a (Probe set id = ILMN_3167691) and clinical characteristics for 210 cases were extracted. These data were subjected to a Cox regression model for distant recurrence-free survival duration (DRFS) with inclusion of the following covariates: patient age, tumor size and grade, nodal involvement, ER expression, and quartile of miR-33 expression.

Statistical analysis

For *in vitro* studies, statistical significance of differences between groups was determined by using the Student *t*-test and calculated by Origin software (OriginLab, Northampton, MA).

4.4 Results

miR-33 and cholesterol transporter expression levels are inversely correlated in breast cancer cells

We first set out to determine the expression levels of miR-33a and miR-33b in five breast cancer cell lines that represent a variety of breast cancer subtypes. The claudin-low breast cancer cell lines (SUM159 and MDA-231) had significantly higher miR-33a expression than the other cell lines, but only SUM159 had higher levels of both miR-33a and miR-33b expression (**Figure 15A**). As ABCA1 and ABCG1 are known targets of miR-33,¹²⁸ we next tested the expression levels of these proteins in these cells through western blotting. Expression of ABCA1 and ABCG1 was inversely correlated with miR-33 expression in four of the five cell lines (**Figure 15B**).

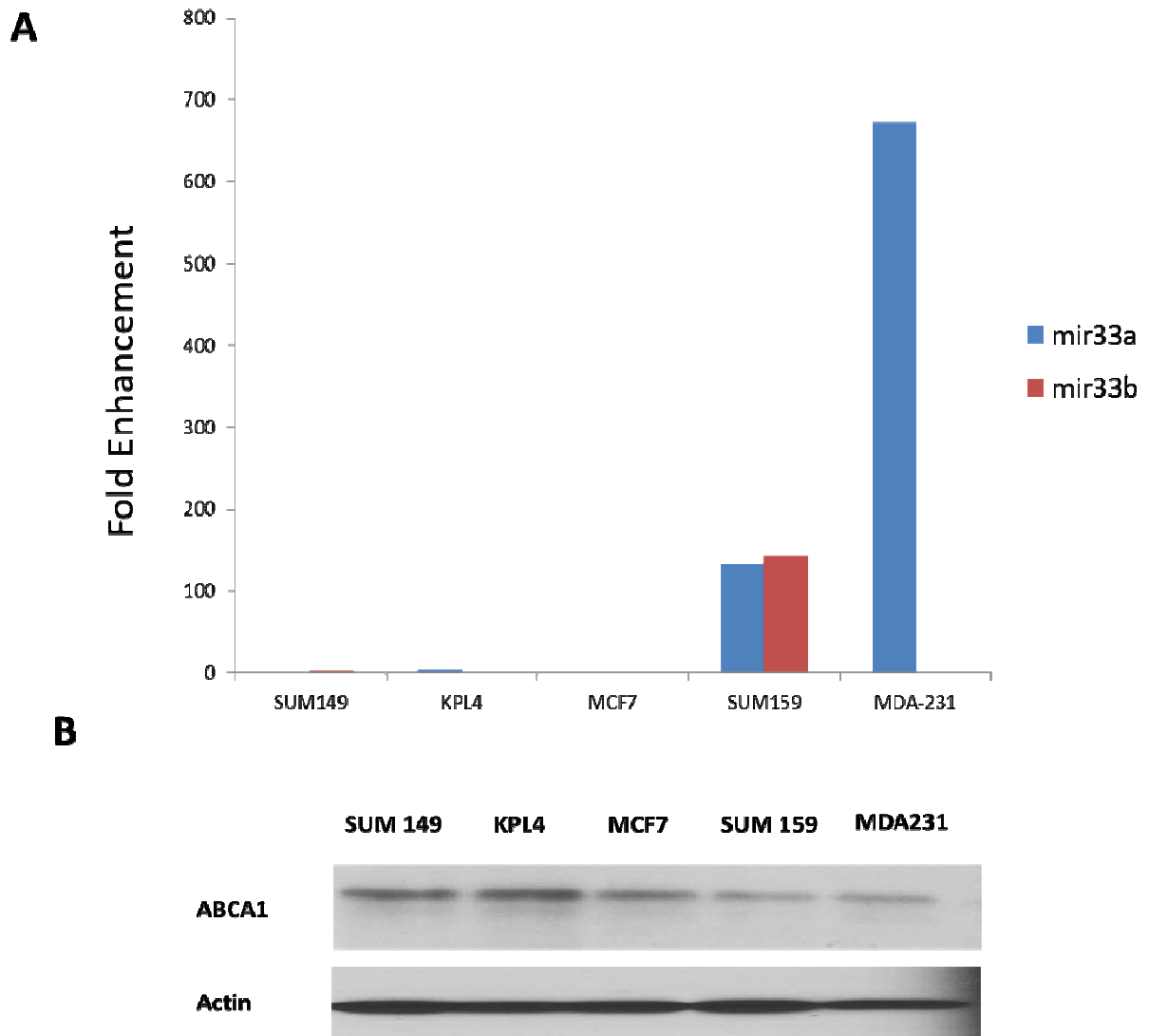


Figure 15. Expression of miR-33 and the protein product of its target gene *ABCA1* in breast cancer cells were detected by qRT-PCR and western blotting. (A) miR-33 expression was significantly higher in claudin-low cell lines (SUM159 and MDA-231) than in claudin-high cell lines (KPL4 and SUM149). (B) Expression of *ABCA1* was higher in KPL4 and SUM149 cells than in SUM159 and MDA-231 cells. MCF7 cells were used as a reference.

HDL-induced radiation sensitivity is correlated with miR-33a expression

Our next experiments were designed to compare the impact of HDL on the sensitivity to radiation of the low miR-33a-expressing cell lines (SUM149 and KPL4) and the high miR-33a-expressing cell lines (MDA-231 and SUM159). Treatment with HDL (100 μ g/mL) for 24 hours radiosensitized the low miR-33a-expressing cell lines, as previously reported (**Figure 16A,B**).¹²⁰ In the high miR-33a-expressing cell lines MDA-231 and SUM159, however, HDL had a slight radioprotective effect (**Figure 16 C, D**). These results suggest that level of expression of miR-33a correlates with radiation sensitivity in response to HDL treatment *in vitro*.

Targeting miR-33a expression alters HDL-induced radiation response

To investigate the role of miR-33a in radiation sensitivity of breast cancer cells in response to HDL, we knocked down miR-33a in SUM159 and MDA-231; two breast cancer cell lines that express miR-33a endogenously (**Figure 15A**). Antagonism of endogenous miR-33a increased ABCA1 protein expression in both cell types (**Figure 17A, B**), resulting in radiosensitization of MDA-231 treated with HDL, a reversal of the results observed in wild-type cells (**Figure 17C**). Knockdown of miR-33a in SUM159 also resulted in radiosensitization in the presence of HDL (**Figure 17D**).

Next, transfection of SUM149 and KPL4 (low miR-33a-expressing cells) with miR-33a mimic decreased ABCA1 protein expression (**Figure 18A, B**). Overexpression of miR-33a resulted in the reversal of HDL-induced radiosensitization seen previously. Transfection of SUM149 cells with miR-33a mimic resulted in no change in the clonogenic survival following HDL treatment (**Figure 18C**), and a similar result was observed in KPL4 cells (**Figure 18D**).

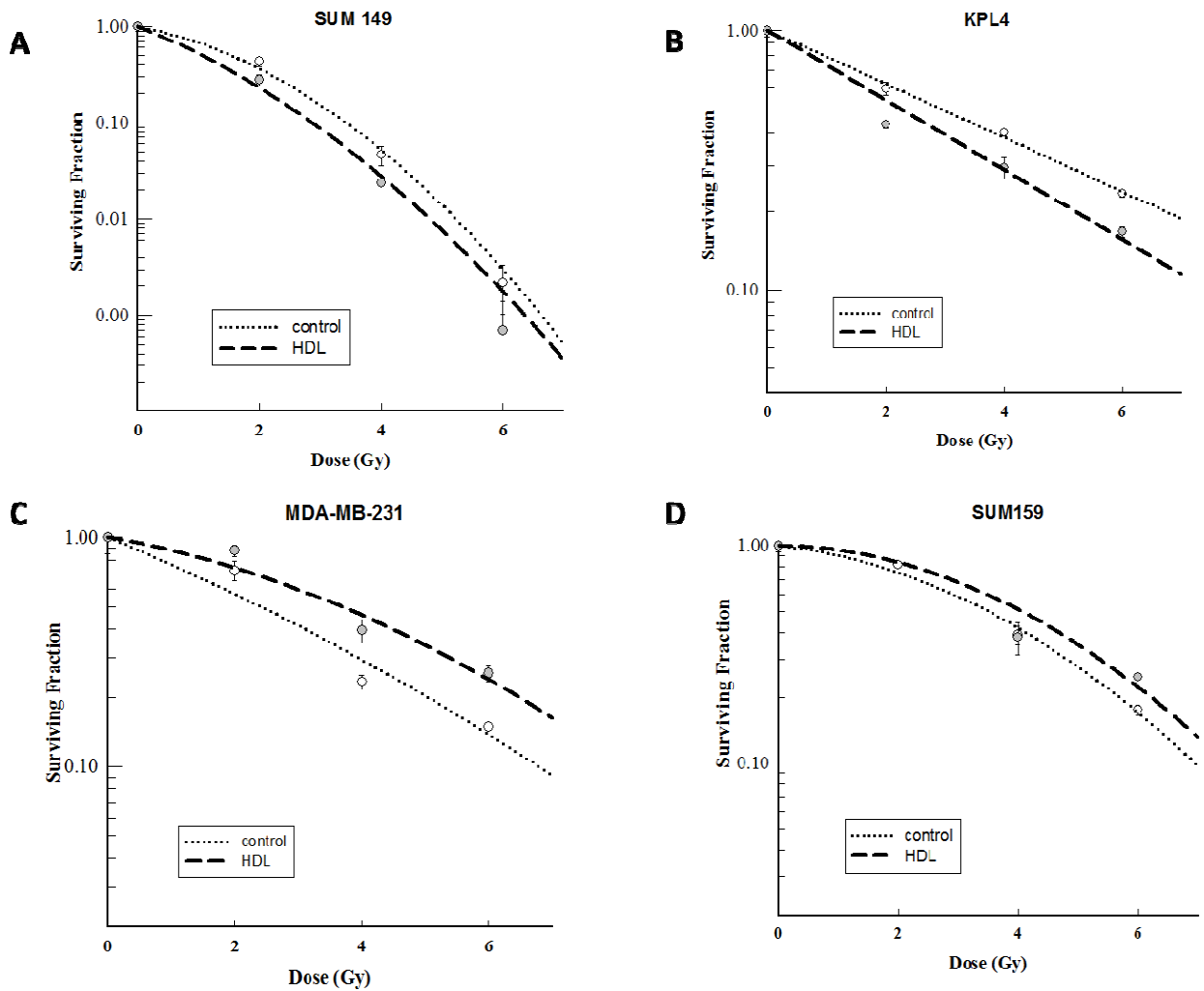


Figure 16. Clonogenic survival curves indicate effect of miR-33 on HDL-induced radiation sensitivity of breast cancer cells. Clonogenic survival assays of (A) SUM149, (B) KPL4, (C) MDA-MB-231, and (D) SUM159 breast cancer cells irradiated at different doses (x axis) with or without HDL pretreatment. HDL pretreatment comprised incubation for 24 hours with HDL 100 $\mu\text{g}/\text{mL}$. After irradiation, colonies were allowed to form for 14 days. The surviving fractions with or without HDL at each dose of radiation are shown.

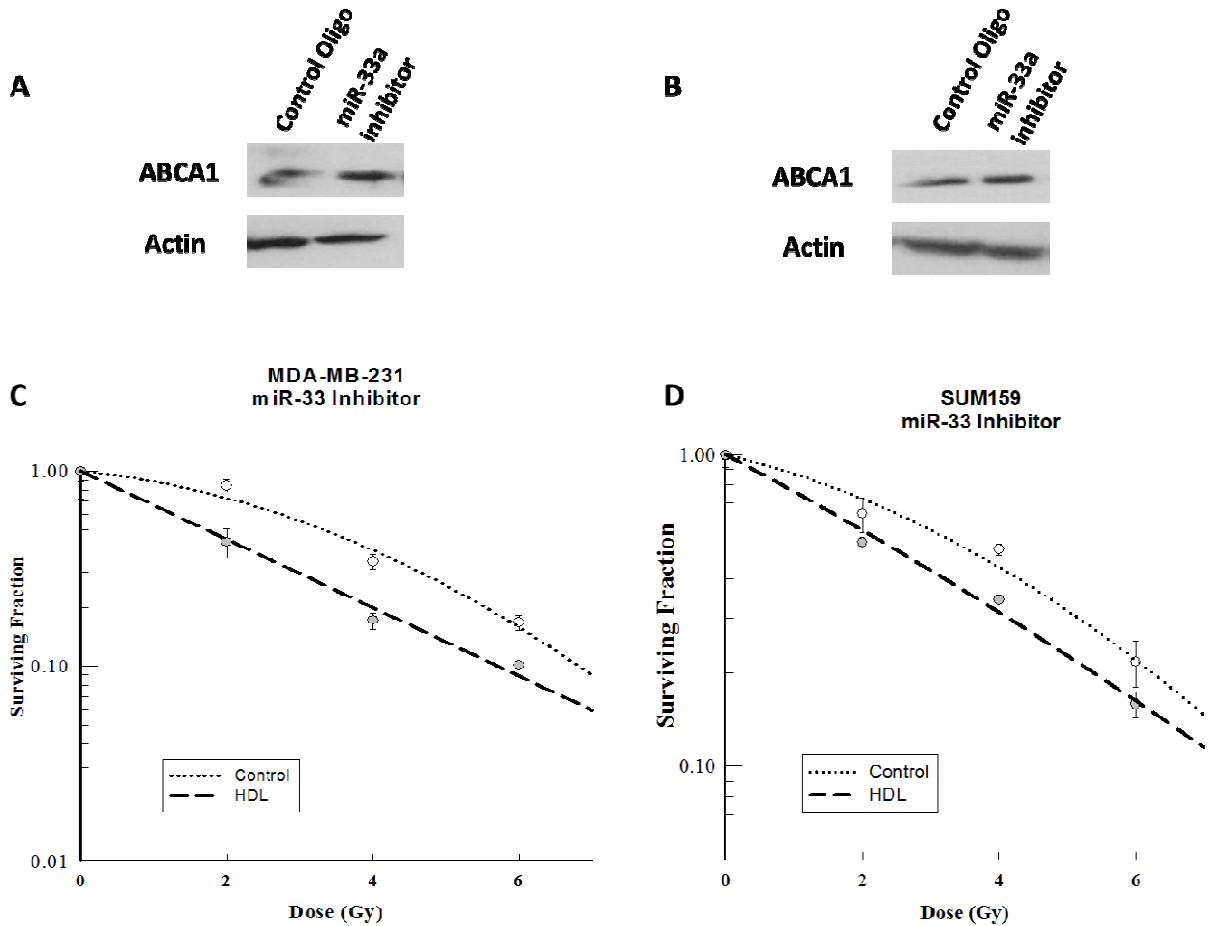


Figure 17. Inhibition of miR-33a increases HDL-induced radiation sensitivity. (A,B)

Knockdown of miR-33a in SUM159 and MDA-MB-231 cell lines resulted in greater ABCA1 expression than in cells transfected with control oligonucleotides. (C,D) Clonogenic survival assays of miR-33a knockdown MDA-MB-231 and SUM159 breast cancer cells irradiated at different doses (x axis) with or without HDL pretreatment. HDL pretreatment comprised incubation for 24 hours with HDL 100 $\mu\text{g}/\text{mL}$. After irradiation, colonies were allowed to form for 14 days. The surviving fractions with or without HDL at each dose of radiation are shown.

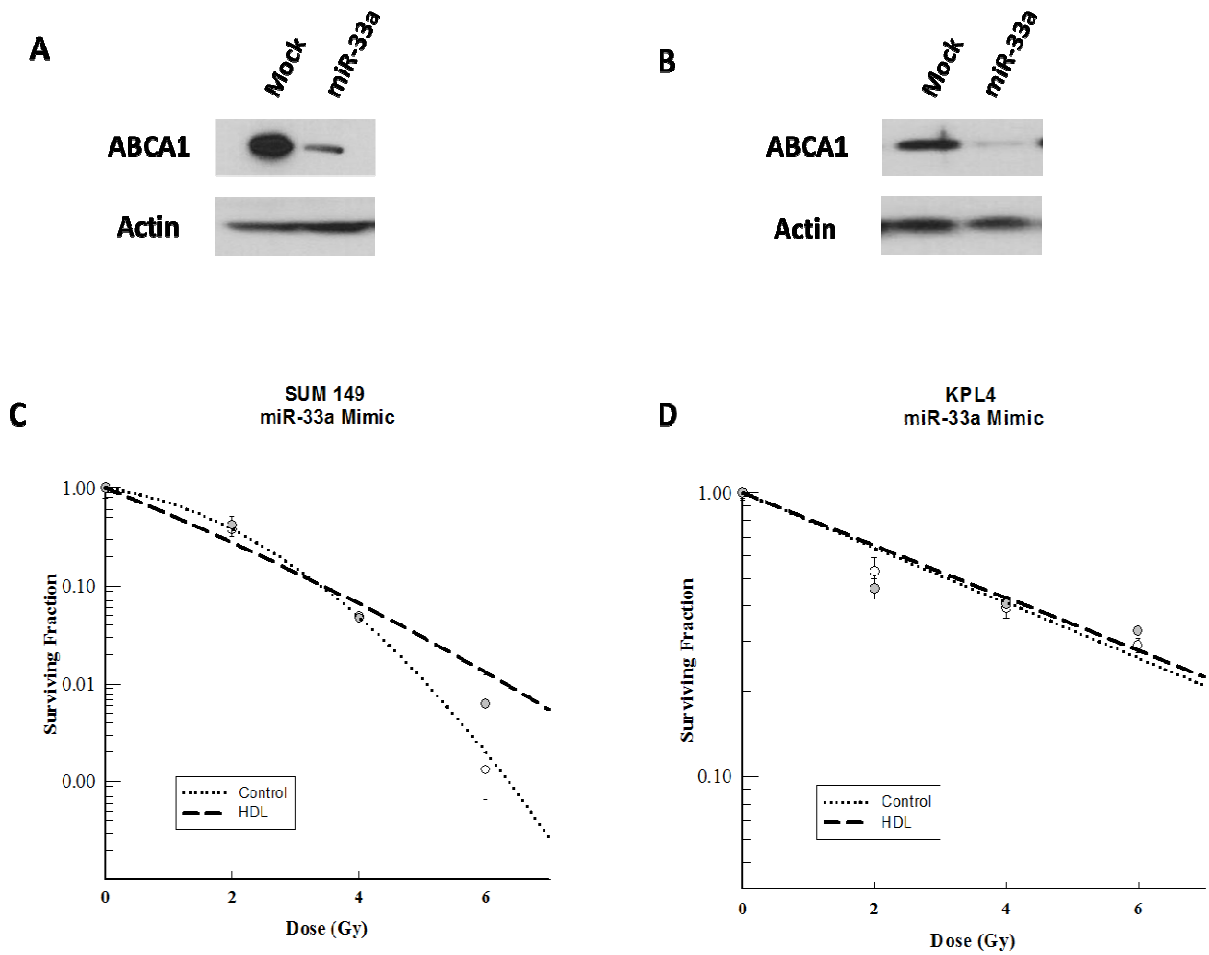


Figure 18. Ectopic expression of miR-33a inhibits HDL-induced radiosensitization. (A, B) Overexpression of miR-33a via transfection of miR-33 mimic in SUM149 and KPL4 cells resulted in lower ABCA1 expression than mock transfection. **(C, D)** Clonogenic survival assays of miR-33a–overexpressing SUM149 and KPL4 breast cancer cells irradiated at different doses (x axis) with or without HDL pretreatment. HDL pretreatment comprised incubation with HDL 100 μ g/mL for 24 hours. After irradiation, colonies were allowed to form for 14 days. The surviving fractions at each dose of radiation are shown.

These results led us to conclude that miR-33a regulates the radiation response to HDL in breast cancer cells.

miR-33a expression in breast cancer patients predicts local recurrence

We downloaded a previously published dataset from the NCBI GEO website to determine prognostic significance of miR-33 on DRFS¹²⁹. The 210 cases analyzed were separated into four quartiles based on miR-33a expression (**Figure 19A**). We tested for differences (log-rank test) in DRFS by miR-33a expression quartile and found a significant difference in DRFS between the highest and lowest quartiles ($p=0.0228$) (**Figure 19B**). Multivariate Cox regression analysis for DRFS revealed that patients in quartile 4 (greatest miR-33a expression) had a DRFS hazard ratio of 2.0, which was nearly significantly higher than that of patients in quartile 1 ($p=0.076$). These results suggest that miR-33a expression warrants further investigation as a potential biomarker for breast cancer patient outcome.

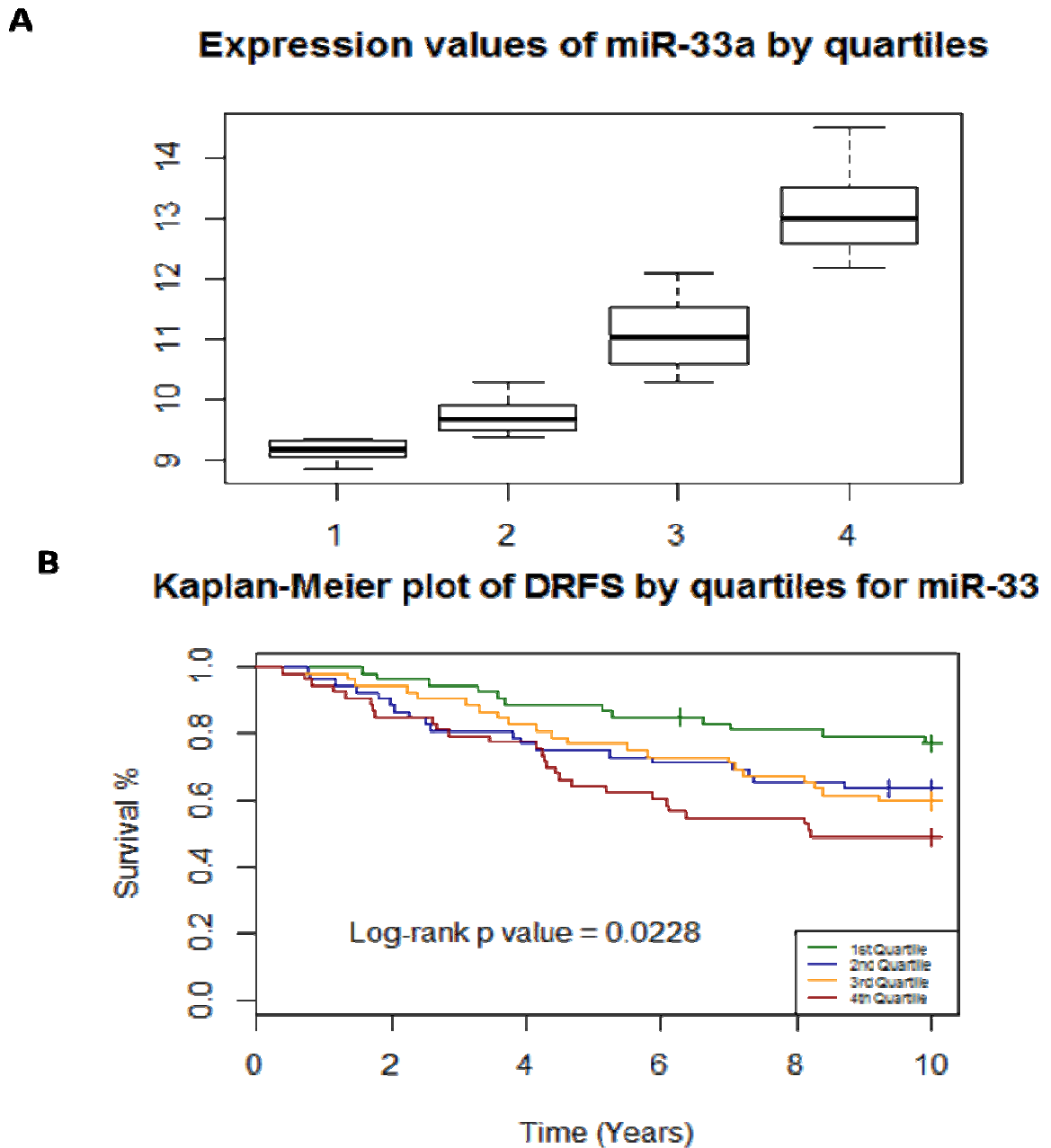


Figure 19. High serum miR-33a level is associated with worse outcome in breast cancer patients. (A) Expression of miR-33a in tumors from 210 patients whose data were downloaded from the Oxford breast cancer dataset was separated into four quartiles. (B) Kaplan-Meier curves representing distant recurrence-free survival (DRFS) for each miR-33a quartile.

4.5 Discussion

In this study, we found that expression of miR-33a was inversely correlated with HDL-induced radiation sensitivity in breast cancer cells. Our results support the importance of cholesterol metabolism in breast cancer cells' response to radiation therapy.

MiR-33 is expressed in various cell types and tissues, and miR-33 is a key regulator of cholesterol homeostasis by regulating the cholesterol transport that removes cholesterol stores from cells to HDL lipoproteins.¹²⁸ Our results show that miR-33 expression varies in breast cancer cell lines. The regulation of intracellular cholesterol is complex and is influenced by genetic factors and by posttranscriptional mechanisms.¹³⁰ ABCA1 functions as the primary gatekeeper in regulating removal of excess free cholesterol from tissues by effluxing cellular cholesterol to lipid-free apoA-1, resulting in the formation of HDL particles.¹³¹ ABCA1 is known to be associated with HDL from the observation that patients with *ABCA1* mutations (i.e., Tangier disease) have a deficiency in plasma HDL.¹³² Recent studies showed evidence that miR-33 functions as a negative feedback loop triggered by low intracellular cholesterol. Transcription of miR-33 is stimulated under low sterol conditions and represses genes, including *ABCA1* and *ABCG1*, that are involved in cholesterol export.³⁷ Furthermore, that miR-33 controls both liver HDL biosynthesis and cellular efflux of cholesterol to nascent HDL particles has been shown by *in vivo* manipulation of miR-33 levels leading to changes in both circulating HDL levels and cellular cholesterol concentrations.³⁷

In this study, we showed for the first time that targeting miR-33a expression in breast cancer cells can alter the effect of HDL on response to radiation. These conclusions were based on the response of four cell lines and so might not reflect processes in the intact body, although it was previously showed a strong correlation between *in vitro* radiation sensitivity and patient

radiation response.⁶⁵ Inhibition of miR-33a increased the radiosensitization of high miR-33–expressing breast cancer cell lines in response to HDL treatment, while promotion of miR-33a expression in low miR-33a–expressing breast cancer cell lines inhibited HDL-induced radiosensitization. The ability of miR-33 to negatively regulate genes that regulate cholesterol transport makes it an attractive potential target for cancer therapy. Targeting miR-33 may have the potential to both raise the level of circulating HDL and increase its radiosensitizing effect. Furthermore, since miRNAs can be rapidly measured in blood samples, our finding that miR-33 can predict DRFS suggests that miR-33 is a potential biomarker for breast cancer outcome for patients with a high HDL level.

4.6 Conclusions

Our results reveal that miR-33 regulates HDL-induced radiosensitivity.

Chapter V

Mesenchymal Stem Cells and Macrophage Cross-Talk through IL-6 to Promote Inflammatory Breast Cancer Cell Invasion and Self Renewal

5.1 Abstract

Background: Inflammatory breast cancer (IBC) is responsible for 10% of breast cancer deaths. The hallmarks of IBC are skin involvement and a high propensity to metastasize. “Normal” breast tissue from women with an IBC diagnosis had significantly greater macrophage infiltration and increased cells with stem cell markers compared to non IBC “normal” breast tissue. These changes were present prior to diagnosis in two patients where pre-IBC biopsies were available. Therefore, we hypothesized changes in the normal breast microenvironment prior to tumor formation contributes to the IBC phenotype.

Methods: To study our hypothesis we used a co-culture system to measure the interactions between normal macrophages (Raw 264.7 cell line), bone-marrow derived mesenchymal stem cells (MSCs), and IBC cells (SUM 149 and MDA-IBC3). Conditioned media (CM) from MSC culture was added to macrophages overnight. The macrophages were subsequently analyzed for their surface markers and cytokine production. Reciprocally, MSCs were “educated” by macrophages by co-culturing polarized M2 macrophages with MSCs at a 1:1 ratio. MSCs and cancer cells were co-cultured in trans-wells (Boyden chambers) for 24 hours. Migration and invasion in vitro was determined by adding MSCs or IBC cells to the insert of the trans-well and cultured in combination with either parental MSCs or educated MSCs for 24 hours. After co-culture, IBC cells were analyzed for their ability to invade and form mammospheres. For mouse models, SUM 149 cells and mesenchymal stem cells were co-injected orthotopically of immunocompromised mice on day 0. On day 1 and continuing weekly, either IgG or anti-CSF1 antibodies were injected intraperitoneally up until the tumors reached a volume of 500 mm³.

Results: The addition of MSC CM to the macrophage culture for 24 hours polarized the macrophages into a M2 phenotype expressing CD206 and arginase 1. When M2 macrophages

were co-cultured with MSCs, the number of MSCs migrating increased 2 fold with the addition of M2 macrophages compared to media alone, M1, or unstimulated macrophages ($P < 0.05$). IBC cells showed a 2 fold enhancement of invasion towards M2 educated MSCs compared to either uneducated MSCs, or media alone ($P < 0.05$). IBC cells co cultured with M2 educated MSCs grew 3 fold more mammospheres compared to IBC cells grown with uneducated MSCs ($P < 0.01$). Lastly, the addition of IL-6 neutralizing antibody or simvastatin inhibited the effects of educated MSCs on IBC cells. In vivo, the treatment with anti-CSF1 significantly delayed tumor growth and time to tumor resection compared to the IgG group. In addition the anti-CSF1 group had fewer mice with skin invasion and local recurrence.

Conclusions: Herein we demonstrate reciprocal tumor interactions between normal cells in the IBC microenvironment. MSC and macrophages can influence each other to increase the tumor promoting influence of each on IBC cells. Our results suggest IL-6 a mediator of these tumor promoting influences and is important for the IBC induced migration of MSCs.

5.2 Introduction

Inflammatory breast cancer is a devastating, variant of breast cancer that presents with skin changes on the breast and spreads rapidly. These signs are caused by blockage of lymphatics and skin invasion, not by classic inflammation.¹² To date, studies comparing IBC and non-IBC tumor cells have identified more similarities than differences. Our preliminary studies of non-tumor containing breast tissue at least 5 cm away from IBC tumor cells have identified interesting differences that the number of CD 68+ cells (macrophages) was significantly elevated in IBC normal adjacent tissues compared to non-IBC.¹³³ In two cases where pre-malignancy biopsies were available, the macrophage infiltrate was demonstrated 10 years prior to diagnosis suggesting the normal breast tissue was altered prior to the initiation of cancer. Macrophages are known to fall into two categories, Th1 stimulated pro-inflammatory or Th2 stimulated, anti-inflammatory.¹³⁴ Tumor associated macrophages (TAMs) are prognostic in non-IBC and have been shown in vivo to promote lymphatic emboli, the hallmark of IBC.¹³⁵ The state and plasticity of macrophages (tumor or normal adjacent) in IBC patients and models has not been examined nor has their interaction with other cell types in the IBC stroma been examined. Lack of such knowledge is important because these cells are potentially mediators of field effects that lead to the clinical characteristics of IBC, and targets for prevention and treatment of IBC.

We have shown that mammosphere cultured MSCs promote tumor stem cells and in vivo growth¹³⁶, and Liu et al have shown that ALDH1+ MSCs do the same.¹³⁷ While numerous studies have demonstrated that MSCs mediate macrophage polarization and function¹³⁸ far fewer have looked at the impact of macrophages on MSCs.

We hypothesized that pre-malignant macrophage-educated MSCs in the breast mediate the IBC phenotype including diffuse migration, skin involvement, and treatment resistance. This hypothesis is based on our data demonstrating in vitro and in vivo data demonstrating MSCs promote stem cell surrogates and skin invasion of IBC, as well as published studies highlighting the role of macrophage-educated MSCs in supporting the hematopoietic stem cell niche.

5.3 Materials and Methods

Cell culture

The IBC cell line SUM149 was obtained from Asterand (Detroit, MI, USA) and cultured in Ham's F-12 media supplemented with 10% fetal bovine serum (FBS), 1 mg/mL hydrocortisone, 5 mg/mL insulin, and 1% antibiotic-antimycotic. Human-derived bone marrow MSCs were obtained from EMD Millipore (Billerica, MA, USA) (Part #SCC034, Lot N61710996) and cultured in alpha minimum essential medium (MEM) supplemented with 20% FBS and 1% penicillin/streptomycin/glutamine. The mouse macrophage cell line RAW 264.7 was purchased from ATCC and maintained in DMEM supplemented with 10% FBS.

Transwell co-culture assay

5×10^4 of either breast cancer cells, macrophages, or MSCS/well were seeded in the lower compartment of 12 well transwell polyethylene terephthalate (PET) permeable supports or 75 mm polycarbonate transwell inserts pore size 8 μm (Corning), respectively, and let to adhere overnight. The medium was replaced serum free media one hour before adding 5×10^4 of breast cancer cells, macrophages, or MSCS into the upper compartment of the transwell inserts. The co-cultures were incubated for 24 hours without medium change in a humidified chamber at 37°C.

Migration and Invasion Assays

Cells were assayed for their ability to migrate or invade using the cytoselect 24 well Cell Migration and Invasion Assay Kit (Cell Bio Labs). The Cell Migration portion of this kit uses polycarbonate membrane inserts (8 μm pore size) in a 24- well plate. The membrane serves as a barrier to discriminate migratory cells from non-migratory cells. 5.0×10^4 cells were seeded in the top of the insert on the membrane. Finally, the cells are removed from the top of the membrane and the migratory cells are stained with crystal violet and quantified. The Cell Invasion Assay portion of this kit uses a 24-well plate containing polycarbonate membrane inserts (8 μm pore size); the upper surface of the insert membrane is coated with a uniform layer of dried basement membrane matrix solution. This basement membrane layer serves as a barrier to discriminate invasive cells from non-invasive cells. Invasive cells are able to degrade the matrix proteins in the layer, and ultimately pass through the pores of the polycarbonate membrane. Finally, the cells are removed from the top of the membrane and the invaded cells are stained and quantified.

Sphere Formation Assay

To generate primary mammospheres, cells in monolayer culture were pre-treated with lipoproteins for 24 hours, and untreated cells were grown in standard mammosphere medium (serum-free, growth factor enriched medium). Low attachment plates were used as described previously [14]. For secondary mammosphere assay, cells from primary mammospheres were dispersed with 0.05% trypsin, seeded in ultra-low attachment plates (20,000 cells/ml) in mammosphere medium, incubated for seven days and counted. A concentration of 10 $\mu\text{g/mL}$ was used in the in vitro experiments to simulate normal cholesterol lipoprotein levels found in human blood samples. After 24 hours treated and untreated cells were suspended into single

cell suspension and plated in mammosphere conditions (further referred to as 3D culture) at concentration of 20,000 cells/mL.

Co-injection of SUM149 cells with MSCs

SUM149 cells were injected into the cleared mammary fat pads of female immunocompromised SCID/Beige mice (3 to 5 weeks old), with or without 5% MSCs, in a total of 2.5×10^5 cells per injection. SUM149 were labeled with dual luciferase-GFP reporter gene (pFULG) vector. For co-injections, 2.5×10^4 MSCs were premixed with SUM149 cells and the mixture co-injected in the #4 (left side) mammary fat pad of the mice. Transplants were allowed to grow to 500 mm^3 (monitored with caliper measurements) and were then resected in a survival surgery.

Follow-up of tumor-skin involvement and metastasis development

Tumor-skin involvement was accessed visually during primary tumor growth (loss of fur at tumor site, redness and thickness of skin), during tumor excision (tumors firmly connected with skin) and after tumor resection (loss of fur, redness, and thickness of skin at any site). The development and localization of metastasis was monitored by bioimaging the luciferase signal (IVIS Spectrum system (Caliper Life Sciences, Hopkinton, MA, USA)). Findings between groups were compared with Fisher's exact test.

In vivo treatment with anti-CSF1

After SUM149 cells with 10% MSCs had been injected into the cleared mammary fat pads of female immunocompromised SCID/Beige mice as described above, mice were injected intraperitoneally (IP) with either IgG or anti-CSF1 (a dose of 0.5 mg per injection), started on day 1 following injection of cells and continued for weekly up until the time of resection.

5.4 Results

Characterizing the interactions between MSCs and macrophages in a co-culture system

To characterize the differences in MSC activation under the influence of macrophages, we cultured RAW 241.7 mouse macrophage cells with human derived MSC cells in an in vitro transwell co-culture assay (**Figure 20**). The transwell setting allowed us to investigate the effect of soluble mediators on MSC activation since direct cell contact of these cells was inhibited by a polyethylene terephthalate (PET) membrane (pore size 8 μm). Macrophages grown for 24 hours in MSC CM displayed a higher degree of M2 type markers in CD206 and Arginase-1 compared with macrophages alone (**Figure 21A**). The MSCs grown in the M2 macrophage co-culture migrated at a 2 fold increase compared to MSCs grown with serum alone, M0, or M1 macrophages ($p < 0.05$) (**Figure 21B**). Furthermore, The MSCs co-cultured with M2 macrophage co-culture secreted 1.6 fold more IL-6 compared to MSCs grown with serum alone, M0, or M1 macrophages ($p < 0.05$) (**Figure 21C**). To investigate the impact of M2 educated MSCs influence on IBC cells, we took MSCs from M2 co culture and co-cultured them with IBC cells for 24 hours. We found M2 educated MSCs co-cultured with IBC cells (SUM149 and IBC3) migrated significantly more than uneducated MSCs compared with the controls ($p < 0.05$) (**Figure 21D**). This effect could be reversed with the addition of an anti-IL-6 antibody during the 24 hour co-culture with IBC cells (**Figure 21D**).

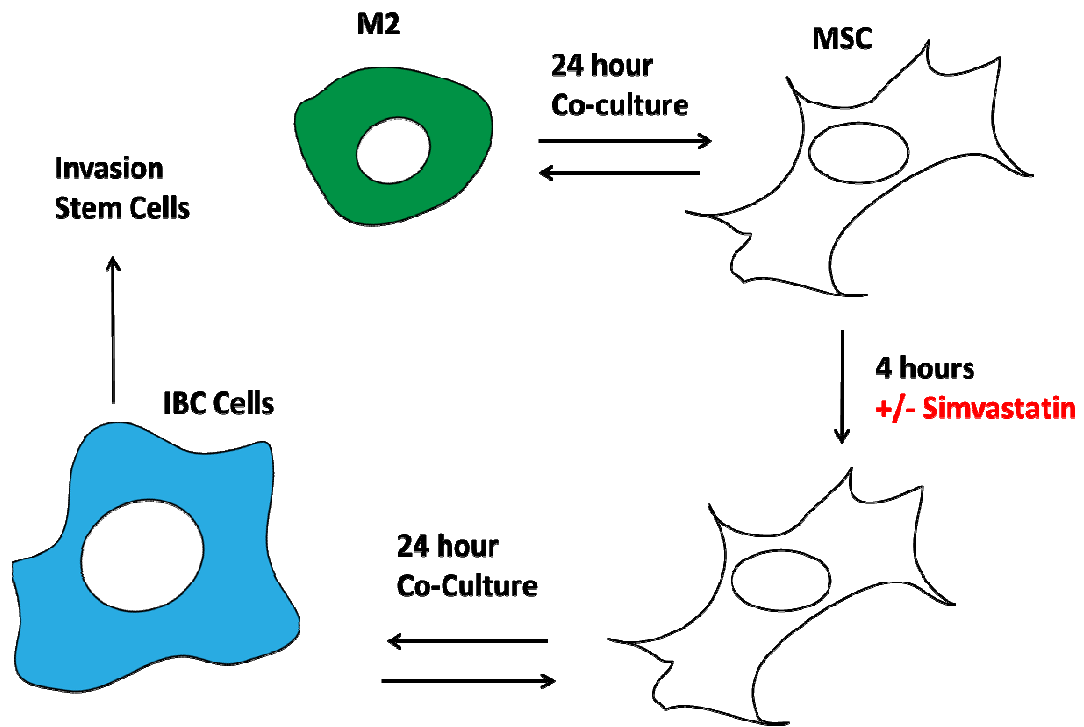


Figure 20. Model of Co-Culture System. Macrophages were polarized with IL-4/IL-13 to become M2 macrophages prior to co-culture. Using a Boyden chamber MSCs were seeded with M2 macrophages for 24 hours. Macrophages were removed and MSCs were washed with either PBS or Simvastatin for 4 hours. MSCs were then co-cultured in Boyden chambers with IBC cells for 24 hours. Following co-culture MSCs and IBC cells were analyzed for migration, invasion, and mammosphere formation.

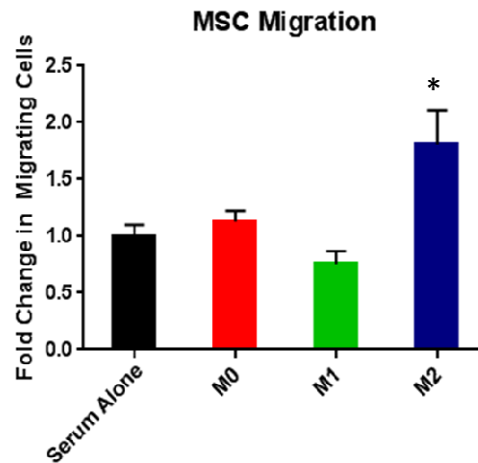
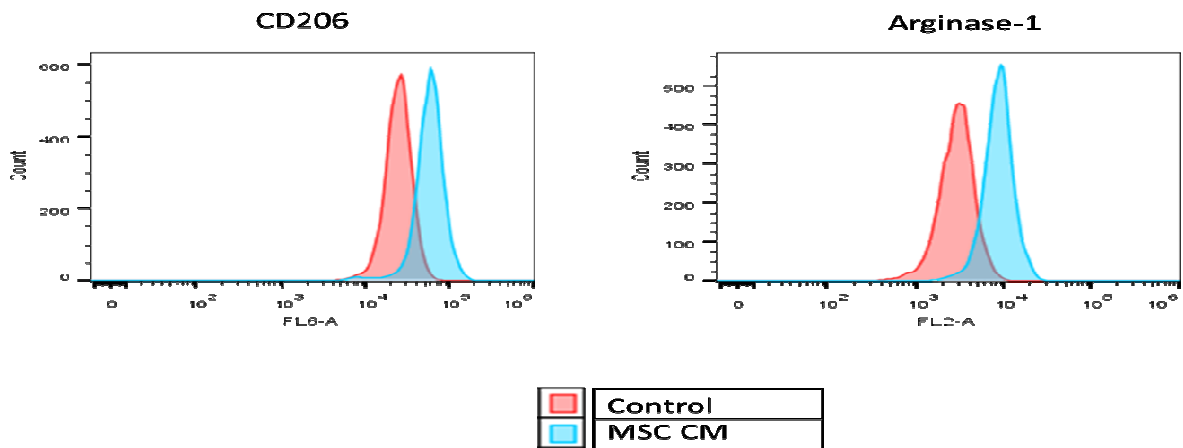
A**B**

Figure 21. MSCs and M2 macrophages cross-talk through IL-6. Following co-culture of with either unpolarized (M0), LPS induced (M1), or IL-4/IL-13 induced (M2), and MSCs for 24 hours. **(A)** The number of MSCs that passed through the transwell membrane after 24 hours was counted. Significant differences are shown as follows: *, $P < 0.05$ for unpaired 2-tailed Student's t-test ($n = 3$). **(B)** Macrophages were grown in the presence of MSC conditioned media (CM) (1:1) for 24 hours and then stained with either anti-CD206 or anti-arginase-1 antibodies and submitted for flow cytometry analysis.

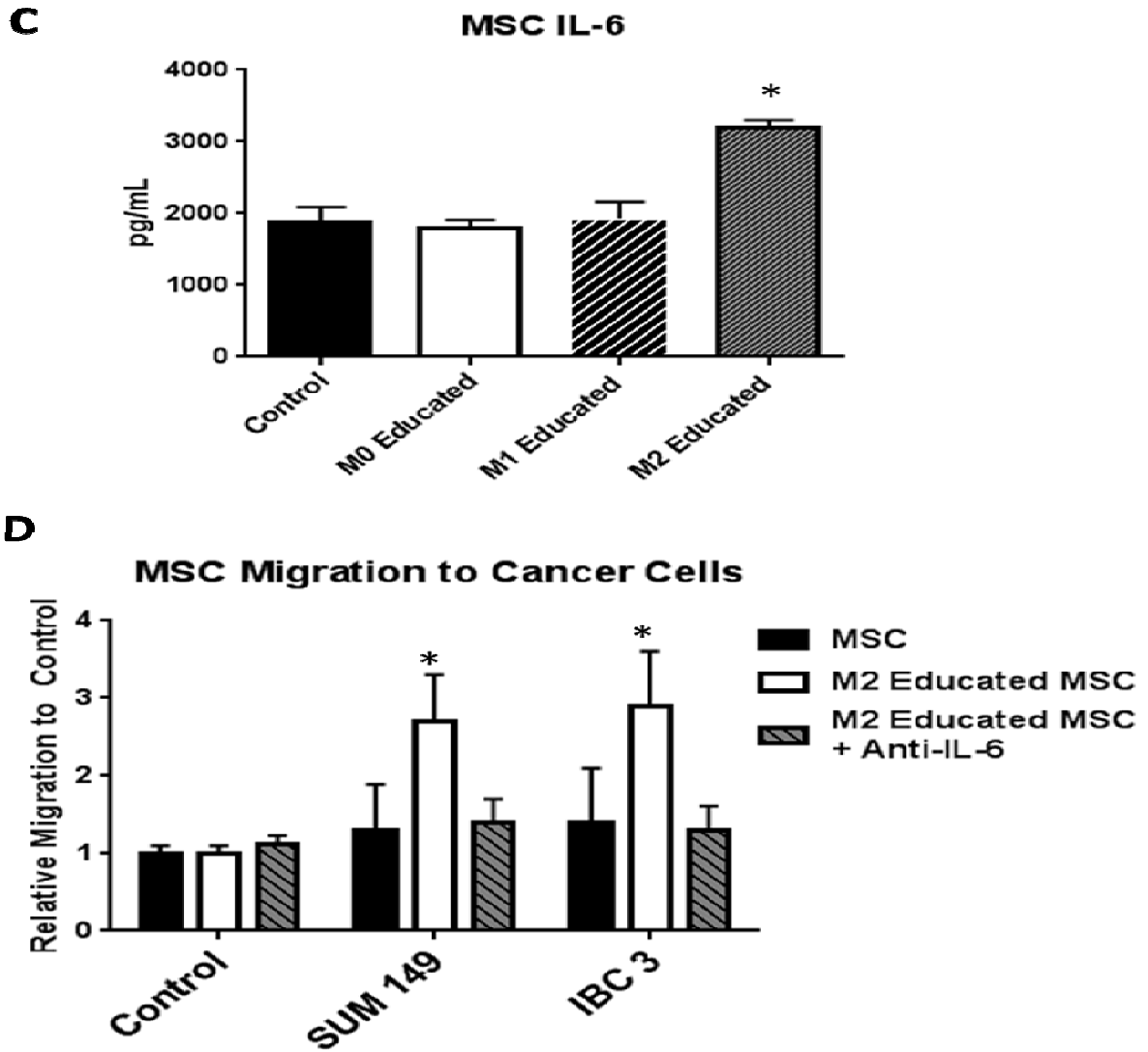


Figure 21. MSCs and M2 macrophages cross-talk through IL-6. (C) Following 24 hours of co-culture with macrophages and MSCs, MSCs were washed with PBS 3X and 4 hours later the supernatant was collected. ELISA was performed for IL-6. (D) Following 24 hours of co-culture with M2 macrophages, the “educated” MSCs were co-cultured with SUM149 and IBC3 cells for 24 hours with or without anti-IL6 antibodies. The number of MSCs that passed through the transwell membrane after 24 hours was counted. Significant differences are shown as follows: *, $P < 0.05$ for unpaired 2-tailed Student’s t-test ($n = 3$).

Crosstalk between educated MSCs and IBC cells increases IBC invasion and self-renewal through IL-6

We next investigated how the IBC cells would respond following 24 hours co-culture with M2 educated MSCs. The IBC cells co-cultured with M2 educated MSCs had a higher number of invading cells in both the uneducated and M2 educated MSCs co-culture in SUM149 cells (**Figure 22A**). Only IBC3 cells grown in co-culture with M2 educated MSCs observed to have a 3 fold increase in invasion (**Figure 22B**). The increase in invasion of M2 educated MSCs was inhibited with the addition of the anti-IL-6 antibodies during the co-culture (**Figure 22A, B**). We next tested for mammosphere formation following co-culture. Both MSCs and M2 educated MSCs increased SUM149 and IBC3 sphere formation efficiency, but only M2 educated MSCs increased sphere formation to a 2 fold higher number compared to MSCs. Once again this effect on mammosphere formation could be blocked with anti-IL6 antibodies (**Figure 22 C, D**).

Simvastatin blocks IL-6 secretion and inhibits the effects of M2 educated MSCs on IBC invasion and self-renewal

Numerous studies have shown that statins increase infiltrating macrophages in other diseases and recently Fujita et al further showed that statins also promote the pro-inflammatory macrophage subtypes in renal disease.¹³⁹ Due to the large data showing statins have both an anti-tumor effect in breast cancer and also have the ability to alter the inflammatory response we tested the effects of statins in our co-culture system. Simvastatin significantly reduced by over 2 fold the secretion of IL-6 in both uneducated and educated MSCs (**Figure 23A**).

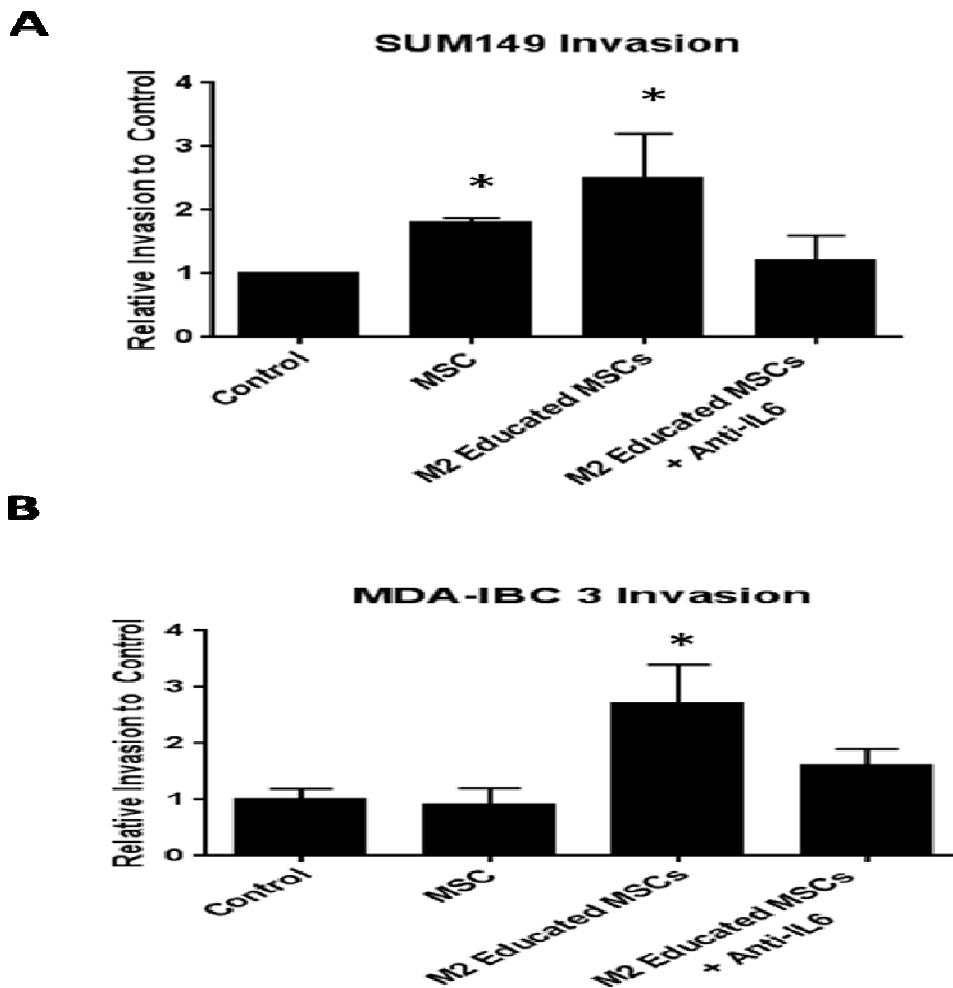


Figure 22 Crosstalk between educated MSCs and IBC cells increases IBC invasion and self-renewal through IL-6. Following 24 hours of co-culture with M2 macrophages, the “educated” MSCs or parental MSCs were co-cultured with (A) SUM149 or (B) MDA-IBC3 for 24 hours with or without anti-IL6 antibodies. The number of IBC cells that invaded through the basement membrane transwell after 24 hours was counted. Significant differences are shown as follows: *, $P < 0.05$ for unpaired 2-tailed Student’s t-test ($n = 3$).

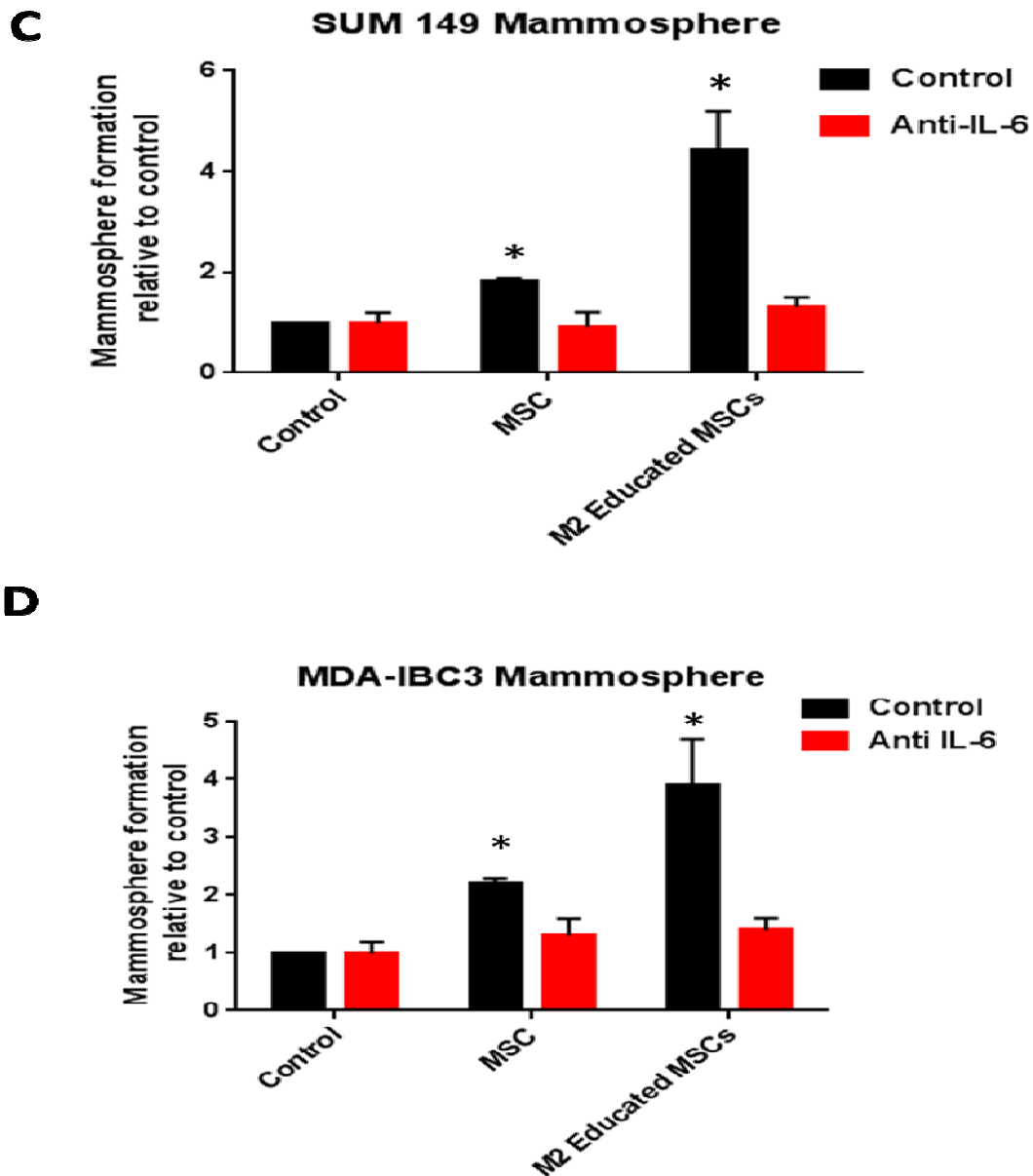


Figure 22 Crosstalk between educated MSCs and IBC cells increases IBC invasion and self-renewal through IL-6. Following 24 hours of co-culture with M2 macrophages, the “educated” MSCs or parental MSCs were co-cultured with (C) SUM149 or (D) MDA-IBC3 for 24 hours with or without anti-IL6 antibodies. IBC cells were seeded in self-renewal promoting suspension culture conditions. Significant differences are shown as follows: *, $P < 0.05$ for unpaired 2-tailed Student’s t-test ($n = 3$).

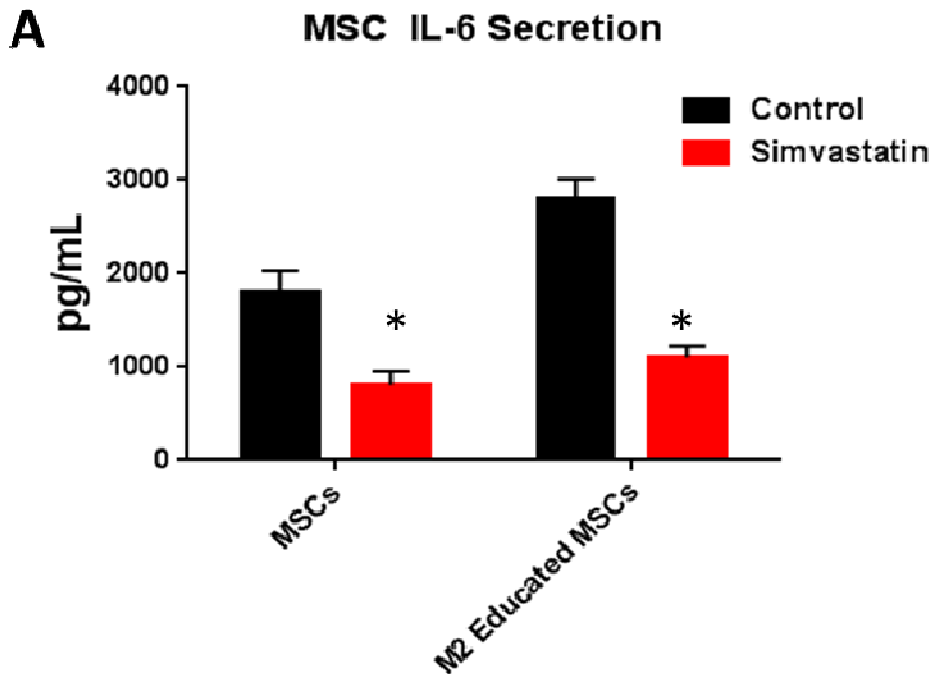


Figure 23. Simvastatin blocks IL-6 secretion and inhibits the effects of M2 educated MSCs on IBC invasion and self-renewal. (A) Macrophages were polarized with IL-4/IL-13 to become M2 macrophages prior to co-culture. Using a Boyden chamber MSCs were seeded with M2 macrophages for 24 hours. Macrophages were removed and MSCs were washed with either PBS or simvastatin (2.5 μ M) for 4 hours. The supernatant was collected and ELISA performed for IL-6.

To test if simvastatin could inhibit the previous results mediated through IL-6 secretion, we designed an experiment wherein MSCs or M2 educated MSCs were first treated with simvastatin for 4 hours prior to being co-cultured with IBC cells for 24 hours. Half of the groups received simvastatin treated MSCs and the other half received both simvastatin treated MSCs and IL-6 cytokines. As observed before M2 educated MSCs significantly increased the number of mammospheres and invading cells. The treatment of the MSCs with simvastatin prior to co-culture with SUM149 cells blocked the increase in both invasion and mammosphere formation. The rescue experiment with IL-6 reversed the effects of simvastatin on M2 educated MSC inhibition of SUM149 mammosphere and invasion (**Figure 23 B, C**).

Blocking M2 macrophage recruitment in the in vivo IBC model delayed tumor formation and decreased

Colony stimulating factor-1 (CSF1) is a key cytokine involved in recruitment and activation of tissue macrophages.¹⁴⁰ Denardo et al showed an antibody against CSF1 blocked the binding of CSF1 to its CSF1 receptor and inhibited tumor associated macrophages (TAM) within the breast tumor.¹⁴¹ Cell suspensions of SUM149 cells and human bone marrow derived MSCs were prepared from monolayer cultures. In both groups, SUM149 and MSCs (9:1 ratio) were mixed and then co-injected into the mammary cleared fat pad as previously described.⁵⁷ 24 hours following co-injection of tumor cells and MSCs, we started treatment with either anti-CSF1 antibody or IgG intraperitoneally. We continued with injections of these antibodies weekly up until the week before resection of the tumor.

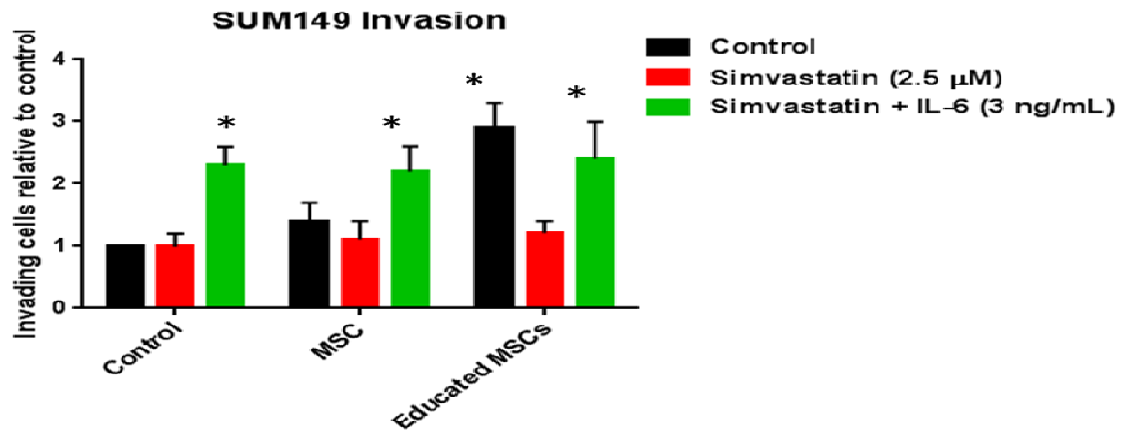
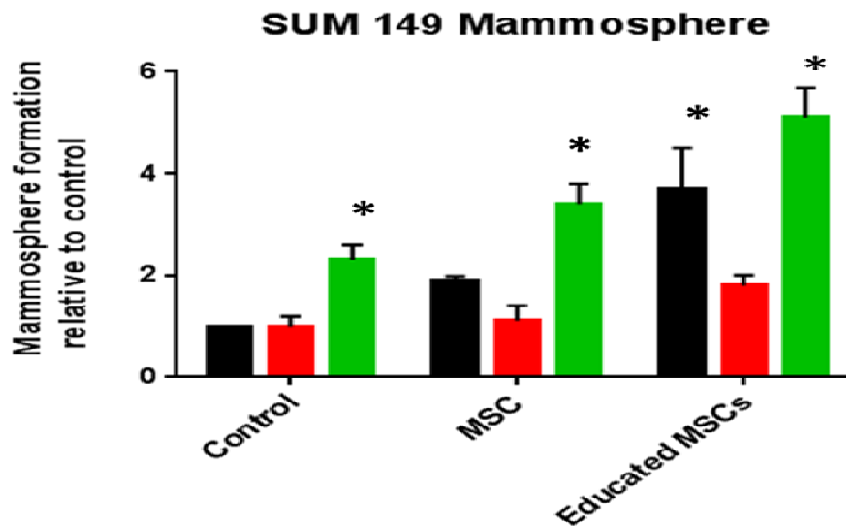
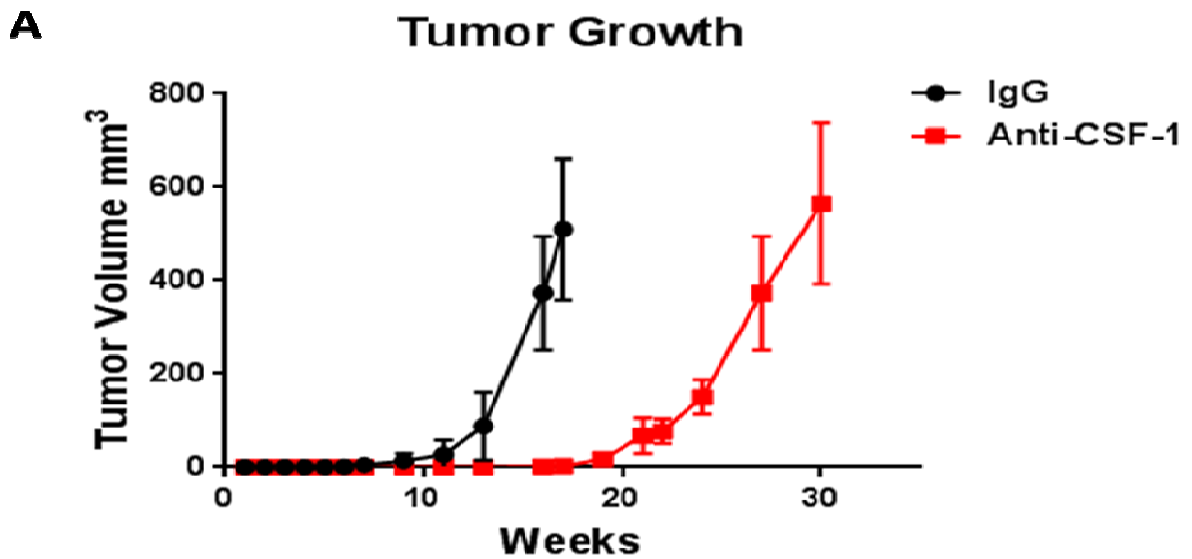
B**C**

Figure 23. Simvastatin blocks IL-6 secretion and inhibits the effects of M2 educated MSCs on IBC invasion and self-renewal. MSCs and educated MSCs either pre-treated with simvastatin or simvastatin plus IL-6 for 4 hours were co-cultured with SUM149 cells for 24 hours. **(B)** Following co-culture the the number of SUM149 cells that invaded through the basement membrane transwell after 24 hours was counted. Significant differences are shown as follows: *, P < 0.05 for unpaired 2-tailed Student's t-test (n = 3). **(C)** SUM149 cells were seeded in self-renewal promoting suspension culture conditions. Significant differences are shown as follows: *, P < 0.05 for unpaired 2-tailed Student's t-test (n = 3).

Monitoring tumor growth we observed that tumor latency was significantly shorter in the IgG treated mice (68.3 days vs. 124.4 days, $P < 0.001$; **Figure 24A**), and the time for the anti-CSF1 group to reach 500 mm³ was slower than tumors in the control IgG group (105.7 days vs. 209.3 days, $P < 0.001$; **Figure 24A**). At the time of resection of the primary tumor, we recorded whether or not the tumor had grossly attached and invaded into the epidermis layer. The group of mice treated with anti-CSF1 had significantly less number of mice with invading tumors into the skin compared to the IgG (7/10 IgG vs 1/10 Anti-CSF1 $p=0.02$). Further, following resection we monitored for metastasis using live bioimaging to detect luciferase signal. Within 8 weeks, mice developed similar rates of spontaneous metastasis to the lung (not shown), but the IgG group had significantly more events of local recurrence compared to the anti-CSF1 group (9/10 IgG vs 4/10 $p=0.05$) (**Figure 24B**). The tumors were collected following resection and stained with macrophage antibodies F4/80 and the M2 marker CD206 and analyzed by flow cytometry. The anti-CSF1 group had a lower percentage of F4/80+ cells compared to the IgG but the result was not significant (**Figure 24C**). However when analyzing the double positive F4/80+ CD206+ cells, the anti-CSF1 group had a significantly lower percentage of double positive cells, TAMs, compared to the IgG group ($p < 0.01$) (**Figure 24D**). This suggests the anti-CSF1 antibody specifically blocks type 2 macrophage recruitment into the tumor.



B

	IgG	CSF1
Skin Invasion	7/10	1/10*
Local Recurrence	9/10	4/10*

Figure 24. Blocking M2 macrophage recruitment in the in vivo IBC model. Cell suspensions of SUM149 cells and human bone marrow derived MSCs were prepared from monolayer cultures. In both groups, SUM149 and MSCs (9:1 ratio) were mixed and then co-injected into the mammary cleared fat pad as previously described. 24 hours following co-injection of tumor cells and MSCs, we started treatment with either anti-CSF1 antibody or IgG intraperitoneally. We continued with injections of these antibodies weekly up until the week before resection of the tumor. (A) Weekly tumor measurements were made and (B) the presence of skin invasion and following tumor resection the presence of local recurrence was recorded.

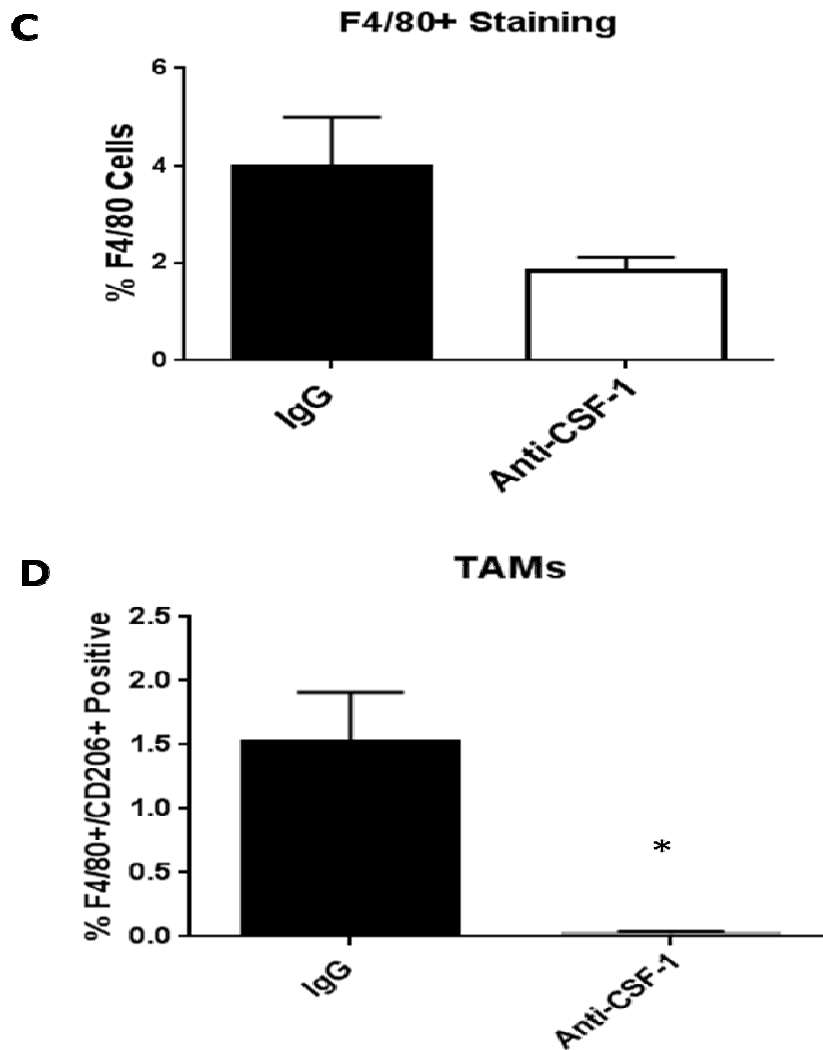


Figure 24. Blocking M2 macrophage recruitment in the in vivo IBC model. Tumors from both groups were resected and collected for digestion. Tumor samples were either stained with (C) anti-F4/80 antibodies or (D) both anti-F4/80 and anti-CD206 antibodies. The results of 3 replicates are shown by flow cytometry.

5.5 Discussion

Macrophages are a major component of the innate immunity and are distributed throughout every tissue. After circulating monocytes differentiate into macrophages they invade into tissues and increase immune reactions to the response of injury.¹⁴² In addition, macrophages remove cellular debris and clear dead or apoptotic cells.¹⁴³ Macrophages can be polarized in the environment in response to different stimuli.¹⁴⁴ The two classes of polarized macrophages are classically activated (M1) alternatively-activated (M2) macrophages.¹⁴⁵ M1 and M2 secrete different cytokines, and M2 is known to secrete IL-10, TNF- α and IL-6.¹⁴⁶

Upon addition of MSC CM to macrophages, we observed an increase in expression of cell surface marker CD206 and Arginase 1, markers up-regulated in M2 macrophages. Additional studies by Ortiz et al. showed MSC-conditioned media inhibits the capacity of RAW-264.7 cells activated by silica or LPS to secrete TNF α ¹⁴⁷, and Nemeth et al. investigated the effect of mouse BM-derived MSCs in a murine model of septicemia and showed LPS-stimulated macrophages produced more IL-10 when co-cultured with BM-derived MSCs.¹⁴⁸ In our study MSCs co-cultured with only M2 macrophages had an increased level of IL-6 secretion. We speculate that this crosstalk between MSCs and macrophages (increasing the M2 phenotype) and between M2 macrophages and MSCs (increasing the secretion of IL-6) can be a promoter of IBC. In fact, these M2 educated MSCs did enhance IBC cell invasion and mammosphere formation. IL-6 signaling in tumor cells increases tumor growth by promoting tumor invasiveness, metastasis and angiogenesis.¹⁴⁹ Secretion of IL-6 leads to recruitment of metastatic cells out of the circulation to the primary tumor sites.¹⁵⁰

In addition to the effects on the tumor itself, recent studies show IL-6 controls tumor growth by activating the normal stromal cells located in the tumor microenvironment. For example, STAT3 activation initiated by IL-6 in tumor-associated endothelial cells, TAM, and

MSCs induces their ability to express VEGF and bFGF in a feed-forward loop that positively regulates angiogenesis within tumor tissues.¹⁵¹ Recent evidence suggests that MSCs coordinate with tumor cells that triggers increased IL-6 production, which correlates with accumulation of MSCs.¹⁵²

In a *in vivo* study, the combined treatment of MMTV-PyMT mice with PTX and anti-CSF1 antibody slowed primary tumor development, reduced development of high-grade carcinomas, and decreased pulmonary metastasis by 85% and increased CD4+ and CD8+ T-cell infiltration in primary tumors. CSF1R blockade by PLX3397 depleted TAMs, but not neutrophils.¹⁵³ Similarly in our *in vivo* experiment, CSF1 inhibition delayed SUM149 tumor initiation and reduced the percentage of TAMs (F4/80⁺ CD206⁺). Importantly since IBC is characterized by rapid skin involvement, the reduction we saw in skin invasion is noteworthy. These results suggest that the induction of the IBC phenotype with the addition of MSC cells is mediated by the host's macrophage infiltration, specifically M2 macrophages. Future studies are warranted looking at targeting M2 type macrophages in patients with IBC. Our preliminary data suggest statins would be a well-tolerated FDA approved drug to begin with.

5.6 Conclusions

We demonstrate reciprocal tumor interactions between normal cells in the IBC microenvironment. MSC and macrophages can influence each other to increase the tumor promoting influence of each on IBC cells. Our results suggest IL-6 a mediator of these tumor promoting influences and is important for the IBC induced migration of MSCs. Currently we are investigating the *in vivo* interactions between macrophages and MSCs in an orthotopic IBC mouse model.

Chapter VI

Discussion

6.1 Overall Conclusions

Taken together, the body of work presented here makes a strong case that cholesterol plays a major role in the pathogenesis of aggressive breast cancers. The therapeutic concentration of simvastatin inhibited TNBC cells in vitro CSC formation, invasion, and in vivo metastasis. The mechanism of action was shown to be through increasing the expression of FOXO3a, a tumor suppressor, by inhibiting its phosphorylation and subsequent degradation. Furthermore, FOXO3a mRNA in patients could predict for metastasis free survival. If the effects seen by simvastatin were through reducing cellular cholesterol concentrations, then one would expect to see the same effects with HDL, which removes cellular cholesterol. Indeed in Chapter 3, HDL removed cellular cholesterol and, as seen with simvastatin, blocked the phosphorylation of FOXO3a. HDL inhibited mammosphere formation and VLDL had the opposite effect in IBC cells in vitro. The translational piece to this study was the radiosensitization of IBC cells with HDL in vitro. This was shown to be caused by the increase in DNA damage after HDL treatment.

Not all breast cancers are alike. This was highlighted by the results in Chapter 4. The expression of miR-33 varied between breast cancer subtypes. In the IBC cells the expression of miR-33 was low and in the claudin low TNBC cells it was high. Since miR-33 regulates cholesterol efflux to HDL, we characterized the effects of HDL on each subtype with radiation treatment. We found that miR-33 regulates radiosensitivity to HDL treatment and that high miR-33 expression in patients predicted for poor outcomes. These results further show the importance of cholesterol in resistance to therapies.

Lastly co-culturing M2 macrophages and MSCs resulted in an “educated” MSC that in turn promoted IBC cell invasion and increased self-renewal. The educated MSCs secreted IL-6

which if blocked reversed the effects seen on invasion and self-renewal. Importantly, simvastatin inhibited the effects of educated MSCs on IBC cells by blocking IL-6 secretion. These results suggest that statins could be not only targeting the tumor cells, as shown in earlier chapters, but could have an additional anti-tumor effect by targeting the supporting stromal cells in the microenvironment.

6.2 Research Significance

The significance of this thesis work is influential, from demonstrating the relevance of the effect of cholesterol regulation in aggressive breast cancer subtypes, identifying the impact of lipoproteins in radiation therapy, identifying biomarkers for tumors susceptible to this radiation therapy, and demonstrating the importance of normal cells that make up the IBC microenvironment.

Targeted therapies are the focus of cancer therapy today. This work suggests we might want to take a step back and look at some non-targeted therapies. Targeted pathways can be ineffective in cancer due to redundancy and cross talk between pathways that provide for resistance. Further, tumor heterogeneity provides increased difficulties in targeting single mutated genes. This thesis provides the framework to begin to study drugs, such as statins, that have multiple targets. These already FDA approved drugs can potentially be used in high risk populations to prevent cancer or in combination with current therapies to improve survival outcomes.

The key to harnessing the benefits of cholesterol targeting is designing appropriate clinical trials to address the questions raised in this work. From our work we know that patients with low HDL levels have worse outcomes and that HDL improves radiation sensitivity. An appropriate clinical trial would separate patients prior to radiation based on HDL levels. The

patients with low HDL should receive therapies driven to raise the levels of HDL prior to radiation therapy. Of course statins should be considered not only because of their potential positive HDL impact but on their impact on the tumors themselves. The patients with high HDL levels should be further analyzed for their miR-33 expression. We know that HDL has only an impact in cancer cells with low miR-33 expression. So in these patients with both high HDL and high miR-33, the strategy should be to block miR-33 before performing radiation.

6.3 Future Investigations

To explain the broad effects seen in these studies to one overarching mechanism, we must look at where cholesterol is utilized in the cell. Cholesterol is most predominating in the plasma membrane. Within the plasma membrane, cholesterol is heavily concentrated in lipid rafts. Lipid rafts are detergent-insoluble, sphingolipid- and cholesterol-rich membrane microdomains that form lateral assemblies in the plasma membrane.^{154,155} Lipid rafts also sequester glycosylphosphatidylinositol (GPI)-linked proteins and other signaling proteins and receptors, which may be regulated by their selective interactions with these membrane microdomains.¹⁵⁶ Recent research has demonstrated that lipid rafts play a role in a variety of cellular processes — including the compartmentalization of cell-signaling events,^{157,158} the regulation of apoptosis¹⁵⁹ and the intracellular trafficking of certain membrane proteins and lipids¹⁶⁰ as well as in the infectious cycles of several viruses and bacterial pathogens.^{161,162} Examining the formation and regulation of lipid rafts is a critical step in understanding these aspects of eukaryotic cell function. Several tools are available to study lipid rafts including: sucrose density centrifugation, immunoisolation of caveolae, and imaging with cholera-toxin B-subunit which binds to the GM1 of the lipid raft.¹⁶³ Comparing lipid raft composition in TNBC and IBC cells following statin and HDL treatment will provide us with the answer of whether targeting cholesterol disrupts lipid raft formation. Further using drugs that specifically target

lipid rafts, such as methyl- β -cyclodextrin, should recapitulate the findings we have observed with statins and HDL. Because of the importance of downstream signaling associated with lipid rafts this would be an important finding.

Currently our lab is collecting cell lysates from a wide variety of breast cancer cell types and different treatment conditions among the subtypes. We are submitting these samples to a lipidomics core to provide analytics on what are the differences in lipids and cholesterol concentrations between breast cancer subtypes, differentiated vs undifferentiated, statin treated, HDL treated, and many more. These results should give us a better understanding of the potential targets for future studies. Other future studies should study the impact of cholesterol manipulation on radiation resistance in vivo. Importantly our lab has developed a brain metastasis model that was utilized in chapter 2. Interestingly the top overexpressed canonical pathways in brain derived metastasis were cholesterol biosynthesis related. The lab will perform in vivo brain metastatic experiments in dyslipidemic Apo E^{-/-} mice. These experiments will reveal whether HDL levels can impact metastasis, like we showed with simvastatin.

Lastly our lab will be interested in how the IBC microenvironment regulates radiation sensitivity and important signaling pathways, specifically FOXO3a. Co-cultured macrophages and MSCs will be cultured with IBC and TNBC cells and clonogenics performed to assess radiation sensitivity. Western blots will be performed on co-cultured educated MSC and tumor cells to assess the changes in FOXO3a expression following co-culture.

Novel functions of cholesterol synthesis and metabolism are constantly being described, and my results combined with those of future studies will aid in developing new treatments for this important process.

Appendix

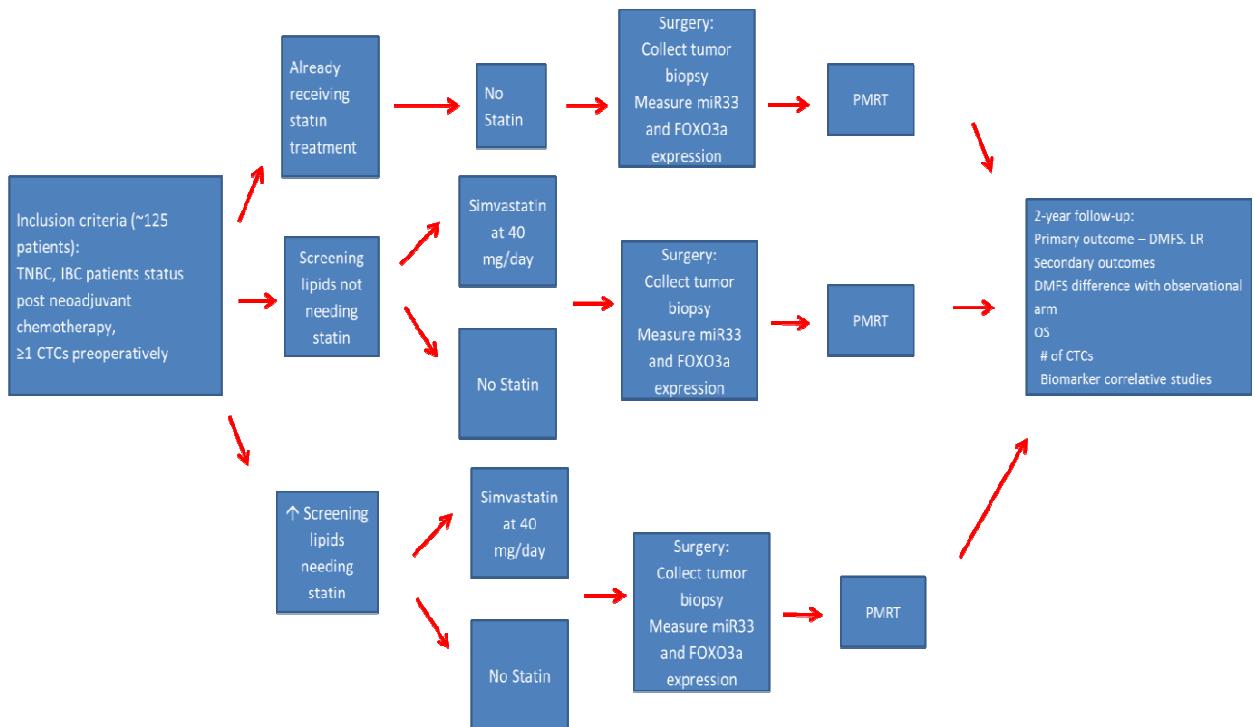
Clinical Trial

This thesis has the potential to have an impact in the clinic. In order to successfully translate these results into positive patient outcomes, a well-designed clinical trial is needed. With any clinical trial, enrolling the proper patient population is important. I therefore propose a phase 2 study with which to evaluate patients at highest risk of relapse—IBC and TNBC breast cancer patients with minimal residual disease (i.e., the presence of ≥ 1 circulating tumor cells [CTCs]) after neoadjuvant chemotherapy. Minimal residual disease has been shown to be negatively prognostic, with median progression-free survival (PFS) duration of 18 months in TNBC and IBC patients.

Primary and Secondary Objectives

- a. Primary objective: Detect a positive signal of long-term use of post-diagnosis simvastatin, 40 mg daily, on distant metastasis free survival (DMFS) and local recurrence (LR) following post-mastectomy radiation therapy (PMRT) in a high-risk IBC and TNBC population.
- b. Secondary objective: Explore the underlying mechanisms for statin efficacy via cancer signaling pathways and cholesterol pathway. Establish if lipid profiles influence the effects of simvastatin and if miR-33 and FOXO3a expression is a predictor to response with simvastatin.

Study Design



We would initially enroll approximately 125 IBC and TNBC patients who are not currently receiving statin treatment or with clear indication for statin therapy who are completing neoadjuvant chemotherapy and have ≥ 1 CTCs (approximately 35% of the population). We will check the lipid profile and exclude patients with elevated lipid levels and already on a statin; this group will be placed in observational arm and continue to be treated with statin as indicated by the latest AHA lipid treatment guidelines. The remaining patients will receive simvastatin at 40 mg daily and will be monitored for 2 years; our goal is to enroll 90 patients into this experimental arm.

Primary and Secondary Endpoints/Criteria for Evaluation

- a. Primary endpoint: Estimated DMFS rate as determined by diagnostic imaging and physical examination every 6 months by a physician
- b. Secondary endpoint:

- i. Overall survival
- ii. Locoregional recurrence to assess efficacy of statin as radiosensitizer
- iii. Toxic effects of simvastatin in breast cancer population
- iv. Comparison of DMFS between experimental and observational arms to assess the importance of lipids in pathophysiology
- v. Change in the number of CTCs
- vi. Change in biomarkers (miR-33 and FOXO3a) measured in CTCs and serum

This clinical trial we will allow us to obtain several answers from the pre-clinical data. First and most important we will answer whether patients that present with TNBC or IBC that have dyslipidemia that receive a statin prior to radiation will lower metastasis and improve local control? Importantly, this clinical trial will allow us to determine if statins effects are dependent on dyslipidemia or if lipoproteins are unimportant for their anti-tumor effects. We hypothesize that lipoproteins are critical for the potential beneficial effects of simvastatin.

We will obtain tumor biopsies and determine expression of miR-33 and FOXO3a and will correlate their expression to the outcomes from patients taking simvastatin. This will allow us to determine if the expression of these markers impact statin survival. In the patients already on statins (observational arm) we will be able to determine if miR-33 or FOXO3a effect survival and possible in the future it will be important to try to modulate their expression in addition to prescribing a statin.

Investigating the effects of statins on breast cancer cells

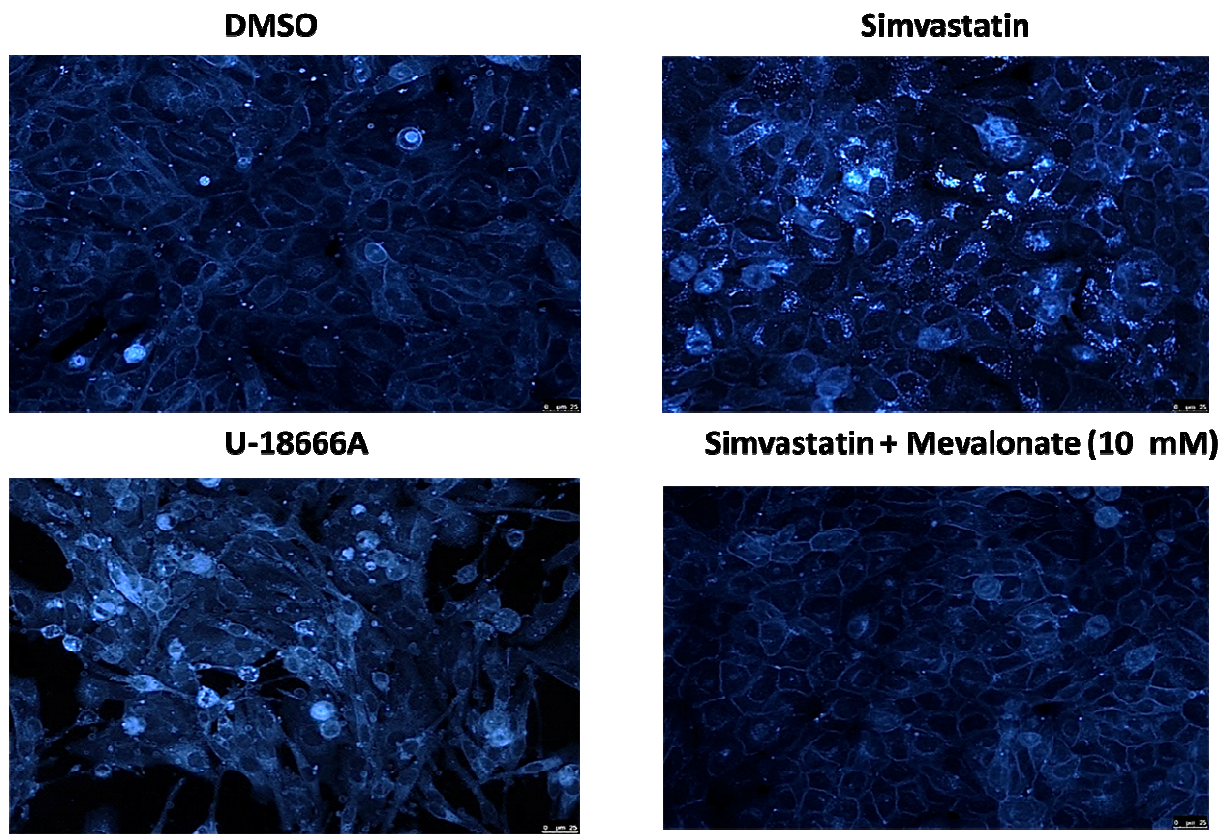


Figure A1. SUM 149 Cells were treated with simvastatin, U-186661 (a cholesterol transport inhibitor), or simvastatin and mevalonate for 24 hours and then stained with filipin. Cholesterol is more equally dispersed in the plasma membrane in the DMSO and simvastatin + mevalonate group. In the simvastatin and U-18666A groups, the cholesterol is more concentrated in the cytoplasm.

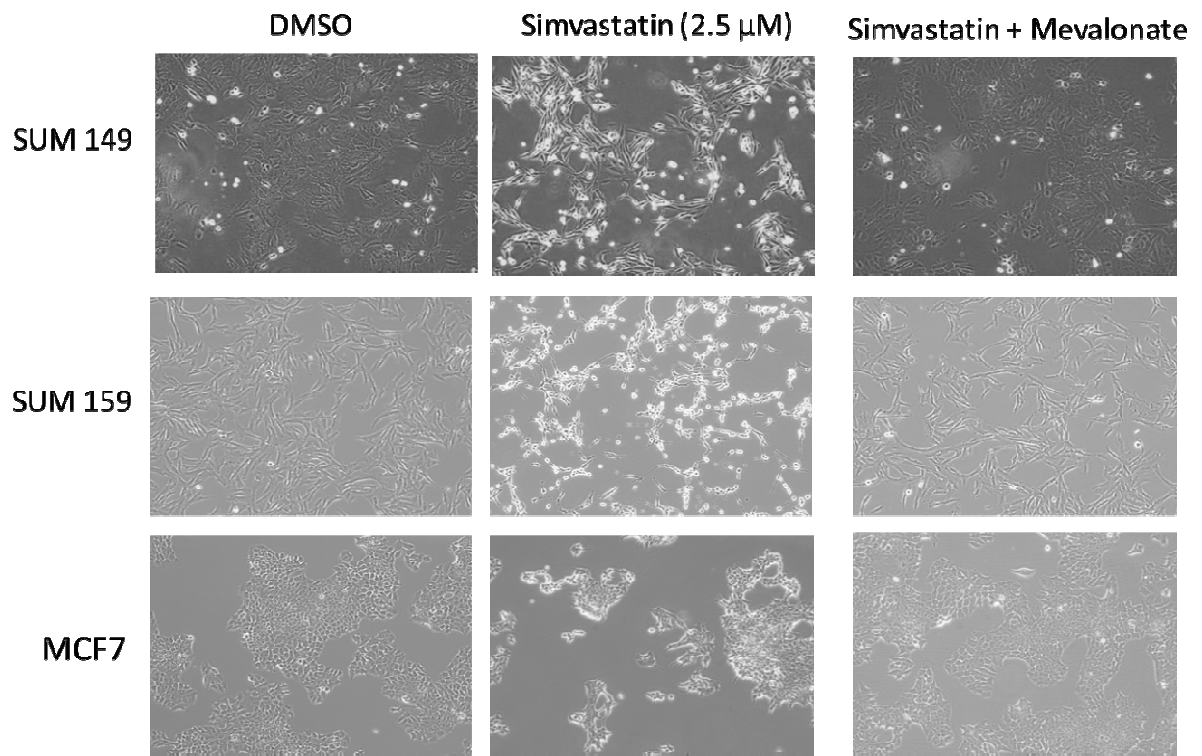


Figure A2. Simvastatin was added to cell culture of three cell lines for 24 hours. The cells after simvastatin treatment appear more mesenchymal.

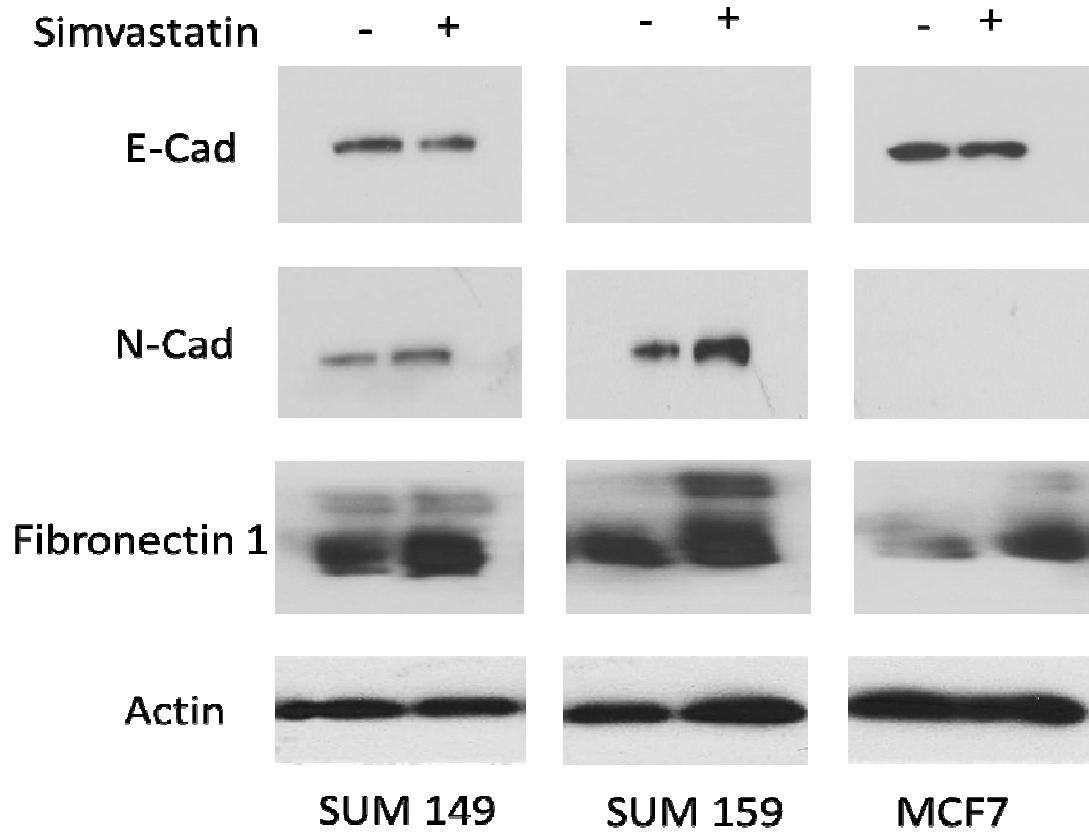


Figure A3. Simvastatin changes the mesenchymal and epithelial markers.

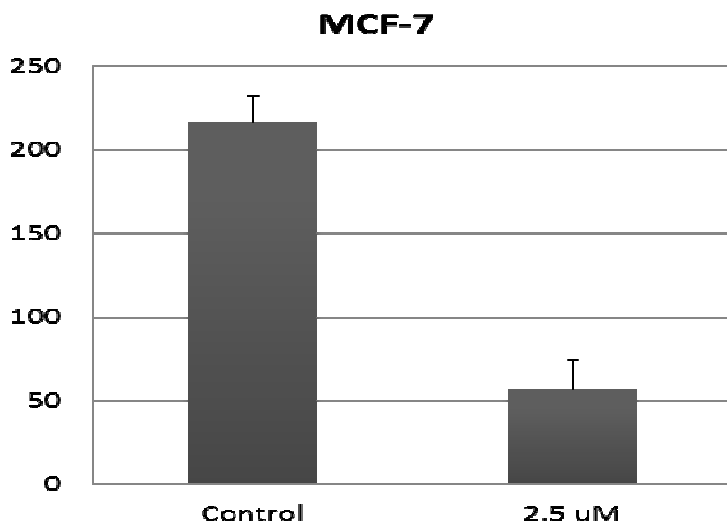


Figure A4. Simvastatin inhibits mammosphere formation in MCF7 cells.

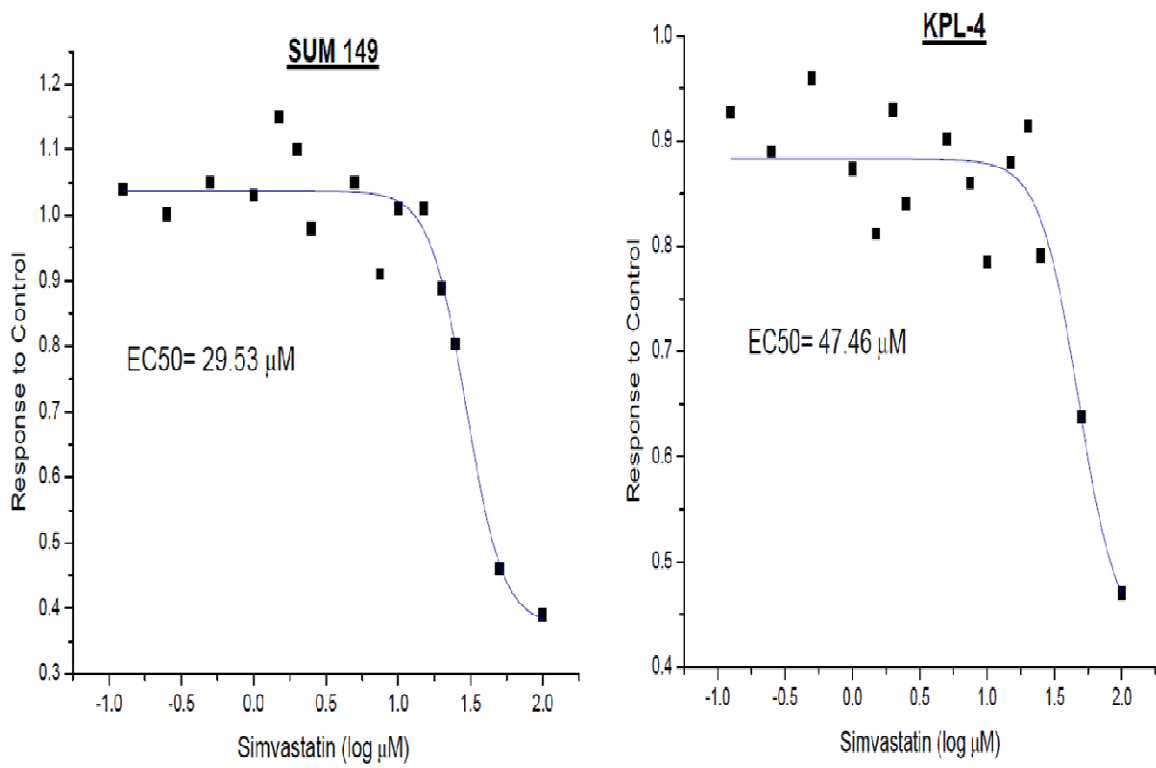


Figure A5. Simvastatin EC50 concentrations for SUM 149 and KPL4. The EC50 is well above the concentrations used in experiments.

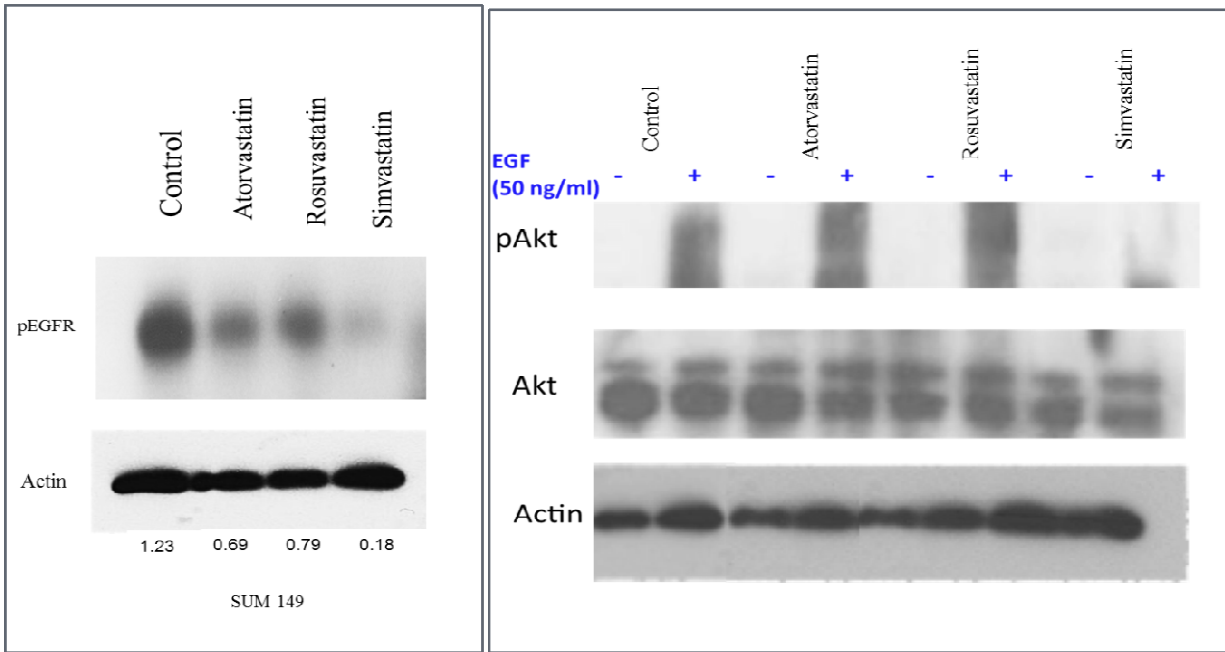


Figure A6. Simvastatin inhibited pEGFR more than any other statin. Simvastatin was the only statin to inhibit pAkt.

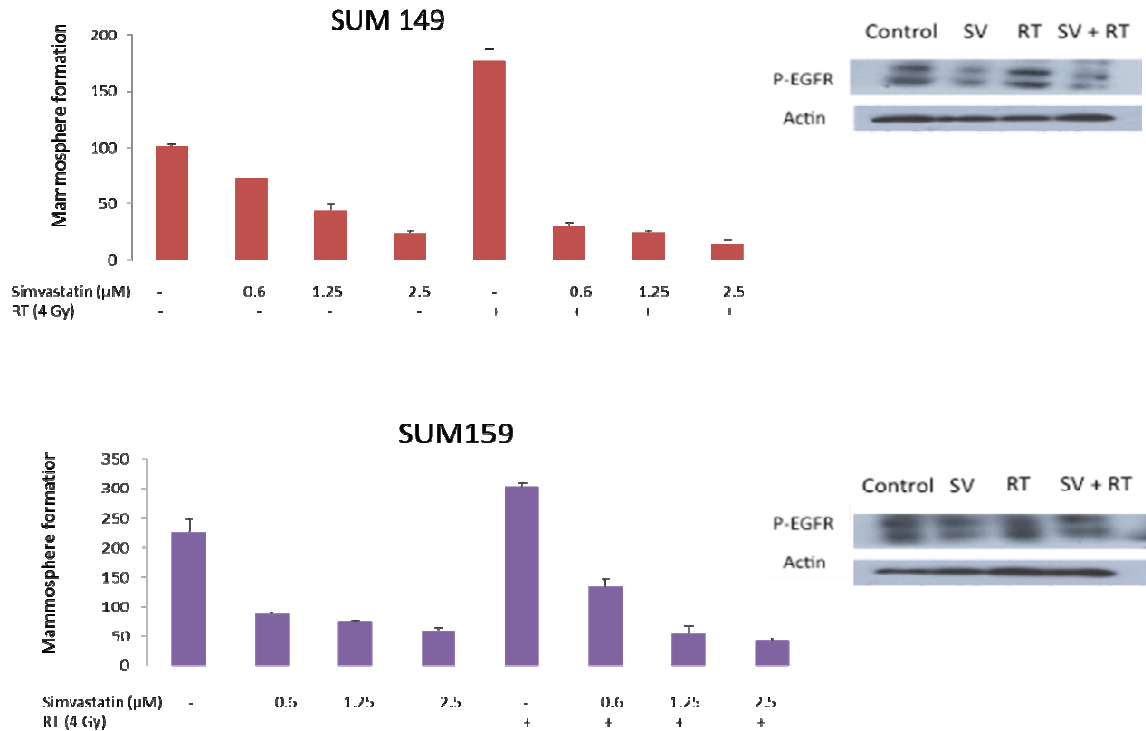


Figure A7. Simvastatin inhibited mammospheres and radiation increased mammosphere formation. Simvastatin inhibited the p-EGFR in both controls and radiation treated cells.

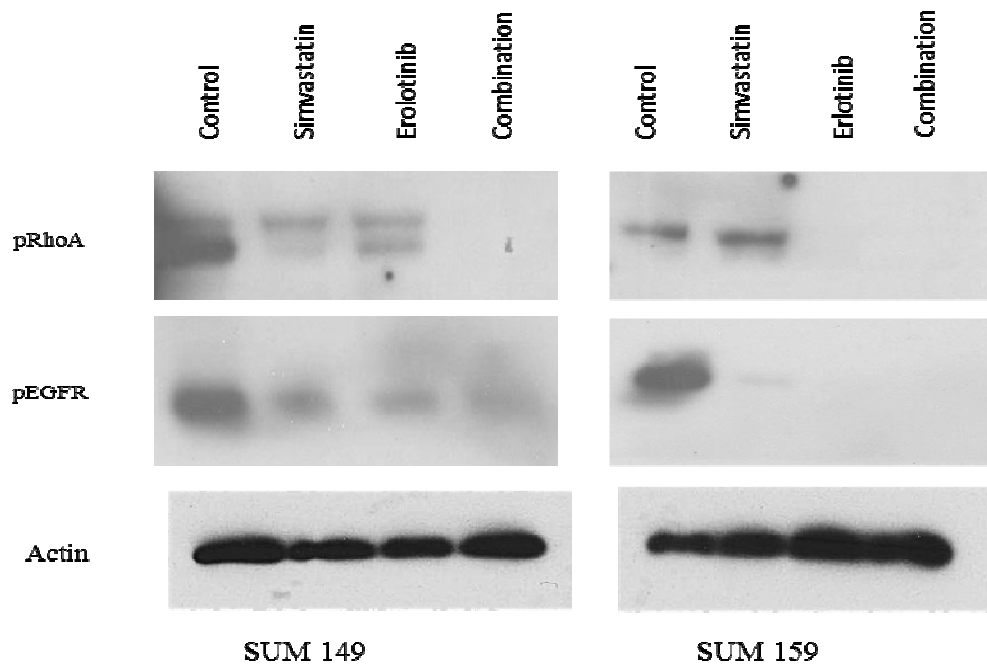


Figure A8. The combination of simvastatin and erlotinib inhibits the phosphorylation of RhoA and EGFR in SUM 149 cells. The SUM 159 cells had full inhibition of pEGFR after simvastatin or erlotinib.

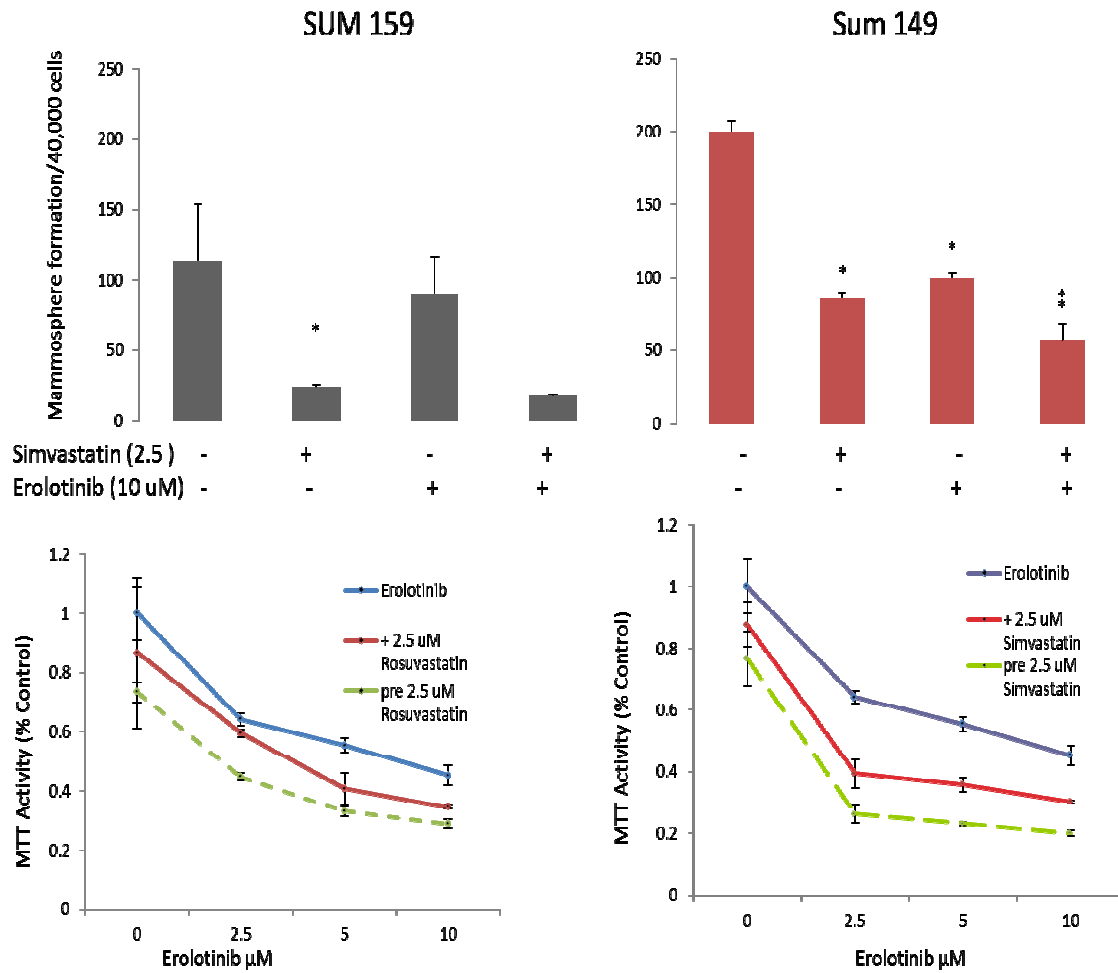


Figure A9. Simvastatin and erlotinib in combination inhibits both SUM 149 and SUM 159 mammospheres more than either drug alone. Treatment with statins in combination with increasing erlotinib concentrations had more of an effect on MTT activity than erlotinib alone.

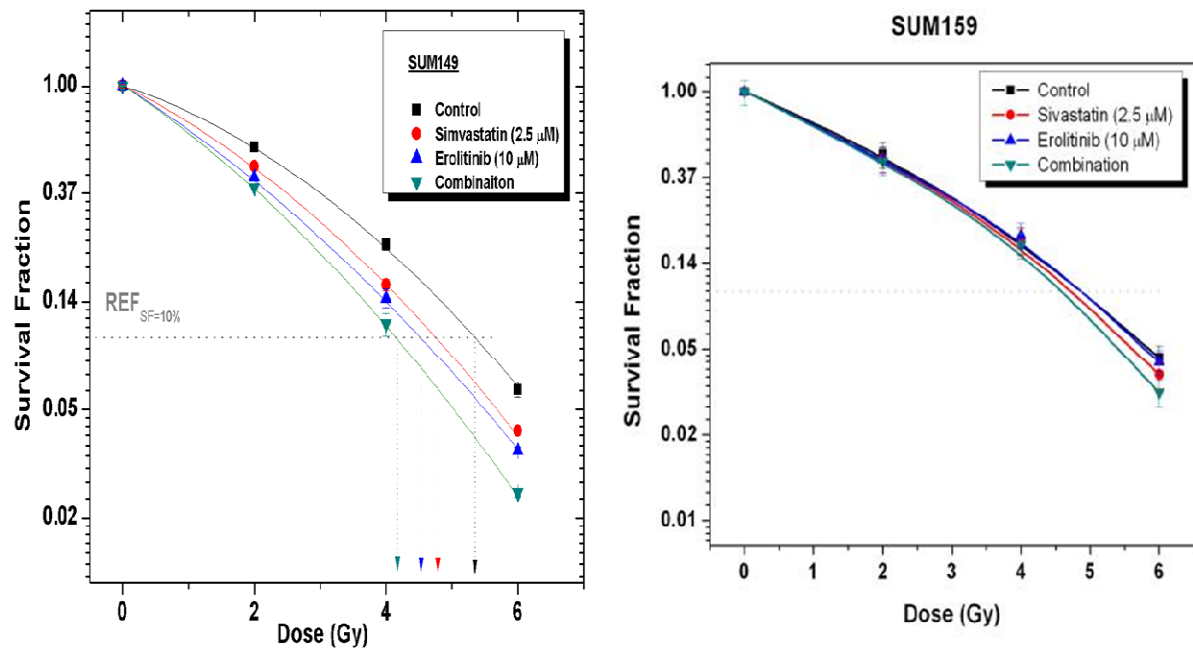


Figure A10. The combination of simvastatin and erlotinib radiosensitizes SUM 149 cells more than either drug alone. No effects seen in combination for SUM 159 cells.

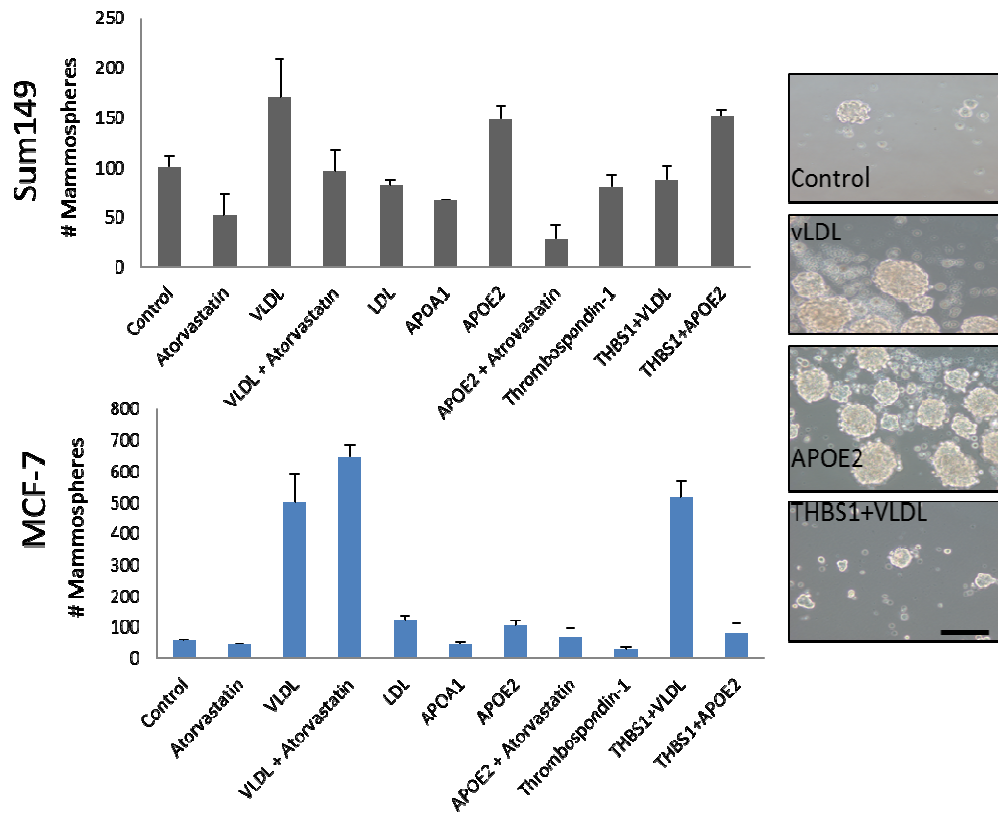


Figure A11. The effects of lipoproteins and apolipoproteins on SUM 149 and MCF7 mammosphre formation.

Analyzing the effects of polarization on macrophages and MSCs

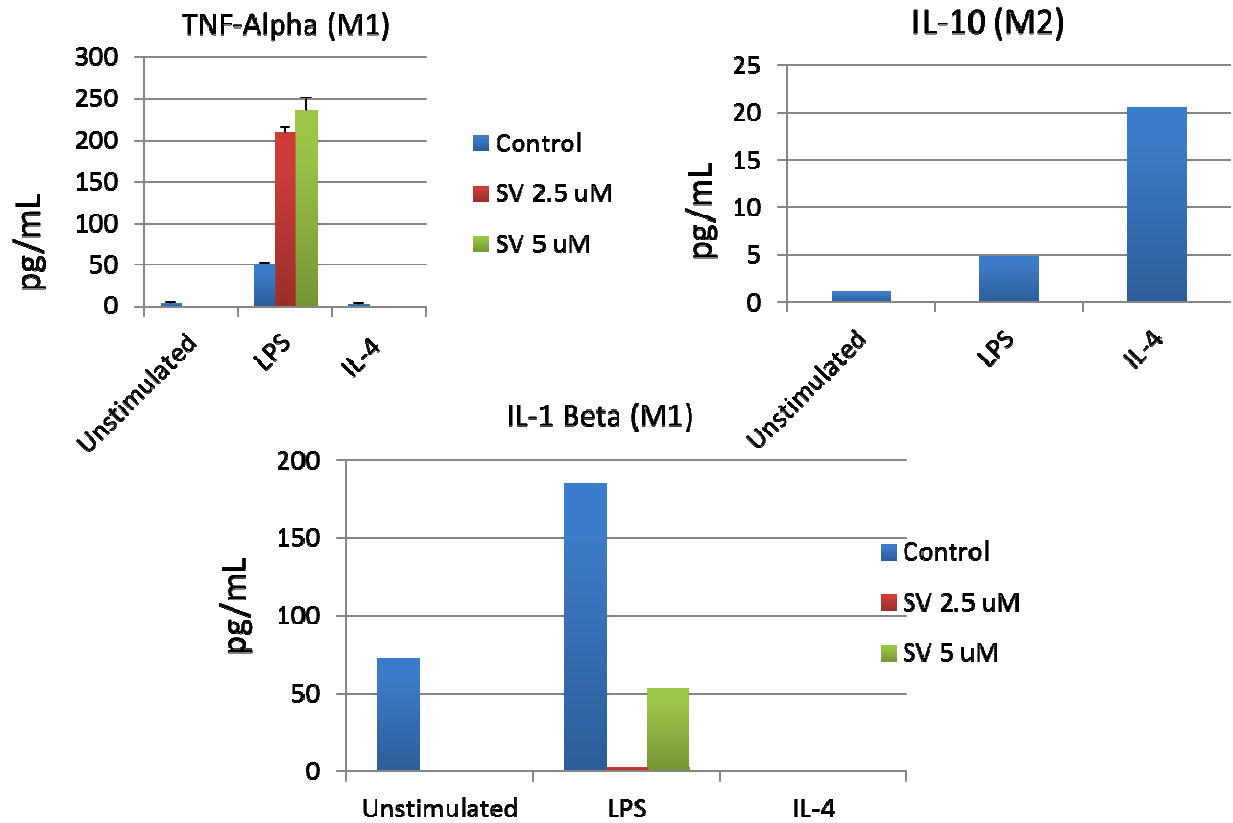


Figure A12. Raw 264.7 macrophage cells were stimulated with LPS or IL-4 for 24 hours and treated with +/- simvastatin. The cell supernatant was used for ELISAs of TNF-alpha (M1 cytokine), IL-1 beta (M1), or IL-10 (M2 cytokine). Simvastatin increased the effects of LPS on TNF-alpha and blocked cytokine secretion of IL-1 beta.

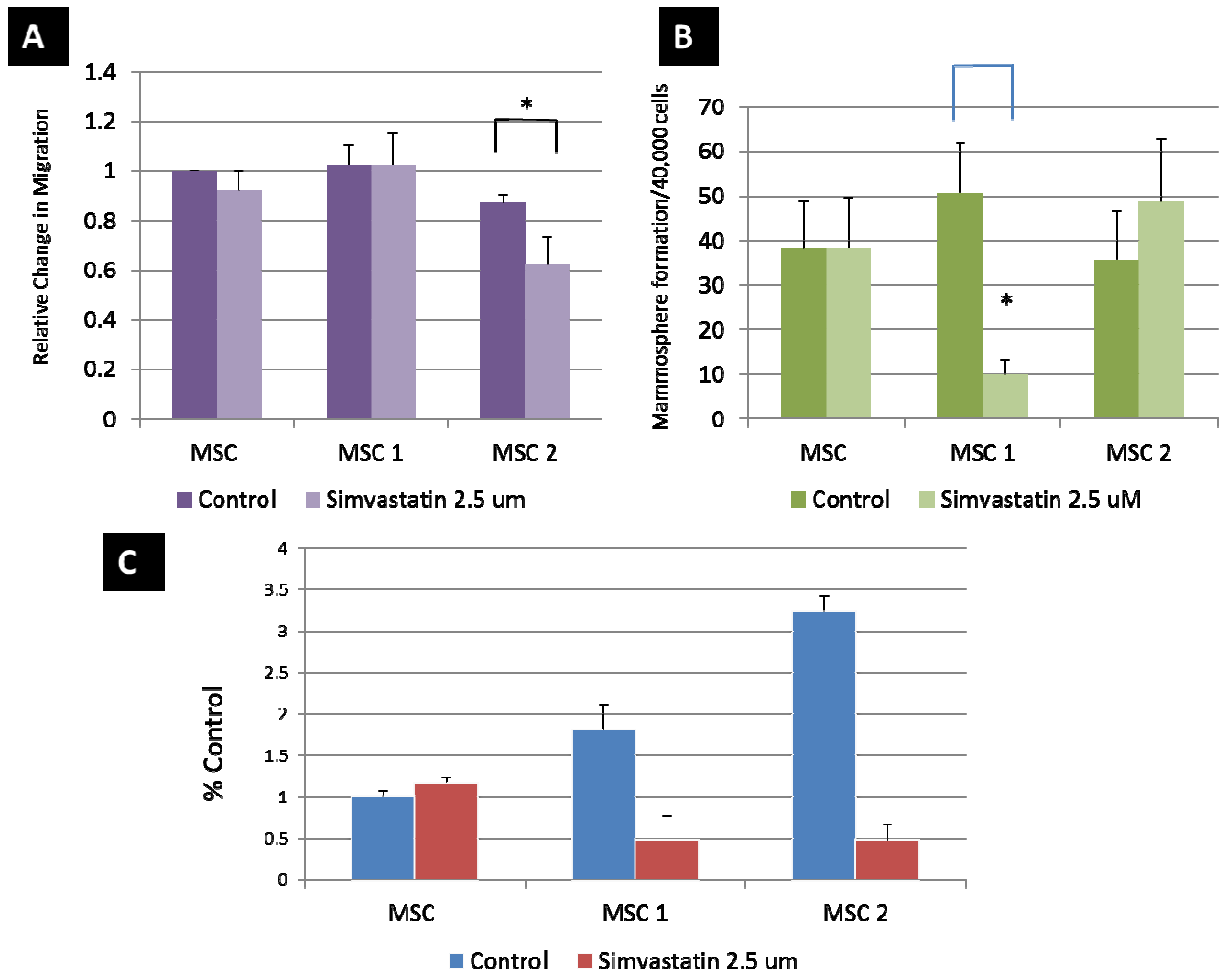


Figure A13. MSC cells were polarized with either LPS (MSC1) or IL-4 (MSC2) for 24 hours. (A) MSC 2 (IL-4 treated) migration was inhibited by simvastatin. (B) MSC1 (LPS) mammospheres were inhibited by simvastatin. (C) MSC1 and MSC2 proliferation was inhibited by simvastatin.

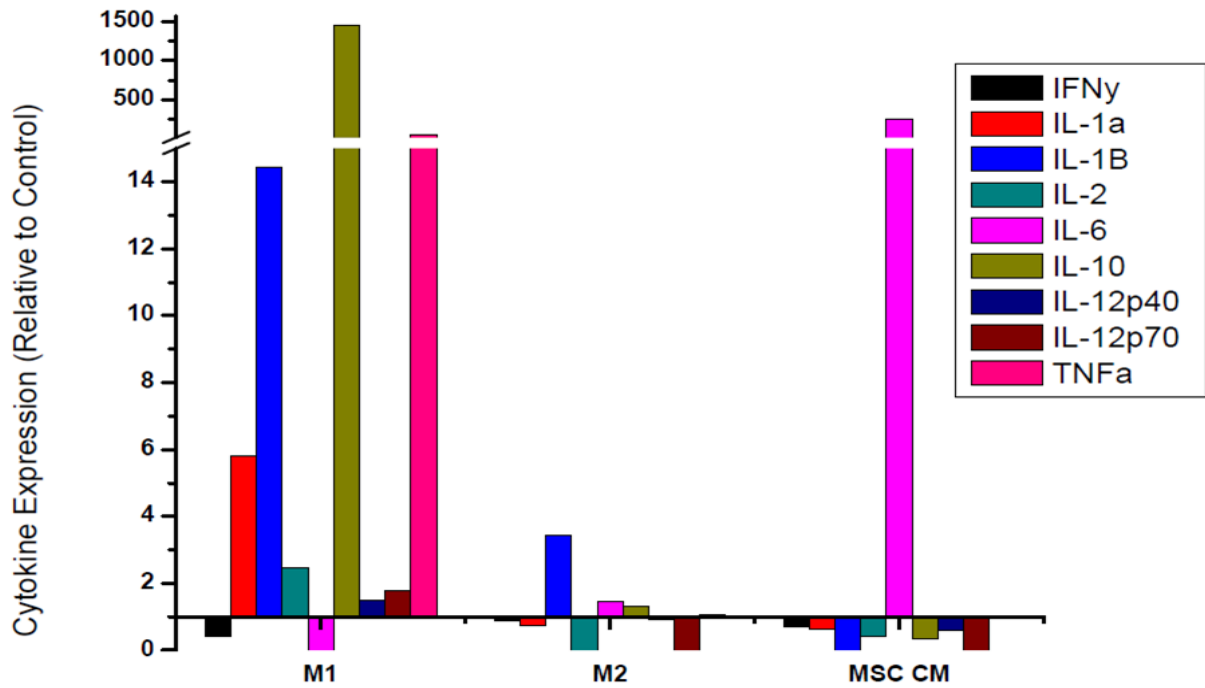


Figure A14. Raw cell supernatants was submitted for luminex magnetic bead assay. The M1 (LPS treated) macrophages had high cytokine secretion profile while the M2 (IL-4) had low cytokine secretion. The untreated Raw cells grown in MSC conditioned media (CM) for 24 hours had very high IL-6 secretion.

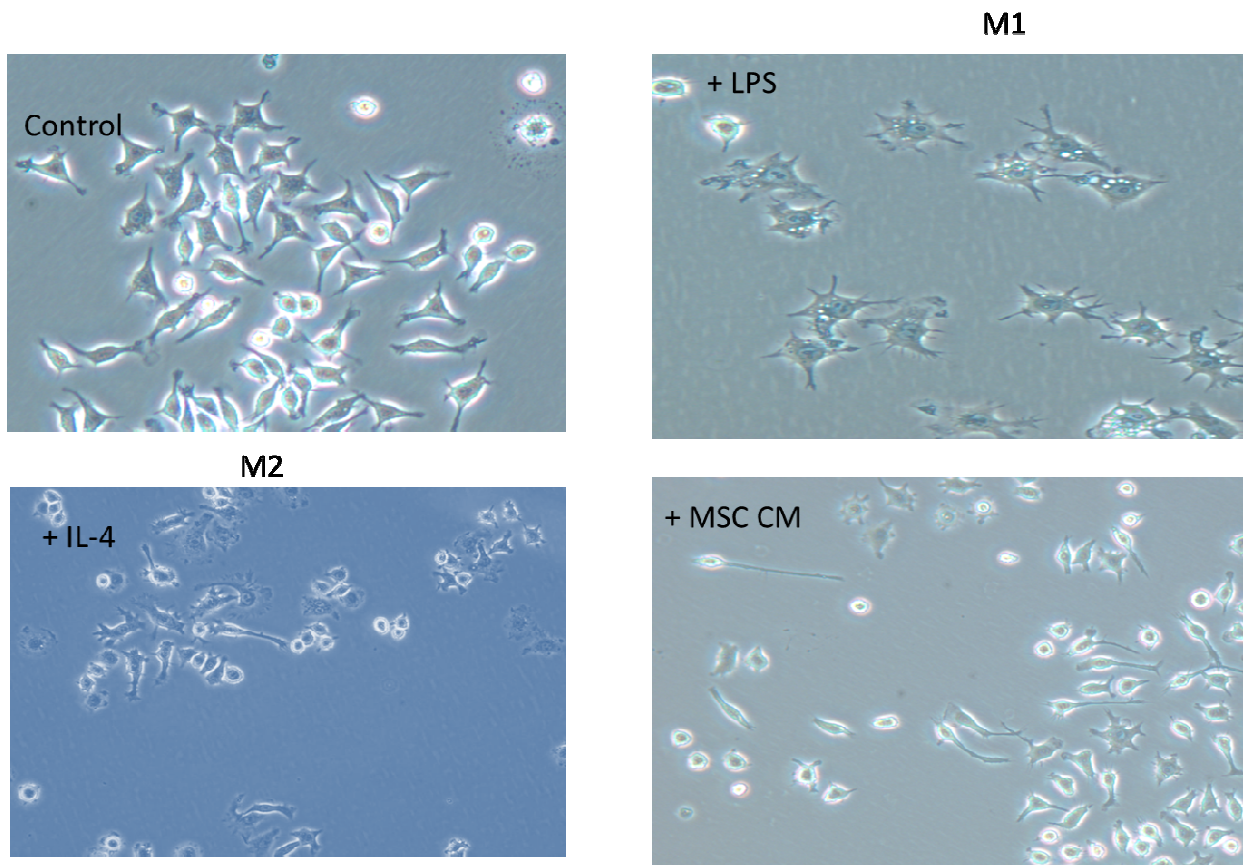


Figure A15. The morphology of macrophages (Raw cells) under light microscope after polarization for 24 hours. MSC CM turns macrophages into a M2 morphology with long protrusions.

MSC CM	-	-	-	-	+	+	-	-
Simvastatin	-	-	-	+	-	+	+	+
IL 4	-	-	+	-	-	-	-	+
LPS & IFN γ	-	+	-	-	-	-	+	-

Arg-1



Actin

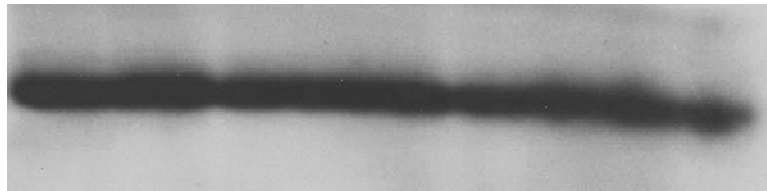


Figure A16. Raw cell lysates submitted for western blotting and probed with anti-Arginase 1 antibody (M2 marker). Raw cells have high expression at baseline of arginase 1 suggesting Raw cells at baseline are M2 like.

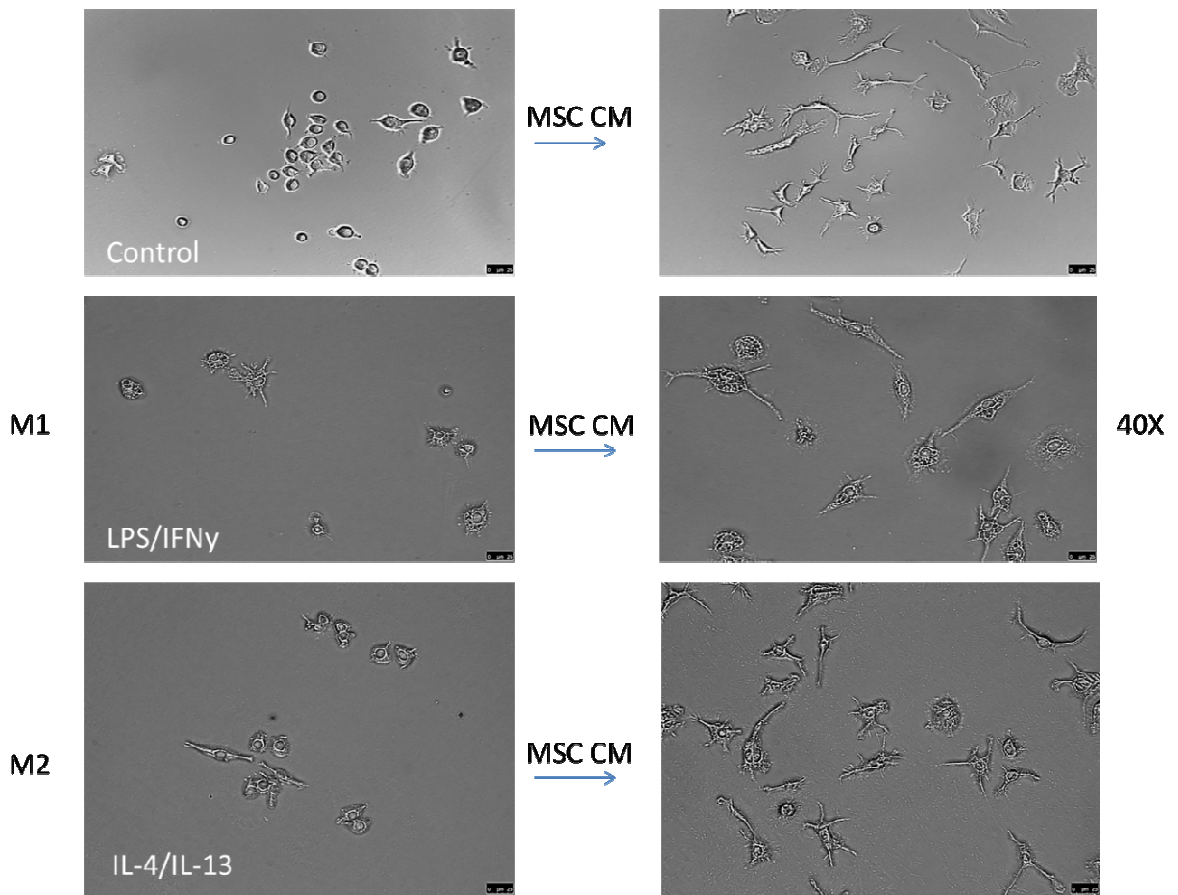


Figure A17. The macrophage morphology changes after 24 hours of MSC CM culture.

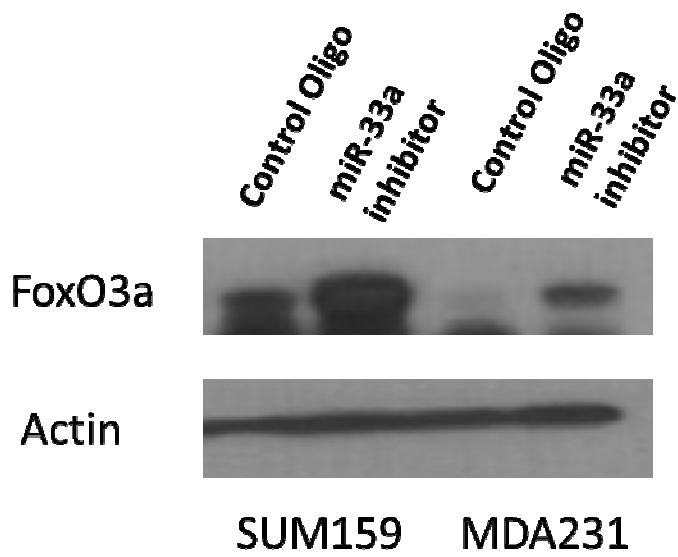


Figure A18. miR-33a inhibition in TNBC cells leads to increased FOXO3a expression.

Bibliography

1. Halsted CP, Benson JR, Jatoi I. A historical account of breast cancer surgery: beware of local recurrence but be not radical. *Future oncology* 2014; **10**(9): 1649-57.
2. Scatliff JH, Morris PJ. From Roentgen to magnetic resonance imaging: the history of medical imaging. *North Carolina medical journal* 2014; **75**(2): 111-3.
3. DeVita VT, Chu E. A History of Cancer Chemotherapy. *Cancer research* 2008; **68**(21): 8643-53.
4. Barrett-Connor E. Book Review. *New England Journal of Medicine* 2007; **357**(16): 1670-1.
5. Thike AA, Iqbal J, Cheok PY, Chong AP, Tse GM, Tan B, Tan P, Wong NS, Tan PH. Triple negative breast cancer: outcome correlation with immunohistochemical detection of basal markers. *The American journal of surgical pathology* 2010; **34**(7): 956-64.
6. Rakha E, Ellis I, Reis-Filho J. Are triple-negative and basal-like breast cancer synonymous? *Clinical cancer research : an official journal of the American Association for Cancer Research* 2008; **14**(2): 618; author reply -9.
7. Rakha EA, Ellis IO. Triple-negative/basal-like breast cancer: review. *Pathology* 2009; **41**(1): 40-7.
8. Ismail-Khan R, Bui MM. A review of triple-negative breast cancer. *Cancer control : journal of the Moffitt Cancer Center* 2010; **17**(3): 173-6.
9. Heitz F, Harter P, Lueck HJ, Fissler-Eckhoff A, Lorenz-Salehi F, Scheil-Bertram S, Traut A, du Bois A. Triple-negative and HER2-overexpressing breast cancers exhibit an elevated risk and an earlier occurrence of cerebral metastases. *Eur J Cancer* 2009; **45**(16): 2792-8.
10. Medema JP. Cancer stem cells: the challenges ahead. *Nat Cell Biol* 2013; **15**(4): 338-44.

11. Dawood S, Merajver SD, Viens P, Vermeulen PB, Swain SM, Buchholz TA, Dirix LY, Levine PH, Lucci A, Krishnamurthy S, Robertson FM, Woodward WA, Yang WT, Ueno NT, Cristofanilli M. International expert panel on inflammatory breast cancer: consensus statement for standardized diagnosis and treatment. *Ann Oncol* 2011; **22**(3): 515-23.
12. Robertson FM, Bondy M, Yang W, Yamauchi H, Wiggins S, Kamrudin S, Krishnamurthy S, Le-Petross H, Bidaut L, Player AN, Barsky SH, Woodward WA, Buchholz T, Lucci A, Ueno NT, Cristofanilli M. Inflammatory breast cancer: the disease, the biology, the treatment. *CA Cancer J Clin* 2010; **60**(6): 351-75.
13. Piras F, Ionta MT, Lai S, Perra MT, Atzori F, Minerba L, Pusceddu V, Maxia C, Murtas D, Demurtas P, Massidda B, Sirigu P. Nestin expression associates with poor prognosis and triple negative phenotype in locally advanced (T4) breast cancer. *European Journal of Histochemistry : EJH* 2011; **55**(4): e39.
14. Vrieling A, Buck K, Kaaks R, Chang-Claude J. Adult weight gain in relation to breast cancer risk by estrogen and progesterone receptor status: a meta-analysis. *Breast cancer research and treatment* 2010; **123**(3): 641-9.
15. Renehan AG, Roberts DL, Dive C. Obesity and cancer: Pathophysiological and biological mechanisms. *Archives Of Physiology And Biochemistry* 2008; **114**(1): 71-83.
16. Key TJ, Appleby PN, Cairns BJ, Luben R, Dahm CC, Akbaraly T, Brunner EJ, Burley V, Cade JE, Greenwood DC, Stephen AM, Mishra G, Kuh D, Keogh RH, White IR, Bhaniani A, Borgulya G, Mulligan AA, Khaw KT. Dietary fat and breast cancer: comparison of results from food diaries and food-frequency questionnaires in the UK Dietary Cohort Consortium. *Am J Clin Nutr* 2011; **94**(4): 1043-52.

17. Ikeda T, Sekiguchi C, Shimamura K, Ozawa I, Inada T, Hishinuma S, Shimizu H, Kotake K, Ogata Y, Koyama Y. Breast cancer developing after chemotherapy for osteosarcoma: a case report. *Japanese journal of clinical oncology* 1991; **21**(6): 444-6.
18. Danilo C, Frank PG. Cholesterol and breast cancer development. *Curr Opin Pharmacol* 2012; **12**(6): 677-82.
19. Hu J, La Vecchia C, de Groh M, Negri E, Morrison H, Mery L, Canadian Cancer Registries Epidemiology Research G. Dietary cholesterol intake and cancer. *Ann Oncol* 2012; **23**(2): 491-500.
20. Llaverias G, Danilo C, Mercier I, Daumer K, Capozza F, Williams TM, Sotgia F, Lisanti MP, Frank PG. Role of cholesterol in the development and progression of breast cancer. *The American journal of pathology* 2011; **178**(1): 402-12.
21. Nelson ER, Wardell SE, Jasper JS, Park S, Suchindran S, Howe MK, Carver NJ, Pillai RV, Sullivan PM, Sondhi V, Umetani M, Geradts J, McDonnell DP. 27-Hydroxycholesterol links hypercholesterolemia and breast cancer pathophysiology. *Science* 2013; **342**(6162): 1094-8.
22. Martin BJ, van Golen KL. A comparison of cholesterol uptake and storage in inflammatory and noninflammatory breast cancer cells. *International journal of breast cancer* 2012; **2012**: 412581.
23. Byers T. Statins, breast cancer, and an invisible switch? *Cancer epidemiology, biomarkers & prevention : a publication of the American Association for Cancer Research, cosponsored by the American Society of Preventive Oncology* 2008; **17**(5): 1026-7.
24. Ahern TP, Pedersen L, Tarp M, Cronin-Fenton DP, Garne JP, Silliman RA, Sorensen HT, Lash TL. Statin prescriptions and breast cancer recurrence risk: a Danish nationwide prospective cohort study. *Journal of the National Cancer Institute* 2011; **103**(19): 1461-8.

25. Hong C-C, Shah AB, Jackowiak CM, Kossoff E, Fu H-W, Nimako GK, Bitikofer D, Edge SB, Ceacareanu AC. Cholesterol drugs improve breast cancer prognosis in women with diabetes mellitus. *Adv Pharmacoepidem Drug Safety* 2013; **2**(130): 2167-1052.1000130.
26. Goldstein JL, Brown MS. Regulation of the mevalonate pathway. *Nature* 1990; **343**(6257): 425-30.
27. Wejde J, Hjertman M, Carlberg M, Egestad B, Griffiths WJ, Sjovall J, Larsson O. Dolichol-like lipids with stimulatory effect on DNA synthesis: substrates for protein dolichylation? *Journal of cellular biochemistry* 1998; **71**(4): 502-14.
28. Rao S, Lowe M, Herliczek TW, Keyomarsi K. Lovastatin mediated G1 arrest in normal and tumor breast cells is through inhibition of CDK2 activity and redistribution of p21 and p27, independent of p53. *Oncogene* 1998; **17**(18): 2393-402.
29. Luan Z, Chase AJ, Newby AC. Statins inhibit secretion of metalloproteinases-1, -2, -3, and -9 from vascular smooth muscle cells and macrophages. *Arteriosclerosis, thrombosis, and vascular biology* 2003; **23**(5): 769-75.
30. Feleszko W, Bałkowiec EZ, Sieberth E, Marczak M, Dabrowska A, Giermasz A, Czajka A, Jakóbiński M. Lovastatin and tumor necrosis factor- α exhibit potentiated antitumor effects against Ha-ras-transformed murine tumor Via inhibition of tumor-induced angiogenesis. *International Journal of Cancer* 1999; **81**(4): 560-7.
31. Franz Alber H, Dulak J, Frick M, Dichtl W, Paul Schwarzacher S, Pachinger O, Weidinger F. Atorvastatin decreases vascular endothelial growth factor in patients with coronary artery disease. *Journal of the American College of Cardiology* 2002; **39**(12): 1951-5.
32. Ginestier C, Monville F, Wicinski J, Cabaud O, Cervera N, Josselin E, Finetti P, Guille A, Larderet G, Viens P, Sebti S, Bertucci F, Birnbaum D, Charafe-Jauffret E. Mevalonate

metabolism regulates Basal breast cancer stem cells and is a potential therapeutic target. *Stem Cells* 2012; **30**(7): 1327-37.

33. Brewer TM, Masuda H, Liu DD, Shen Y, Liu P, Iwamoto T, Kai K, Barnett CM, Woodward WA, Reuben JM, Yang P, Hortobagyi GN, Ueno NT. Statin use in primary inflammatory breast cancer: a cohort study. *British journal of cancer* 2013; **109**(2): 318-24.

34. Lacerda L, Reddy JP, Liu D, Larson R, Li L, Masuda H, Brewer T, Debeb BG, Xu W, Hortobágyi GN, Buchholz TA, Ueno NT, Woodward WA. Simvastatin Radiosensitizes Differentiated and Stem-Like Breast Cancer Cell Lines and Is Associated With Improved Local Control in Inflammatory Breast Cancer Patients Treated With Postmastectomy Radiation. *Stem cells translational medicine* 2014; **3**(7): 849-56.

35. Ray G, Husain SA. Role of lipids, lipoproteins and vitamins in women with breast cancer. *Clinical biochemistry* 2001; **34**(1): 71-6.

36. Yvan-Charvet L, Wang N, Tall AR. Role of HDL, ABCA1, and ABCG1 transporters in cholesterol efflux and immune responses. *Arteriosclerosis, thrombosis, and vascular biology* 2010; **30**(2): 139-43.

37. Rayner KJ, Suarez Y, Davalos A, Parathath S, Fitzgerald ML, Tamehiro N, Fisher EA, Moore KJ, Fernandez-Hernando C. MiR-33 contributes to the regulation of cholesterol homeostasis. *Science* 2010; **328**(5985): 1570-3.

38. Graziani SR, Igreja FA, Hegg R, Meneghetti C, Brandizzi LI, Barboza R, Amancio RF, Pinotti JA, Maranhao RC. Uptake of a cholesterol-rich emulsion by breast cancer. *Gynecologic oncology* 2002; **85**(3): 493-7.

39. Athyros VG, Kakafika AI, Papageorgiou AA, Pagourelas ED, Savvatianos SD, Elisaf M, Karagiannis A, Tziomalos K, Mikhailidis DP. Statin-Induced Increase in HDL-C and Renal

- Function in Coronary Heart Disease Patients. *The open cardiovascular medicine journal* 2007; **1**: 8-14.
40. McGrowder D, Riley C, Morrison EYSA, Gordon L. The Role of High-Density Lipoproteins in Reducing the Risk of Vascular Diseases, Neurogenerative Disorders, and Cancer. *Cholesterol* 2011; **2011**.
41. Laisupasin P, Thompat W, Sukarayodhin S, Sornprom A, Sudjaroen Y. Comparison of Serum Lipid Profiles between Normal Controls and Breast Cancer Patients. *Journal of Laboratory Physicians* 2013; **5**(1): 38-41.
42. Jordan CT, Guzman ML, Noble M. Cancer stem cells. *The New England journal of medicine* 2006; **355**(12): 1253-61.
43. Al-Hajj M, Wicha M, Benito-Hernandez A, Morrison S, Clarke M. Prospective identification of tumorigenic breast cancer cells. *Proc Natl Acad Sci USA* 2003; **100**: 3983 - 8.
44. Singh SK, Hawkins C, Clarke ID, Squire JA, Bayani J, Hide T, Henkelman RM, Cusimano MD, Dirks PB. Identification of human brain tumour initiating cells. *Nature* 2004; **432**(7015): 396-401.
45. Lapidot T, Sirard C, Vormoor J, Murdoch B, Hoang T, Caceres-Cortes J, Minden M, Paterson B, Caligiuri MA, Dick JE. A cell initiating human acute myeloid leukaemia after transplantation into SCID mice. *Nature* 1994; **367**(6464): 645-8.
46. Bonnet D, Dick JE. Human acute myeloid leukemia is organized as a hierarchy that originates from a primitive hematopoietic cell. *Nat Med* 1997; **3**(7): 730-7.
47. Van Keymeulen A, Rocha AS, Ousset M, Beck B, Bouvencourt G, Rock J, Sharma N, Dekoninck S, Blanpain C. Distinct stem cells contribute to mammary gland development and maintenance. *Nature* 2011; **479**(7372): 189-93.

48. van Amerongen R, Bowman AN, Nusse R. Developmental stage and time dictate the fate of Wnt/beta-catenin-responsive stem cells in the mammary gland. *Cell Stem Cell* 2012; **11**(3): 387-400.
49. de Visser KE, Ciampricotti M, Michalak EM, Tan DW, Speksnijder EN, Hau CS, Clevers H, Barker N, Jonkers J. Developmental stage-specific contribution of LGR5(+) cells to basal and luminal epithelial lineages in the postnatal mammary gland. *J Pathol* 2012; **228**(3): 300-9.
50. Visvader JE, Stingl J. Mammary stem cells and the differentiation hierarchy: current status and perspectives. *Genes Dev* 2014; **28**(11): 1143-58.
51. Li J, Gonzalez-Angulo AM, Allen PK, Yu TK, Woodward WA, Ueno NT, Lucci A, Krishnamurthy S, Gong Y, Bondy ML, Yang W, Willey JS, Cristofanilli M, Valero V, Buchholz TA. Triple-negative subtype predicts poor overall survival and high locoregional relapse in inflammatory breast cancer. *Oncologist* 2011; **16**(12): 1675-83.
52. Dawood S, Ueno NT, Valero V, Woodward WA, Buchholz TA, Hortobagyi GN, Gonzalez-Angulo AM, Cristofanilli M. Identifying factors that impact survival among women with inflammatory breast cancer. *Ann Oncol* 2012; **23**(4): 870-5.
53. Dawood S, Ueno NT, Valero V, Woodward WA, Buchholz TA, Hortobagyi GN, Gonzalez-Angulo AM, Cristofanilli M. Differences in survival among women with stage III inflammatory and noninflammatory locally advanced breast cancer appear early: a large population-based study. *Cancer* 2011; **117**(9): 1819-26.
54. Ehninger A, Trumpp A. The bone marrow stem cell niche grows up: mesenchymal stem cells and macrophages move in. *The Journal of experimental medicine* 2011; **208**(3): 421-8.

55. Chow T, Whiteley J, Li M, Rogers IM. The transfer of host MHC class I protein protects donor cells from NK cell and macrophage-mediated rejection during hematopoietic stem cell transplantation and engraftment in mice. *Stem Cells* 2013; **31**(10): 2242-52.
56. Klopp AH, Lacerda L, Gupta A, Debeb BG, Solley T, Li L, Spaeth E, Xu W, Zhang X, Lewis MT, Reuben JM, Krishnamurthy S, Ferrari M, Gaspar R, Buchholz TA, Cristofanilli M, Marini F, Andreeff M, Woodward WA. Mesenchymal stem cells promote mammosphere formation and decrease E-cadherin in normal and malignant breast cells. *PloS one* 2010; **5**(8): e12180.
57. Lacerda L, Debeb BG, Smith D, Larson R, Solley T, Xu W, Krishnamurthy S, Gong Y, Levy LB, Buchholz T, Ueno NT, Klopp A, Woodward WA. Mesenchymal stem cells mediate the clinical phenotype of inflammatory breast cancer in a preclinical model. *Breast cancer research : BCR* 2015; **17**(1): 42.
58. Obeid E, Nanda R, Fu Y-X, Olopade OI. The role of tumor-associated macrophages in breast cancer progression. *International journal of oncology* 2013; **43**(1): 5-12.
59. Mohamed MM, Al-Raawi D, Sabet SF, El-Shinawi M. Inflammatory breast cancer: New factors contribute to disease etiology: A review. *Journal of Advanced Research* 2014; **5**(5): 525-36.
60. Cho KJ, Hill MM, Chigurupati S, Du G, Parton RG, Hancock JF. Therapeutic levels of the hydroxymethylglutaryl-coenzyme A reductase inhibitor lovastatin activate ras signaling via phospholipase D2. *Molecular and cellular biology* 2011; **31**(6): 1110-20.
61. Foulkes WD, Smith IE, Reis-Filho JS. Triple-negative breast cancer. *The New England journal of medicine* 2010; **363**(20): 1938-48.
62. Woodward WA, Sulman EP. Cancer stem cells: markers or biomarkers? *Cancer metastasis reviews* 2008; **27**(3): 459-70.

63. Al-Hajj M, Wicha MS, Benito-Hernandez A, Morrison SJ, Clarke MF. Prospective identification of tumorigenic breast cancer cells. *Proceedings of the National Academy of Sciences of the United States of America* 2003; **100**(7): 3983-8.
64. Liu H, Patel MR, Prescher JA, Patsialou A, Qian D, Lin J, Wen S, Chang YF, Bachmann MH, Shimono Y, Dalerba P, Adorno M, Lobo N, Bueno J, Dirbas FM, Goswami S, Somlo G, Condeelis J, Contag CH, Gambhir SS, Clarke MF. Cancer stem cells from human breast tumors are involved in spontaneous metastases in orthotopic mouse models. *Proceedings of the National Academy of Sciences of the United States of America* 2010; **107**(42): 18115-20.
65. Lacerda L, Reddy JP, Liu D, Larson R, Li L, Masuda H, Brewer T, Debeb BG, Xu W, Hortobagyi GN, Buchholz TA, Ueno NT, Woodward WA. Simvastatin radiosensitizes differentiated and stem-like breast cancer cell lines and is associated with improved local control in inflammatory breast cancer patients treated with postmastectomy radiation. *Stem cells translational medicine* 2014; **3**(7): 849-56.
66. Chan KK, Oza AM, Siu LL. The statins as anticancer agents. *Clinical cancer research : an official journal of the American Association for Cancer Research* 2003; **9**(1): 10-9.
67. Bansal D, Undela K, D'Cruz S, Schifano F. Statin use and risk of prostate cancer: a meta-analysis of observational studies. *PloS one* 2012; **7**(10): e46691.
68. Bonovas S, Filioussi K, Tsavaris N, Sitaras NM. Use of statins and breast cancer: a meta-analysis of seven randomized clinical trials and nine observational studies. *Journal of clinical oncology : official journal of the American Society of Clinical Oncology* 2005; **23**(34): 8606-12.
69. Mantha AJ, McFee KE, Niknejad N, Goss G, Lorimer IA, Dimitroulakos J. Epidermal growth factor receptor-targeted therapy potentiates lovastatin-induced apoptosis in head and

neck squamous cell carcinoma cells. *Journal of cancer research and clinical oncology* 2003; **129**(11): 631-41.

70. Kotamraju S, Williams CL, Kalyanaraman B. Statin-induced breast cancer cell death: role of inducible nitric oxide and arginase-dependent pathways. *Cancer research* 2007; **67**(15): 7386-94.

71. Hakamada-Taguchi R, Uehara Y, Kuribayashi K, Numabe A, Saito K, Negoro H, Fujita T, Toyo-oka T, Kato T. Inhibition of hydroxymethylglutaryl-coenzyme a reductase reduces Th1 development and promotes Th2 development. *Circulation research* 2003; **93**(10): 948-56.

72. Alber HF, Dulak J, Frick M, Dichtl W, Schwarzacher SP, Pachinger O, Weidinger F. Atorvastatin decreases vascular endothelial growth factor in patients with coronary artery disease. *Journal of the American College of Cardiology* 2002; **39**(12): 1951-5.

73. Dontu G, Abdallah WM, Foley JM, Jackson KW, Clarke MF, Kawamura MJ, Wicha MS. In vitro propagation and transcriptional profiling of human mammary stem/progenitor cells. *Genes Dev* 2003; **17**(10): 1253-70.

74. Irizarry RA, Hobbs B, Collin F, Beazer-Barclay YD, Antonellis KJ, Scherf U, Speed TP. Exploration, normalization, and summaries of high density oligonucleotide array probe level data. *Biostatistics* 2003; **4**(2): 249-64.

75. Lehmann BD, Bauer JA, Chen X, Sanders ME, Chakravarthy AB, Shyr Y, Pietenpol JA. Identification of human triple-negative breast cancer subtypes and preclinical models for selection of targeted therapies. *The Journal of clinical investigation* 2011; **121**(7): 2750-67.

76. Sabatier R, Finetti P, Mamessier E, Adelaide J, Chaffanet M, Ali HR, Viens P, Caldas C, Birnbaum D, Bertucci F. Prognostic and predictive value of PDL1 expression in breast cancer; 2015.

77. McShane LM, Altman DG, Sauerbrei W, Taube SE, Gion M, Clark GM. REporting recommendations for tumour MARKer prognostic studies (REMARK). *British journal of cancer* 2005; **93**(4): 387-91.
78. Fu Z, Tindall DJ. FOXOs, cancer and regulation of apoptosis. *Oncogene* 2008; **27**(16): 2312-9.
79. Hindler K, Cleeland CS, Rivera E, Collard CD. The role of statins in cancer therapy. *Oncologist* 2006; **11**(3): 306-15.
80. Keyomarsi K, Sandoval L, Band V, Pardee AB. Synchronization of tumor and normal cells from G1 to multiple cell cycles by lovastatin. *Cancer research* 1991; **51**(13): 3602-9.
81. Wejde J, Blegen H, Larsson O. Requirement for mevalonate in the control of proliferation of human breast cancer cells. *Anticancer research* 1992; **12**(2): 317-24.
82. Seeger H, Wallwiener D, Mueck AO. Statins can inhibit proliferation of human breast cancer cells in vitro. *Experimental and clinical endocrinology & diabetes : official journal, German Society of Endocrinology [and] German Diabetes Association* 2003; **111**(1): 47-8.
83. Issat T, Nowis D, Legat M, Makowski M, Klejman MP, Urbanski J, Skierski J, Koronkiewicz M, Stoklosa T, Brzezinska A, Bil J, Gietka J, Jakobisiak M, Golab J. Potentiated antitumor effects of the combination treatment with statins and pamidronate in vitro and in vivo. *International journal of oncology* 2007; **30**(6): 1413-25.
84. Koyuturk M, Ersoz M, Altioek N. Simvastatin induces apoptosis in human breast cancer cells: p53 and estrogen receptor independent pathway requiring signalling through JNK. *Cancer letters* 2007; **250**(2): 220-8.
85. Kang S, Kim ES, Moon A. Simvastatin and lovastatin inhibit breast cell invasion induced by H-Ras. *Oncology reports* 2009; **21**(5): 1317-22.

86. Klawitter J, Shokati T, Moll V, Christians U. Effects of lovastatin on breast cancer cells: a proteo-metabonomic study. *Breast cancer research : BCR* 2010; **12**(2): R16.
87. Undela K, Srikanth V, Bansal D. Statin use and risk of breast cancer: a meta-analysis of observational studies. *Breast cancer research and treatment* 2012; **135**(1): 261-9.
88. Brunet A, Sweeney LB, Sturgill JF, Chua KF, Greer PL, Lin Y, Tran H, Ross SE, Mostoslavsky R, Cohen HY, Hu LS, Cheng HL, Jedrychowski MP, Gygi SP, Sinclair DA, Alt FW, Greenberg ME. Stress-dependent regulation of FOXO transcription factors by the SIRT1 deacetylase. *Science* 2004; **303**(5666): 2011-5.
89. Ni D, Ma X, Li HZ, Gao Y, Li XT, Zhang Y, Ai Q, Zhang P, Song EL, Huang QB, Fan Y, Zhang X. Downregulation of FOXO3a promotes tumor metastasis and is associated with metastasis-free survival of patients with clear cell renal cell carcinoma. *Clinical cancer research : an official journal of the American Association for Cancer Research* 2014; **20**(7): 1779-90.
90. Gopinath SD, Webb AE, Brunet A, Rando TA. FOXO3 promotes quiescence in adult muscle stem cells during the process of self-renewal. *Stem cell reports* 2014; **2**(4): 414-26.
91. Jiang Y, Zou L, Lu WQ, Zhang Y, Shen AG. Foxo3a expression is a prognostic marker in breast cancer. *PloS one* 2013; **8**(8): e70746.
92. Gray-Bablin J, Rao S, Keyomarsi K. Lovastatin induction of cyclin-dependent kinase inhibitors in human breast cells occurs in a cell cycle-independent fashion. *Cancer research* 1997; **57**(4): 604-9.
93. Cheng T. Cell cycle inhibitors in normal and tumor stem cells. *Oncogene* 2004; **23**(43): 7256-66.
94. Chappell J, Dalton S. Altered cell cycle regulation helps stem-like carcinoma cells resist apoptosis. *BMC biology* 2010; **8**: 63.

95. Li CJ, Chang JK, Chou CH, Wang GJ, Ho ML. The PI3K/Akt/FOXO3a/p27Kip1 signaling contributes to anti-inflammatory drug-suppressed proliferation of human osteoblasts. *Biochemical pharmacology* 2010; **79**(6): 926-37.
96. Gonzalez-Angulo AM, Hennessy BT, Broglio K, Meric-Bernstam F, Cristofanilli M, Giordano SH, Buchholz TA, Sahin A, Singletary SE, Buzdar AU, Hortobagyi GN. Trends for inflammatory breast cancer: is survival improving? *Oncologist* 2007; **12**(8): 904-12.
97. Cristofanilli M, Valero V, Buzdar AU, Kau SW, Broglio KR, Gonzalez-Angulo AM, Sneige N, Islam R, Ueno NT, Buchholz TA, Singletary SE, Hortobagyi GN. Inflammatory breast cancer (IBC) and patterns of recurrence: understanding the biology of a unique disease. *Cancer* 2007; **110**(7): 1436-44.
98. Van Laere S, Limame R, Van Marck EA, Vermeulen PB, Dirix LY. Is there a role for mammary stem cells in inflammatory breast carcinoma?: a review of evidence from cell line, animal model, and human tissue sample experiments. *Cancer*; **116**(11 Suppl): 2794-805.
99. Clarke M, Collins R, Darby S, Davies C, Elphinstone P, Evans E, Godwin J, Gray R, Hicks C, James S, MacKinnon E, McGale P, McHugh T, Peto R, Taylor C, Wang Y, Early Breast Cancer Trialists' Collaborative G. Effects of radiotherapy and of differences in the extent of surgery for early breast cancer on local recurrence and 15-year survival: an overview of the randomised trials. *Lancet* 2005; **366**(9503): 2087-106.
100. Baumann M, Krause M, Hill R. Exploring the role of cancer stem cells in radioresistance. *Nature reviews Cancer* 2008; **8**(7): 545-54.
101. Fillmore CM, Kuperwasser C. Human breast cancer cell lines contain stem-like cells that self-renew, give rise to phenotypically diverse progeny and survive chemotherapy. *Breast cancer research : BCR* 2008; **10**(2): R25.

102. Maugeri-Sacca M, Bartucci M, De Maria R. DNA damage repair pathways in cancer stem cells. *Mol Cancer Ther* 2012; **11**(8): 1627-36.
103. Mathews LA, Cabarcas SM, Farrar WL. DNA repair: the culprit for tumor-initiating cell survival? *Cancer metastasis reviews* 2011; **30**(2): 185-97.
104. Hegele RA. Plasma lipoproteins: genetic influences and clinical implications. *Nat Rev Genet* 2009; **10**(2): 109-21.
105. McTaggart F, Jones P. Effects of statins on high-density lipoproteins: a potential contribution to cardiovascular benefit. *Cardiovascular drugs and therapy / sponsored by the International Society of Cardiovascular Pharmacotherapy* 2008; **22**(4): 321-38.
106. Pianetti S, Arsura M, Romieu-Mourez R, Coffey RJ, Sonenshein GE. Her-2/neu overexpression induces NF-kappaB via a PI3-kinase/Akt pathway involving calpain-mediated degradation of IkappaB-alpha that can be inhibited by the tumor suppressor PTEN. *Oncogene* 2001; **20**(11): 1287-99.
107. Tran H, Brunet A, Grenier JM, Datta SR, Fornace AJ, Jr., DiStefano PS, Chiang LW, Greenberg ME. DNA repair pathway stimulated by the forkhead transcription factor FOXO3a through the Gadd45 protein. *Science* 2002; **296**(5567): 530-4.
108. Rogakou EP, Pilch DR, Orr AH, Ivanova VS, Bonner WM. DNA double-stranded breaks induce histone H2AX phosphorylation on serine 139. *The Journal of biological chemistry* 1998; **273**(10): 5858-68.
109. Boyd NF, McGuire V. Evidence of association between plasma high-density lipoprotein cholesterol and risk factors for breast cancer. *Journal of the National Cancer Institute* 1990; **82**(6): 460-8.

110. Ferraroni M, Gerber M, Decarli A, Richardson S, Marubini E, Crastes de Paulet P, Crastes de Paulet A, Pujol H. HDL-cholesterol and breast cancer: a joint study in northern Italy and southern France. *International journal of epidemiology* 1993; **22**(5): 772-80.
111. Kitahara CM, Berrington de Gonzalez A, Freedman ND, Huxley R, Mok Y, Jee SH, Samet JM. Total cholesterol and cancer risk in a large prospective study in Korea. *Journal of clinical oncology : official journal of the American Society of Clinical Oncology* 2011; **29**(12): 1592-8.
112. Bavari S, Bosio CM, Wiegand E, Ruthel G, Will AB, Geisbert TW, Hevey M, Schmaljohn C, Schmaljohn A, Aman MJ. Lipid raft microdomains: a gateway for compartmentalized trafficking of Ebola and Marburg viruses. *The Journal of experimental medicine* 2002; **195**(5): 593-602.
113. Chatterjee S, Mayor S. The GPI-anchor and protein sorting. *Cellular and molecular life sciences : CMLS* 2001; **58**(14): 1969-87.
114. Varma R, Mayor S. GPI-anchored proteins are organized in submicron domains at the cell surface. *Nature* 1998; **394**(6695): 798-801.
115. Prevo R, Deutsch E, Sampson O, Diplexcito J, Cengel K, Harper J, O'Neill P, McKenna WG, Patel S, Bernhard EJ. Class I PI3 kinase inhibition by the pyridinylfuranopyrimidine inhibitor PI-103 enhances tumor radiosensitivity. *Cancer research* 2008; **68**(14): 5915-23.
116. Fuhrman CB, Kilgore J, LaCoursiere YD, Lee CM, Milash BA, Soisson AP, Zempolich KA. Radiosensitization of cervical cancer cells via double-strand DNA break repair inhibition. *Gynecologic oncology* 2008; **110**(1): 93-8.
117. Choi EJ, Ryu YK, Kim SY, Wu HG, Kim JS, Kim IH, Kim IA. Targeting epidermal growth factor receptor-associated signaling pathways in non-small cell lung cancer cells: implication in radiation response. *Mol Cancer Res* 2010; **8**(7): 1027-36.

118. Luo X, Puig O, Hyun J, Bohmann D, Jasper H. Foxo and Fos regulate the decision between cell death and survival in response to UV irradiation. *The EMBO journal* 2007; **26**(2): 380-90.
119. Early Breast Cancer Trialists' Collaborative G. Effect of radiotherapy after breast-conserving surgery on 10-year recurrence and 15-year breast cancer death: meta-analysis of individual patient data for 10 801 women in 17 randomised trials. *Lancet* 2011; **378**(9804): 1707-16.
120. Wolfe AR, Atkinson RL, Reddy JP, Debeb BG, Larson R, Li L, Masuda H, Brewer T, Atkinson BJ, Brewster A, Ueno NT, Woodward WA. High-Density and Very-Low-Density Lipoprotein Have Opposing Roles in Regulating Tumor-Initiating Cells and Sensitivity to Radiation in Inflammatory Breast Cancer. *International Journal of Radiation Oncology*Biography*Physics* 2015; **91**(5): 1072-80.
121. McDonnell DP, Park S, Goulet MT, Jasper J, Wardell SE, Chang CY, Norris JD, Guyton JR, Nelson ER. Obesity, cholesterol metabolism, and breast cancer pathogenesis. *Cancer research* 2014; **74**(18): 4976-82.
122. Smith B, Land H. Anti-cancer activity of the cholesterol exporter ABCA1 gene. *Cell reports* 2012; **2**(3): 580-90.
123. Lee BH, Taylor MG, Robinet P, Smith JD, Schweitzer J, Sehayek E, Falzarano SM, Magi-Galluzzi C, Klein EA, Ting AH. Dysregulation of cholesterol homeostasis in human prostate cancer through loss of ABCA1. *Cancer research* 2013; **73**(3): 1211-8.
124. Ma R, Jiang T, Kang X. Circulating microRNAs in cancer: origin, function and application. *Journal of experimental & clinical cancer research : CR* 2012; **31**(1): 38-.
125. Fernández-Hernando C, Suárez Y, Rayner KJ, Moore KJ. MicroRNAs in lipid metabolism. *Current opinion in lipidology* 2011; **22**(2): 86-92.

126. Wang H, Sun T, Hu J, Zhang R, Rao Y, Wang S, Chen R, McLendon RE, Friedman AH, Keir ST, Bigner DD, Li QJ, Wang H, Wang XF. miR-33a promotes glioma-initiating cell self-renewal via PKA and NOTCH pathways. *The Journal of clinical investigation* 2014; **124**(10): 4489-502.
127. Zhou Y, Huang Z, Wu S, Zang X, Liu M, Shi J. miR-33a is up-regulated in chemoresistant osteosarcoma and promotes osteosarcoma cell resistance to cisplatin by down-regulating TWIST. *Journal of experimental & clinical cancer research : CR* 2014; **33**: 12.
128. Moore KJ, Rayner KJ, Suárez Y, Fernández-Hernando C. microRNAs and cholesterol metabolism. *Trends in endocrinology and metabolism: TEM* 2010; **21**(12): 699-706.
129. Buffa FM, Camps C, Winchester L, Snell CE, Gee HE, Sheldon H, Taylor M, Harris AL, Ragoussis J. microRNA-associated progression pathways and potential therapeutic targets identified by integrated mRNA and microRNA expression profiling in breast cancer. *Cancer research* 2011; **71**(17): 5635-45.
130. Wellington CL, Walker EK, Suarez A, Kwok A, Bissada N, Singaraja R, Yang YZ, Zhang LH, James E, Wilson JE, Francone O, McManus BM, Hayden MR. ABCA1 mRNA and protein distribution patterns predict multiple different roles and levels of regulation. *Lab Invest* 2002; **82**(3): 273-83.
131. Oram JF, Lawn RM. ABCA1. The gatekeeper for eliminating excess tissue cholesterol. *Journal of lipid research* 2001; **42**(8): 1173-9.
132. Bodzioch M, Orso E, Klucken J, Langmann T, Bottcher A, Diederich W, Drobnik W, Barlage S, Buchler C, Porsch-Ozcurumez M, Kaminski WE, Hahmann HW, Oette K, Rothe G, Aslanidis C, Lackner KJ, Schmitz G. The gene encoding ATP-binding cassette transporter 1 is mutated in Tangier disease. *Nature genetics* 1999; **22**(4): 347-51.

133. Atkinson R, Yang W, Rosen D, Landis M, Wong H, Lewis M, Creighton C, Sexton K, Hilsenbeck S, Sahin A, Brewster A, Woodward W, Chang J. Cancer stem cell markers are enriched in normal tissue adjacent to triple negative breast cancer and inversely correlated with DNA repair deficiency. *Breast Cancer Research* 2013; **15**(5): R77.
134. Baumgarten SC, Frasor J. Minireview: Inflammation: an instigator of more aggressive estrogen receptor (ER) positive breast cancers. *Mol Endocrinol* 2012; **26**(3): 360-71.
135. Hussein MR, Hassan HI. Analysis of the mononuclear inflammatory cell infiltrate in the normal breast, benign proliferative breast disease, in situ and infiltrating ductal breast carcinomas: preliminary observations. *J Clin Pathol* 2006; **59**(9): 972-7.
136. Klopp AH, Spaeth EL, Dembinski JL, Woodward WA, Munshi A, Meyn RE, Cox JD, Andreeff M, Marini FC. Tumor irradiation increases the recruitment of circulating mesenchymal stem cells into the tumor microenvironment. *Cancer research* 2007; **67**(24): 11687-95.
137. Liu S, Ginestier C, Ou SJ, Clouthier SG, Patel SH, Monville F, Korkaya H, Heath A, Dutcher J, Klier CG, Jung Y, Dontu G, Taichman R, Wicha MS. Breast cancer stem cells are regulated by mesenchymal stem cells through cytokine networks. *Cancer research* 2011; **71**(2): 614-24.
138. Adutler-Lieber S, Ben-Mordechai T, Naftali-Shani N, Asher E, Loberman D, Raanani E, Leor J. Human Macrophage Regulation Via Interaction With Cardiac Adipose Tissue-Derived Mesenchymal Stromal Cells. *J Cardiovasc Pharmacol Ther* 2012.
139. Fujita E, Soyama A, Momoi T. RA175, which is the mouse ortholog of TSLC1, a tumor suppressor gene in human lung cancer, is a cell adhesion molecule. *Experimental cell research* 2003; **287**(1): 57-66.
140. Priceman SJ, Sung JL, Shaposhnik Z, Burton JB, Torres-Collado AX, Moughon DL, Johnson M, Lusic AJ, Cohen DA, Iruela-Arispe ML, Wu L. Targeting distinct tumor-infiltrating

- myeloid cells by inhibiting CSF-1 receptor: combating tumor evasion of antiangiogenic therapy. *Blood* 2010; **115**(7): 1461-71.
141. DeNardo DG, Barreto JB, Andreu P, Vasquez L, Tawfik D, Kolhatkar N, Coussens LM. CD4(+) T cells regulate pulmonary metastasis of mammary carcinomas by enhancing protumor properties of macrophages. *Cancer Cell* 2009; **16**(2): 91-102.
142. Gordon S. The macrophage: past, present and future. *European journal of immunology* 2007; **37 Suppl 1**: S9-17.
143. Pollard JW. Trophic macrophages in development and disease. *Nature reviews Immunology* 2009; **9**(4): 259-70.
144. Stout RD, Jiang C, Matta B, Tietzel I, Watkins SK, Suttles J. Macrophages sequentially change their functional phenotype in response to changes in microenvironmental influences. *J Immunol* 2005; **175**(1): 342-9.
145. Martinez FO, Helming L, Gordon S. Alternative activation of macrophages: an immunologic functional perspective. *Annual review of immunology* 2009; **27**: 451-83.
146. Mosser DM. The many faces of macrophage activation. *J Leukoc Biol* 2003; **73**(2): 209-12.
147. Ortiz LA, Dutreil M, Fattman C, Pandey AC, Torres G, Go K, Phinney DG. Interleukin 1 receptor antagonist mediates the antiinflammatory and antifibrotic effect of mesenchymal stem cells during lung injury. *Proceedings of the National Academy of Sciences of the United States of America* 2007; **104**(26): 11002-7.
148. Nemeth K, Leelahavanichkul A, Yuen PS, Mayer B, Parmelee A, Doi K, Robey PG, Leelahavanichkul K, Koller BH, Brown JM, Hu X, Jelinek I, Star RA, Mezey E. Bone marrow stromal cells attenuate sepsis via prostaglandin E(2)-dependent reprogramming of host macrophages to increase their interleukin-10 production. *Nat Med* 2009; **15**(1): 42-9.

149. Wei LH, Kuo ML, Chen CA, Chou CH, Lai KB, Lee CN, Hsieh CY. Interleukin-6 promotes cervical tumor growth by VEGF-dependent angiogenesis via a STAT3 pathway. *Oncogene* 2003; **22**(10): 1517-27.
150. Kim MY, Oskarsson T, Acharyya S, Nguyen DX, Zhang XH, Norton L, Massague J. Tumor self-seeding by circulating cancer cells. *Cell* 2009; **139**(7): 1315-26.
151. Kujawski M, Kortylewski M, Lee H, Herrmann A, Kay H, Yu H. Stat3 mediates myeloid cell-dependent tumor angiogenesis in mice. *The Journal of clinical investigation* 2008; **118**(10): 3367-77.
152. Oh K, Lee OY, Shon SY, Nam O, Ryu PM, Seo MW, Lee DS. A mutual activation loop between breast cancer cells and myeloid-derived suppressor cells facilitates spontaneous metastasis through IL-6 trans-signaling in a murine model. *Breast cancer research : BCR* 2013; **15**(5): R79.
153. DeNardo DG, Brennan DJ, Rexhepaj E, Ruffell B, Shiao SL, Madden SF, Gallagher WM, Wadhvani N, Keil SD, Junaid SA, Rugo HS, Hwang ES, Jirstrom K, West BL, Coussens LM. Leukocyte complexity predicts breast cancer survival and functionally regulates response to chemotherapy. *Cancer discovery* 2011; **1**(1): 54-67.
154. Lai EC. Lipid rafts make for slippery platforms. *The Journal of cell biology* 2003; **162**(3): 365-70.
155. Pike LJ. Lipid rafts: bringing order to chaos. *Journal of lipid research* 2003; **44**(4): 655-67.
156. Foster LJ, de Hoog CL, Mann M. Unbiased quantitative proteomics of lipid rafts reveals high specificity for signaling factors. *Proceedings of the National Academy of Sciences* 2003; **100**(10): 5813-8.

157. Silvius JR. Role of cholesterol in lipid raft formation: lessons from lipid model systems. *Biochimica et Biophysica Acta (BBA) - Biomembranes* 2003; **1610**(2): 174-83.
158. Dykstra M, Cherukuri A, Sohn HW, Tzeng S-J, Pierce SK. LOCATION IS EVERYTHING: Lipid Rafts and Immune Cell Signaling*. *Annual review of immunology* 2003; **21**(1): 457-81.
159. Legler DF, Micheau O, Doucey M-A, Tschopp J, Bron C. Recruitment of TNF Receptor 1 to Lipid Rafts Is Essential for TNF α -Mediated NF- κ B Activation. *Immunity* 2003; **18**(5): 655-64.
160. Bagnat M, Simons K. Lipid Rafts in Protein Sorting and Cell Polarity in Budding Yeast *Saccharomyces cerevisiae*. *Biological Chemistry*; 2002. p. 1475.
161. Krummenacher C, Baribaud I, Sanzo JF, Cohen GH, Eisenberg RJ. Effects of Herpes Simplex Virus on Structure and Function of Nectin-1/HveC. *Journal of Virology* 2002; **76**(5): 2424-33.
162. Stuart ES, Webley WC, Norkin LC. Lipid rafts, caveolae, caveolin-1, and entry by *Chlamydiae* into host cells. *Experimental cell research* 2003; **287**(1): 67-78.
163. Ostrom RS, Insel PA. Methods for the study of signaling molecules in membrane lipid rafts and caveolae. *Methods Mol Biol* 2006; **332**: 181-91.

Vita

Adam was born in Houston, Texas on December 15, 1986, the son of Michael Neil Wolfe and Peggy Ann Wolfe. After graduating from Clear Lake High School in May 2005, he entered Texas Tech University in Lubbock, Texas. He received a Bachelor of Science in Cell and Molecular Biology, summa cum laude with honors in May 2009. In August 2009 he enrolled as a dual degree student at the University of Texas Health Science Center at Houston, in the combined M.D./PhD. Program. His research has been recognized in several national meetings, and he received the AACR Scholar-in-Training Award for his research. Adam is intending to graduate with both M.D. and PhD. degrees in May 2016 and start a Radiation Oncology Residency in July 2016.

Permanent address:

1937 Dryden Rd Apt 2

Houston, Texas 77030